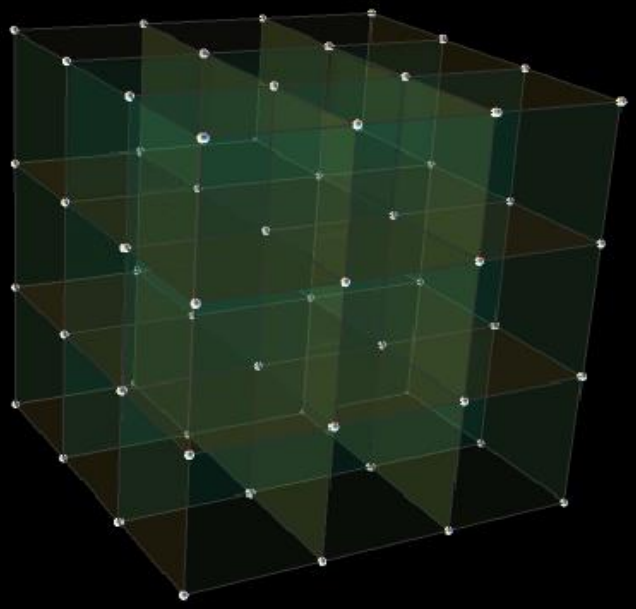

Anthony Gomes Duarte

Correlation Functions in Pure Gauge Theories: Propagators and Vertices in Lattice QCD

Dissertation presented to the Physics Department at
University of Coimbra to obtain the Master's degree in Physics

September 2016

· U C ·

UNIVERSIDADE DE COIMBRA

Correlation Functions in Pure Gauge Theories

Propagators and vertices in Lattice QCD

Anthony Gomes Duarte

Supervisor: Prof. Dr. Orlando Olavo Aragão Aleixo e Neves de Oliveira;
Dr. Paulo de Jesus Henriques da Silva

Departamento de Física
Universidade de Coimbra

This dissertation is submitted for the degree of
Master

Faculdade de Ciências e Tecnologia September 2016

I would like to dedicate this thesis to my loving parents ...

Acknowledgements

I would like to take the oportunity to thank all people that somehow supported me throughout this whole process of creating and developing this dissertation.

First, I would like to thank both my supervisors, Prof. Dr. Orlando Olavo Aragão Aleixo e Neves de Oliveira and Dr. Paulo de Jesus Henriques da Silva, for all the continuous support, guidance and kindness towards me. Both have taught me so much and have always been available to answer my questions. I would also like to thank both of them for the time spent reading this dissertation, which certainly improved it.

I would like to ackowledge the Laboratory for Advanced Computing at the University of Coimbra for providing HPC resources such as Milipeia, Centaurus and Navigator, which have contributed to the work developed in this dissertation.

On the other hand, I would like to ackowledge the computing resources provided by the Partnership for Advanced Computing in Europe (PRACE) initiative under DECI-9 project COIMBRALATT and DECI-12 project COIMBRALATT2.

I would also like to express my appreciation to my beloved friends without whom this journey would be much less enjoyable, from which I would like to mention my friends Cátia, Vanda and Miguel for all they have done.

Finally, I would like to mention my gratitude to my family who has always supported me throughout life.

Abstract

This dissertation is a result of the work developed throughout the year by the author in association with his supervisors. There were two main objectives: one was to study the gluon and ghost propagators and the strong coupling constant on the lattice, namely their dependences on the finite lattice spacing and on the physical volume; the other was to compute the three-gluon vertex and provide further evidence of the zero crossing of the gluon factor form associated with the three gluon one particle irreducible function, which is expected so that one has a properly defined set of Dyson-Schwinger equations. These were done in the pure Yang-Mills theory.

Our results showed no noticeable (or, at most, mild) dependence of the gluon and ghost propagators on the physical volume, at least for the lattices used (above $(6.5\,\mathrm{fm})^4$ and below $(13\,\mathrm{fm})^4$); they showed on both propagators a dependence on the lattice spacing in the infrared region, where the dependence is more noticeable in the case of the gluon propagator; they exhibit a supression on the value at the maximum of the running coupling for smaller lattice spacings. In what concerns the three gluon vertex, our results are in favour of a zero crossing of the gluon form factor for momenta in the range $p \in [220 - 260]\,\mathrm{MeV}$. On the other hand, the data seems to corroborate the predictions of the renormalization group improved perturbation theory in the region of high momentum.

The results obtained originated

• Two papers in international refereed journals,

1. "Lattice Gluon and Ghost Propagators, and the Strong Coupling in Pure SU(3) Yang-Mills Theory: Finite Lattice Spacing and Volume Effects", Anthony G. Duarte and Orlando Oliveira and Paulo J. Silva, *Phys. Rev. **D94**, 014502 (2016)*[1];

2. "Further Evidence For Zero Crossing On The Three Gluon Vertex", Anthony G. Duarte and Orlando Oliveira and Paulo J. Silva, Phys. Rev. D (accepted) [2].

• An oral presentation in an international conference

1. "Landau gauge gluon vertices from Lattice QCD", A. Duarte, O. Oliveira, P.J. Silva, presented in "34th International Symposium on Lattice Field Theory", Southampton, UK, 24-30 July 2016.

which is going to be published in the proceedings,

1. "Landau gauge gluon vertices from Lattice QCD", A. Duarte, O. Oliveira, P.J. Silva, PoS (LATTICE2016) 351 (in preparation).

Keywords

Quantum Field Theory, Quantum Chromodynamics, Lattice Quantum Chromodynamics, Gluon, Ghost, Running Coupling, Propagator, Three Gluon Vertex.

Resumo

Esta dissertação é fruto do trabalho desenvolvido ao longo deste ano pelo autor, juntamente com os seus orientadores. A dissertação consistiu essencialmente em dois objectivos: o estudo do propagador gluónico e dos campos fantasma, bem como da constante de acoplamento associada, na rede, nomeadamente, das suas dependências no espaçamento finito da rede e no volume físico; o estudo do vértice de três gluões, nomeadamente, o seu cálculo na rede, e o estudo do factor de forma gluónico da função $1PI$, de modo a fornecer novas evidências sobre a mudança de sinal deste factor de forma, prevista a fim de termos um conjunto de equações de Dyson-Schwinger bem definidas. Estes objectivos foram estudados numa teoria de Yang-Mills pura.

Os resultados obtidos não mostram nenhuma dependência evidente dos propagadores gluónico e dos campos fantasma no volume físico, pelo menos, para as redes utilizadas (acima de $(6.5\,\mathrm{fm})^4$ e abaixo de $(13\,\mathrm{fm})^4$); mostram em ambos os propagadores (gluónico e de campos fantasma) uma dependência no espaçamento da rede, na região do infravermelho, notando-se uma dependência mais evidente no caso do propagador gluónico; exibem uma supressão no valor da constante de acoplamento correspondente ao seu máximo para espaçamentos da rede menores. No que diz respeito ao vértice de três gluões, os nossos resultados são compatíveis com uma mudança de sinal do factor de forma gluónico na região de momentos $p \in [220 - 260]\,\mathrm{MeV}$. Por outro lado, os nossos dados parecem corroborar as previsões da teoria perturbativa de grupo de renormalização melhorado, na região de momentos altos.

Os resultados obtidos deram origem a

• Dois artigos em revistas científicas de circulação internacional,

1. "Lattice Gluon and Ghost Propagators, and the Strong Coupling in Pure SU(3) Yang-Mills Theory: Finite Lattice Spacing and Volume Effects", Anthony G. Duarte and Orlando Oliveira and Paulo J. Silva, *Phys. Rev. D**94**, 014502 (2016)*[1];

2. "Further Evidence For Zero Crossing On The Three Gluon Vertex", Anthony G. Duarte and Orlando Oliveira and Paulo J. Silva (aceite)[2].

• Uma apresentação oral numa conferência internacional

1. "Landau gauge gluon vertices from Lattice QCD", A. Duarte, O. Oliveira, P.J. Silva, presented in "34th International Symposium on Lattice Field Theory", Southampton, UK, 24-30 July 2016.

que irá ser publicado nas actas da conferência,

1. "Landau gauge gluon vertices from Lattice QCD", A. Duarte, O. Oliveira, P.J. Silva, PoS (LATTICE2016) 351 (em preparação).

Palavras-chave

Teoria Quântica de Campos, Cromodinâmica Quântica, Cromodinâmica Quântica na Rede, Gluão, Campos Fantasma, Constante de Acoplamento, Propagador, Vértice de Três Gluões.

Table of contents

List of figures

List of tables

Notation and Conventions

Units

One set $\hbar = c = 1$. In this system one has

$$[length] = [time] = [energy]^{-1} = [mass]^{-1}$$

Useful functions

The Heaviside function is defined as

$$\theta(x^0 - y^0) = \begin{cases} 1, & \text{if } x^0 - y^0 > 0 \\ 0, & \text{otherwise} \end{cases}$$

Some Notations

The slashed notation is defined as

$$\not{A} := \gamma^\mu A_\mu$$

where γ^μ are the gamma matrices and A_μ is a four-vector (for instance, $\not{\partial} = \gamma^\mu \partial_\mu$).
One also uses the notations

$$\begin{aligned} A_\mu &:= A^a_\mu t^a \\ F_{\mu\nu} &:= F^a_{\mu\nu} t^a \end{aligned} \tag{1}$$

for, respectively, the gauge field and the field strength tensor. Notice that $F^a_{\mu\nu} = \partial_\mu A^a_\nu - \partial_\nu A^a_\mu + g f^{abc} A^b_\mu A^c_\nu$, where f^{abc} are the structure constants of the group (see Appendix A). On the other hand, t^a are the generators of $SU(N)$.

Acronyms / Abbreviations

1PI One Particle Irreducible
LQCD Lattice Quantum Chromodynamics
QCD Quantum Chromodynamics
QED Quantum Elecrodynamics

Introduction

Quantum Chromodynamics is tightly established as the theory of quarks and gluons. It may be viewed as a generalization of Quantum Electrodynamics, for it may be constructed from gauge symmetry as one may see in chapter 2. It is a non-abelian gauge theory with symmetry group $SU(3)$. In this dissertation, in order to study the non-perturbative regime, one adopts the well-established Lattice Quantum Chromodynamics approach, which consists of calculations in a discretized Euclidean space-time, which is particularly suited for computational calculations.

There are two main objectives for this dissertation: one is to study the gluon and ghost propagators and the strong coupling constant on the lattice, namely their dependences on the finite lattice spacing and on the physical volume; the other is to compute the three-gluon vertex and to provide further evidence of the zero crossing of the gluon factor form associated with the three gluon one particle irreducible function, which is expected due to Dyson-Schwinger equations. In this work, we will not consider dynamical fermions, i.e., the aforementioned is studied in a pure Yang-Mills theory in Landau gauge. This is called the *quenched approximation*, which, in terms of Feynman diagrams, means one is not considering the fermion loop contributions.

In what concerns the gluon and ghost propagators, there have been investigations using lattice simulations in the past years for the $SU(2)$ and $SU(3)$ groups, resulting in the consensus that: the gluon propagator is supressed in the infrared and that at zero momentum it has a finite non-vanishing value [3–11]; the ghost propagator appears to be represented substantially by its tree level expression [3–5, 7, 12–16]. It has been shown in [10] after comparing various ensembles with different lattice spacings and physical volumes that the dominant effect in the infrared region was the use of a finite lattice spacing. Furthermore, the same paper reports that in the infrared region the use of large lattice spacing underestimates the value of the propagator. Therefore, this dissertation is an extension of the work developed in [10]. For that purpose, we used large physical volumes $\gtrsim 6.5\,fm$.

On the other hand, notice that the study of the three gluon vertex is important as it is related to several properties of the strong interaction. For instance, one can define from the three point Green's function a static potential between colour charges or even compute

the strong coupling constant [17–25]. It is expected that in the case of pure Yang-Mills theory, in order to make the gluon Dyson Schwinger equations finite, that some form factors related to the three gluon one particle irreducible change sign for some momentum in the infrared region, if one assumes a ghost propagator essentially described by its tree level form, and also that the four-gluon vertex is subleading in the infrared[26, 27]. The change of sign of the three gluon 1PI implies that one has a momentum in which a zero crossing happens. This zero crossing have been observed in the case of $SU(2)$ gauge group for three dimensions in [28, 29]; for $SU(3)$ in four dimensions in pure Yang Mills theory, reported in [25]; in solutions of the three-gluon vertex Dyson-Schwinger equations [30, 31]; in Coulomb gauge using the variational solution of QCD [32]; using the Curci-Ferrari model [33]. The zero crossing where estimated in the range: $150-250\,MeV$ in the case of SU(2) lattice simulation in three dimensions [29]; $130-200\,MeV$ in the study of the gluon using the Dyson Schwinger equations [27]; above $100\,MeV$ in the case of lattice simulations for $SU(3)$ gauge group [25]. Furthermore, if the dynamical effects are included in the three gluon vertex, the zero crossing seems to happen within the same scales of momentum as in the quenched theory [34]. The work developed in the current dissertation intended to provide further evidence of this change of sign for certain kinematic configurations.

This dissertation is divided into six chapters. The first four chapters are a synopsis of the theoretical basis needed to understand the results we obtained. They are not to be understood as a complete description of the topics they cover, but rather as a (hopefully) understandable set of topics that only covers what is needed.

In chapter one, the basic concepts of Quantum Field theory are introduced, as those of correlation functions. One commences with the classical field theory and then introduces the functional integral method approach to quantum field theory. Afterwards, one introduces the essencial concept of correlation functions and finally uses the generating functional to define it.

In chapter two, Quantum Chromodynamics is discussed by taking the gauge symmetry as the starting point. One constructs the Yang-Mills lagrangian from it and then quantize the theory using the Faddeev-Popov method, which is needed due to the redundancy in the functional integration caused by physically equivalent field configurations. Next, one defines the tree-level gluon and ghost propagators and the three gluon vertex factor. Then, the concepts of regularization and renormalization are briefly explained. Finally, the full gluon and ghost propagators and the general form of the three-gluon vertex are defined. The later was done in [35].

In chapter three, Quantum Chromodynamics is reformulated on a space-time lattice. One discusses the need for Euclidean space-time, and then defines the gauge-links which will

be used instead of the gauge fields. Next, the simplest discretized version of the continuum action is defined - the Wilson action. Then one discusses methods used to rotate the lattice configurations to the Landau gauge. Next, one defines the gluon and ghost propagators on the lattice and the running coupling constant, which is a renormalization group invariant.

In chaper four, the computational methods needed to perform lattice computations are introduced. To this end, one discuss Monte Carlo methods (which are needed for one is dealing with high dimensional integrals), and then the methods used in this work in the generation of the lattice configurations, namely, the overrelaxation algorithm and the heatbath method. In order to fix the gauge of the configurations to the Landau gauge, the Fourier Accelerated Steepest Descent method was used, which is also discussed. Finally, one introduces the method used for computing statistical errors - the bootstrap method.

In chapter five, the results obtained in the work described in this dissertation are presented. It is divided in three sections, the first to discuss the lattice setup, and the other two for each main objective of the dissertation already discussed above.

Finally, in chapter six, the main conclusions from the results presented in the previous chapter are summarized.

In order to provide some further topics, calculations or proofs not presented in the first four chapters but slightly mentioned, one refers the reader to some references and some of these are discussed in the appendices.

Chapter 1

Quantum Field Theory: A Brief Overview

Quantum field theory may be understood as the basic theory used to describe the physics of elementary particles. Like its name suggests, it is an application of quantum mechanics to the theory of classical fields. One may wonder why the use of fields is necessary. One could simply quantize particles instead of fields. However, this imposes several issues, for instance, the negative-energy states arising from the Dirac equation. On the other hand, there is the necessity of a multiparticle theory, due to particle-antiparticle pairs [36]. Fortunately, the use of fields solves these issues. For further informations concerning this chapter, one recomends [36] and [37]. The concept of functional derivative was based on the definition presented in [38].

1.1 Classical Field Theory: Lagrangian and Hamiltonian Formulation

1.1.1 Lagrangian Field Theory

The goal of this section is to derive the equation of motion for fields. The action, S, is a fundamental quantity in classical mechanics from which one may derive them. It is related to the Lagrangian, as it is a time integral over it. In a local field theory, however, one usually uses the Lagragian density, denoted by $\mathscr{L}$, instead of the usual Lagrangian. The action is given by,

$$S = \int L dt = \int \mathscr{L}(\phi, \partial_\mu \phi) d^4x \,. \tag{1.1}$$

The principle of least action states that[1] *the path taken by the system between times t_1 and t_2 is the one for which the action is stationary (no change) to first order.* Mathematically, this means that

$$0 = \delta S = \int d^4x \left\{ \frac{\partial \mathscr{L}}{\partial \phi} \delta\phi + \frac{\partial \mathscr{L}}{\partial(\partial_\mu \phi)} \delta(\partial_\mu \phi) \right\} , \tag{1.2}$$

which may be rewritten using the rule of the derivative of a product as

$$0 = \int d^4x \left\{ \frac{\partial \mathscr{L}}{\partial \phi} \delta\phi - \partial_\mu \left(\frac{\partial \mathscr{L}}{\partial(\partial_\mu \phi)} \right) \delta\phi + \partial_\mu \left(\frac{\partial \mathscr{L}}{\partial(\partial_\mu \phi)} \delta\phi \right) \right\} . \tag{1.3}$$

Using Gauss' divergence theorem, the last term may be turned into a surface integral. Assuming that the field is not varied on the boundary of the four-dimensional space-time region of integration, this integral vanishes. Since $\delta\phi$ is arbitrary (except for the surface), one must have:

$$\partial_\mu \left(\frac{\partial \mathscr{L}}{\partial(\partial_\mu \phi)} \right) - \frac{\partial \mathscr{L}}{\partial \phi} = 0 . \tag{1.4}$$

These are the Euler-Lagrange equation of motion for a field[2].

1.1.2 Hamiltonian Field Theory

For a discrete system one can associate with each dynamical variable q a conjugate momentum $p := \partial L/\partial \dot{q}$. The Hamiltonian is defined as $H := \sum p\dot{q} - L$. To generalize to continuous systems, one begins by pretending that the spacial points are discretly spaced,

$$\begin{aligned} p(\mathbf{x}) =& \frac{\partial L}{\partial \dot{\phi}(\mathbf{x})} = \frac{\partial}{\partial \dot{\phi}(\mathbf{x})} \int \mathscr{L}\left(\phi(\mathbf{y}, \dot{\phi}(\mathbf{y})\right) d^3y \\ &\sim \frac{\partial}{\partial \dot{\phi}(\mathbf{x})} \sum_y \mathscr{L}\left(\phi(\mathbf{y}, \dot{\phi}(\mathbf{y})\right) d^3y \\ &= \pi(\mathbf{x}) d^3x , \end{aligned}$$

where

$$\pi(\mathbf{x}) := \frac{\partial \mathscr{L}}{\partial \dot{\phi}(\mathbf{x})} \tag{1.5}$$

[1] R. Penrose (2007). "The Road to Reality". Vintage books. p. 474.

[2] If the Lagrangian involves more than one field, there is one such equation for each field.

is the momentum density conjugate to $\phi(\mathbf{x})$. Hence, the hamiltonian can be written as

$$H = \sum_{\mathbf{x}} p(\mathbf{x})\dot{\phi}(\mathbf{x}) - L\,. \tag{1.6}$$

In the continuum limit, for a field theory, one has

$$H = \int d^3x \left[\pi(\mathbf{x})\dot{\phi}(\mathbf{x}) - \mathscr{L}\right] := \int d^3x \mathscr{H}\,. \tag{1.7}$$

1.2 Functional Integral Formulation

In this section, the method of functional integrals applied to quantum systems are introduced. Let us start from a general quantum system described by a set of coordinates $\{q^k\}_{k=1}^M$, its conjugate momenta $\{p^k\}_{k=1}^M$ and their respective Hamiltonian[3] $H(q,p)$. One is interested in the computation of the transition amplitude, which in Quantum Mechanics may be written as:

$$U(q_a, q_b; T) = \langle q_b | e^{-iHT} | q_a \rangle\,. \tag{1.8}$$

Notice that one uses q or p without superscript to denote the whole set of coordinates or momenta, respectively. Thus, within this simplification,

$$\begin{aligned}
&\int dq := \int dq^1 \int dq^2 ... \int dq^M = \prod_{k=1}^M \left(\int dq^k\right)\,; \\
&\xi_\alpha \xi_\beta := \sum_{k=1}^M \xi_\alpha^k \xi_\beta^k \text{ , where } \xi \text{ is either } q \text{ or } p\,; \\
&\delta(q_i - q_j) = \prod_{k=1}^M \delta(q_i^k - q_j^k)\,.
\end{aligned} \tag{1.9}$$

Our goal is to rewrite (1.8) as a functional integral. To do so, the time interval is divided into N slices of duration ε. Thus, one may write:

[3] One simplifies the notation: $H(q,p) = H(q^1,...,q^M,p^1,...,p^M)$.

$$e^{-iHT} = \prod_{i=1}^{N} e^{-iH\varepsilon} \ .$$

Next, one just has to insert the following complete set of intermediate states q_i between each factor,

$$\mathbf{1} = \int dq_i \, |q_i\rangle \, \langle q_i| \ ,$$

which results in:

$$U(q_a, q_b; T) = \int dq_1 \, dq_2 ... dq_{N-1} \ \langle q_N| e^{-iH\varepsilon} |q_{N-1}\rangle \, \langle q_{N-1}| e^{-iH\varepsilon} |q_{N-2}\rangle ... \langle q_1| e^{-iH\varepsilon} |q_0\rangle \ .$$

Notice that the endpoints have been set as $q_0 = q_a$ and $q_N = q_b$. As one wishes to take the limit $\varepsilon \to 0$, the term $e^{-i\varepsilon H}$ may be considered as $1 - i\varepsilon H$. Now, let us consider the different possibilities of dependencies of the Hamiltonian:

The hamiltonian is solely a function of the coordinates

In that case, one gets

$$\langle q_{i+1}| H(q) |q_i\rangle = H(q_i)\delta(q_i - q_{i+1}) \ ,$$

which may be written as[4]

$$\langle q_{i+1}| H(q) |q_i\rangle = H\left(\frac{q_{i+1} + q_i}{2}\right) \int \frac{dp_i}{2\pi} \, e^{ip_i(q_{i+1} - q_i)} \ ,$$

using the integral definition of the multi-dimensional Dirac's Delta:

$$\delta(q_i - q_{i+1}) = \int \frac{dp_i}{2\pi} \, e^{ip_i(q_{i+1} - q_i)} \ .$$

The hamiltonian is purely a function of the momenta

In that case, one has to introduce a complete set of momentum eigenstates to get:

[4]The mid-point has been used for reasons to be apparent when Weyl ordering will be discussed. Notice that $\langle q_{j+1}|q_j\rangle = \delta(q_{j+1} - q_j) = \int \frac{dp_j}{2\pi} e^{ip_j(q_{j+1} - q_j)}$.

$$\langle q_{i+1}|H(p)|q_i\rangle = \int \frac{dp_i}{2\pi} H(p_i) e^{ip_i(q_{i+1}-q_i)} ,$$

where one used, in order to obtain it,

$$\langle q_\alpha | p_\beta \rangle = e^{ip_\beta q_\alpha} .$$

The Hamiltonian is of the form $H(q,p) = f(q) + g(p)$

Its matrix element follows directly from the previous considerations,

$$\langle q_{i+1}|H(q,p)|q_i\rangle = \int \frac{dp_i}{2\pi} H\left(\frac{q_{i+1}+q_i}{2}, p_i\right) e^{ip_i(q_{i+1}-q_i)} . \tag{1.10}$$

The Hamiltonian is Weyl ordered

The formula (1.10) must not hold in general, since the order of the products of coordinates and momenta matters on the left-hand side (H is an operator), but not on the right-hand side (H is just a function of numbers). However, for one specific ordering of the operators, the formula holds – Weyl ordering.

A Hamiltonian is said to be Weyl ordered if it contains all possible combinations of the products of coordinates and momenta (divided by the number of such possibilities).[5]

It can be shown (see Appendix B) that if the Hamiltonian is Weyl ordered then

$$\langle q_{i+1}| e^{-i\varepsilon H} |q_i\rangle = \int \frac{dp_i}{2\pi} e^{-i\varepsilon H\left(\frac{q_{i+1}+q_i}{2}, p_i\right)} e^{ip_i(q_{i+1}-q_i)} . \tag{1.11}$$

Let us, from now on, consider Weyl ordered Hamiltonians. One has the essencial tools to write the transition amplitude as a functional integral. One just has to multiply N factors of the form (1.11), one for each index i, and integrate over the intermediate coordinates q_i,

$$\begin{aligned} U(q_0,q_N;T) = &\int dq_1 ... dq_{N-1} \int dp_0 ... dp_{N-1} \frac{1}{(2\pi)^N} \\ &\times \exp\left[i \sum_i \left(p_i(q_{i+1}-q_i) - \varepsilon H\left(\frac{q_{i+1}+q_i}{2}, p_i\right)\right)\right] . \end{aligned} \tag{1.12}$$

[5]For instance, the following hamiltonian is Weyl ordered $H = 1/6\{q^2p^2 + pqpq + qpqp + qp^2q + pq^2p + p^2q^2\}$.

If the limit $N \to \infty$ is taken, the aforementioned approximates an integral over $q(t)$ and $p(t)$,

$$\begin{aligned}
&\int dq_1 ... dq_{N-1} \to \int \mathscr{D}q(t) \; ; \\
&\int dp_0 ... dp_{N-1} \frac{1}{(2\pi)^N} \to \int \mathscr{D}p(t) \; ; \\
&\frac{q_{i+1} - q_i}{\varepsilon} \to \dot{q}(i) \; ; \\
&\sum_i \varepsilon \to \int_0^T dt \; .
\end{aligned} \tag{1.13}$$

Then one defines

$$U(q_a, q_b; T) = \left(\prod_k \int \mathscr{D}q(t) \mathscr{D}p(t) \right) \exp \left[i \int_0^T dt \left(\sum_k p^k \dot{q}^k - H(q^k, p^k) \right) \right] \tag{1.14}$$

as the continuum version of (1.12), where $q(t=0) = q_a$ and $q(t=T) = q_b$. This is the most general formula for the formulation via functional integrals of the transition amplitude.

Let us apply the formula (1.14) to a field theory. Using (1.7), the transition amplitude may be written in terms of the Lagrangian density,

$$\langle \phi_b(\mathbf{x}) | \, e^{-iHT} \, | \phi_a(\mathbf{x}) \rangle = \int \mathscr{D}\phi \exp \left[i \int_0^T d^4x \mathscr{L} \right] \; . \tag{1.15}$$

1.3 Correlation Functions

The n-correlation function is defined as the average of n time ordered field operators at some given positions. Physically, it may be interpreted as the amplitude for propagation of a particle or excitation between spatial points. For the sake of simplicity, one starts with the 2-correlation function.

1.3.1 Derivation using Functional Integrals

One would like to compute $\langle \Omega | \, T \left[\phi_H(x_1) \phi_H(x_2) \right] | \Omega \rangle$, where we introduce the notation $|\Omega\rangle$ to represent the ground state; the subscript H in ϕ_H denotes the Heisenberg picture operator; T is the time-ordering symbol, which is related to the Heaviside step function via (for scalar fields)[6]

$$T(\phi(x)\phi(y)) = \theta(x^0 - y^0)\phi(x)\phi(y) + \theta(y^0 - x^0)\phi(y)\phi(x) \; . \tag{1.16}$$

[6]Notice that for fermions one has $T(\psi(x)\bar{\psi}(y)) = \theta(x^0 - y^0)\psi(x)\bar{\psi}(y) - \theta(y^0 - x^0)\bar{\psi}(y)\psi(x)$. See the definition of the Heaviside step function in *Notations and Conventions*.

Let us begin by considering the following boundary conditions $\phi(T,\mathbf{x}) = \phi_b(\mathbf{x})$ and $\phi(-T,\mathbf{x}) = \phi_a(\mathbf{x})$, for some ϕ_a and ϕ_b. Now, one decomposes $|\phi_a\rangle$ into eigenstates $|n\rangle$ of H. Thus, one obtains

$$e^{-iHT}|\phi_a\rangle = \sum_n e^{-iE_nT}|n\rangle\langle n|\phi_a\rangle = e^{-iE_0T}|\Omega\rangle\langle\Omega|\phi_a\rangle + \sum_{n=1} e^{-iE_nT}|n\rangle\langle n|\phi_a\rangle \ ,$$

where $E_0 := \langle\Omega|H|\Omega\rangle$. Notice that one has $E_0 < E_n \ \forall n \neq 0$, so that if the limit[7] $T \to \infty(1-i\varepsilon)$ is taken, one may write

$$\lim_{T\to\infty(1-i\varepsilon)} e^{-iHT}|\phi_a\rangle = \lim_{T\to\infty(1-i\varepsilon)} \langle\Omega|\phi_a\rangle e^{-iE_0T}|\Omega\rangle \ ,$$

which can be rewritten as

$$|\Omega\rangle = \lim_{T\to\infty(1-i\varepsilon)} \left(\langle\Omega|\phi_a\rangle e^{-iE_0T}\right)^{-1} e^{-iHT}|\phi_a\rangle \ .$$

Likewise, one has

$$\langle\Omega| = \lim_{T\to\infty(1-i\varepsilon)} \left(\langle\phi_b|\Omega\rangle e^{-iE_0T}\right)^{-1} \langle\phi_b| e^{-iHT} \ .$$

This decomposition into eigenstates of H allows us to write the 2-correlation function as:

$$\begin{aligned}\langle\Omega|T\left[\phi_H(x_1)\phi_H(x_2)\right]|\Omega\rangle = &\lim_{T\to\infty(1-i\varepsilon)} \left(\langle\phi_b|\Omega\rangle\langle\Omega|\phi_a\rangle e^{-2iE_0T}\right)^{-1} \\ &\times \langle\phi_b| e^{-iHT} T(\phi_H(x_1)\phi_H(x_2)e^{-iHT})|\phi_a\rangle \ .\end{aligned}$$

Now one switches from Heisenberg operators to Schrödinger ones using

$$\phi_H(x) = e^{iHx^0}\phi_S(\mathbf{x})e^{-iHx^0} \ . \tag{1.17}$$

[7]Notice that one has to introduce the slightly imaginary part $-i\varepsilon$ so that the exponencial has a real and negative exponent part. It is multiplied by an exponencial with an imaginary exponent, which, according to the Euler formula $e^{i\theta} = cos(\theta) + i\sin(\theta)$ is a sum of bounded functions.

Let us consider, without loss of generality, that $x_1^0 < x_2^0$. One may write

$$\langle\Omega|\, T\left[\phi_H(x_1)\phi_H(x_2)\right]|\Omega\rangle = \lim_{T\to\infty(1-i\varepsilon)} \beta(T)\,\langle\phi_b|\, e^{-iH(T-x_2^0)}\phi_S(\mathbf{x}_2) \\ \times e^{-iH(x_2^0-x_1^0)}\phi_S(\mathbf{x}_1)e^{-iH(x_1^0+T)})\,|\phi_a\rangle\ ,$$

where $\beta(T) = \left(\langle\phi_b|\Omega\rangle\,\langle\Omega|\phi_a\rangle\, e^{-2iE_0T}\right)^{-1}$. Now, one wishes to turn the Schrödinger operators into fields, so that one can use the completeness relations[8]. To do so, one just has to apply those operators onto the states,

$$\phi_S(\mathbf{x}_i)\,|\phi_i\rangle = \phi_i(\mathbf{x}_i)\,|\phi_i\rangle\,;\ i = 1,2\,. \tag{1.18}$$

Applying (1.18) and the completeness relation to our 2-correlation functions of the fields,

$$\langle\Omega|\, T\left[\phi_H(x_1)\phi_H(x_2)\right]|\Omega\rangle = \lim_{T\to\infty(1-i\varepsilon)} \beta(T)\int \mathscr{D}\phi_1(\mathbf{x})\int \mathscr{D}\phi_2(\mathbf{x})\phi_1(\mathbf{x}_1)\phi_2(\mathbf{x}_2) \\ \times\,\langle\phi_b|\, e^{-iH(T-x_2^0)}\,|\phi_2\rangle\,\langle\phi_2|\, e^{-iH(x_2^0-x_1^0)}\,|\phi_1\rangle\,\langle\phi_1|\, e^{-iH(x_1^0+T)})\,|\phi_a\rangle\ .$$

Now, notice that one may relate

$$\int\limits_{\substack{\phi(x_1^0,\mathbf{x})=\phi_1(\mathbf{x})\\ \phi(x_2^0,\mathbf{x})=\phi_2(\mathbf{x})}} \mathscr{D}\phi(x)\exp\left[\int_{-T}^{T} d^4x\mathscr{L}(\phi)\right] = \langle\phi_b|\, e^{-iH(T-x_2^0)}\,|\phi_2\rangle \\ \times\,\langle\phi_2|\, e^{-iH(x_2^0-x_1^0)}\,|\phi_1\rangle\,\langle\phi_1|\, e^{-iH(x_1^0+T)})\,|\phi_a\rangle\ ,$$

for one has three transition amplitudes: one for $t\in[-T,x_1^0]$, one for $t\in[x_1^0,x_2^0]$ and one for $t\in[x_2^0,T]$. Using the previous relation, the correlation function may be written as

$$\langle\Omega|\, T\left[\phi_H(x_1)\phi_H(x_2)\right]|\Omega\rangle = \lim_{T\to\infty(1-i\varepsilon)} \beta(T)\int \mathscr{D}\phi_1(\mathbf{x})\int \mathscr{D}\phi_2(\mathbf{x})\phi_1(\mathbf{x}_1)\phi_2(\mathbf{x}_2) \\ \times \int\limits_{\substack{\phi(x_1^0,\mathbf{x})=\phi_1(\mathbf{x})\\ \phi(x_2^0,\mathbf{x})=\phi_2(\mathbf{x})}} \mathscr{D}\phi(x)\exp\left[\int_{-T}^{T} d^4x\mathscr{L}(\phi)\right]\ .$$

Now, one just has to notice that the fields $\phi_1(\mathbf{x}_1)$ and $\phi_2(\mathbf{x}_2)$ can be taken inside the main integral and be written as $\phi_1(x)$ and $\phi_2(x)$, respectively. Then, the three integrals may be

[8] $\int \mathscr{D}\phi_i\,|\phi_i\rangle\,\langle\phi_i| = \mathbf{1}; i = 1,2.$

written as one, and finally, one may write,

$$\langle\Omega|\,T\left[\phi_H(x_1)\phi_H(x_2)\right]|\Omega\rangle = \lim_{T\to\infty(1-i\varepsilon)}\beta(T)\int\mathscr{D}\phi(x)\phi(x_1)\phi(x_2) \times\exp\left[i\int_{-T}^{T}d^4x\mathscr{L}(\phi)\right].$$

One would like to get rid of $\beta(T)$. To do so, one just has to apply the following, remembering that it can be obtained retracing the same steps, excluding the fields from the integrand,

$$\langle\Omega|\Omega\rangle = 1 = \lim_{T\to\infty(1-i\varepsilon)}\beta(T)\int\mathscr{D}\phi(x)\exp\left[i\int_{-T}^{T}d^4x\mathscr{L}(\phi)\right]. \tag{1.19}$$

Finally, dividing by the aforementioned expression, one finds that the correlation functions is

$$\langle\Omega|\,T\left[\phi_H(x_1)\phi_H(x_2)\right]|\Omega\rangle = \lim_{T\to\infty(1-i\varepsilon)}\frac{\int\mathscr{D}\phi(x)\phi(x_1)\phi(x_2)\exp\left[i\int_{-T}^{T}d^4x\mathscr{L}(\phi)\right]}{\int\mathscr{D}\phi(x)\exp\left[i\int_{-T}^{T}d^4x\mathscr{L}(\phi)\right]}.$$

This is the 2-correlation function. This formula may be generalized quite naturally using the same reasoning as for the 2-correlation function,

$$\langle\Omega|\,T\mathscr{O}(\phi)\,|\Omega\rangle = \lim_{T\to\infty(1-i\varepsilon)}\frac{\int\mathscr{D}\phi(x)\mathscr{O}(\phi)\exp\left[i\int_{-T}^{T}d^4x\mathscr{L}(\phi)\right]}{\int\mathscr{D}\phi(x)\exp\left[i\int_{-T}^{T}d^4x\mathscr{L}(\phi)\right]}. \tag{1.20}$$

where $\mathscr{O}$ is a general operator containing some field operators ϕ.

1.3.2 Generating Functional

To conclude this topic about correlation functions, one may introduce a different method for computing correlation functions based on functional derivatives. Let us define the functional derivative of a functional $F[f]$. Notice that a functional $F[f]$ may be considered just as a function defined on a variable f which is an ordinary function, so that one may define a gradient derivative $(\delta F/\delta f(x_0))[f]$ in the direction of a Dirac delta density,

$$\frac{\delta F[f]}{\delta f(x_0)} = \lim_{\varepsilon\to 0}\frac{F[f(x)+\varepsilon\delta(x-x_0)]-F[f(x)]}{\varepsilon}. \tag{1.21}$$

This is a generalization of the definition of derivatives from usual calculus with functions. Next, let us introduce the generating functional of correlation functions, $Z[J]$ which is, in a

scalar field theory, defined as[9]

$$Z[J] := \int \mathscr{D}\phi \exp\left[i \int d^4x [\mathscr{L} + J(x)\phi(x)] \right] . \tag{1.22}$$

where $J(x)\phi(x)$ is a source term. The correlation function may then be written as a product of derivatives (one for each scalar field) of the generating functional, using the definition of the derivative of a functional,

$$\langle \Omega | T [\phi(x_1)...\phi(x_N)] | \Omega \rangle = Z[J]^{-1} \left(-i \frac{\delta}{\delta J(x_1)} \right) ... \left(-i \frac{\delta}{\delta J(x_N)} \right) Z[J] \Big|_{J=0} . \tag{1.23}$$

1.4 Summary

In short, so far one has used a functional integral approach to derive the expression of transition amplitudes,

$$\langle \phi_b(x) | e^{-iHT} | \phi_a(x) \rangle = \int \mathscr{D}\phi \exp\left[i \int_0^T d^4x \mathscr{L} \right] ,$$

and derived a general formula to compute correlation functions,

$$\langle \Omega | T \mathscr{O}(\phi) | \Omega \rangle = \lim_{T \to \infty(1-i\varepsilon)} \frac{\int \mathscr{D}\phi(x) \mathscr{O}(\phi) \exp\left[i \int_{-T}^{T} d^4x \mathscr{L}(\phi) \right]}{\int \mathscr{D}\phi(x) \exp\left[i \int_{-T}^{T} d^4x \mathscr{L}(\phi) \right]} , \tag{1.24}$$

and finally, expressed the aforementioned in terms of a generating functional,

$$\langle \Omega | T [\phi(x_1)...\phi(x_N)] | \Omega \rangle = Z[J]^{-1} \left(-i \frac{\delta}{\delta J(x_1)} \right) ... \left(-i \frac{\delta}{\delta J(x_N)} \right) Z[J] \Big|_{J=0}$$

in which the generating functional is defined as

$$Z[J] := \int \mathscr{D}\phi \exp\left[i \int d^4x [\mathscr{L} + J(x)\phi(x)] \right] . \tag{1.25}$$

[9] Recall that the time variable of integration runs from $-T$ to T, with $T \to \infty(1 - i\varepsilon)$.

Chapter 2

Quantum Chromodynamics

Quantum Chromodynamics is the theory of quarks and gluons. It is a non-Abelian gauge theory with gauge group $SU(3)$. Two important properties of the strong interactions are the asymptotic freedom and confinement. It was shown that the only asymptotically free field theories in four dimensions are the non-Abelian gauge theories [39]. These may be viewed as a generalization of Quantum Electrodynamics.

For further informations on the derivation of the Yang-Mills Lagrangian, one would recommend [36]. In order to acquire a better understanding on the subject of the quantization of non-abelian gauge theories via the method of Faddeev-Popov, one would recommend [36], [37] and, of course, [40]. The derivation of the tree-level expressions for the gluon and ghost propagators and three-vertex gluon was based on [41], [42] and [43]. The derivation of the full gluon and ghost propagators was based on [43] and [44]. The discussion about regularization and renormalization was based on [43–45]. The derivation of the general form of the three-gluon vertex was introduced in [35].

2.1 Gauge Invariance: The Yang-Mills Lagrangian

Let us start by considering the Lagrangian describing Quantum Electrodynamics, which is a sum of three parts[1],

$$\begin{aligned}\mathscr{L}_{QED} =& \mathscr{L}_{Dirac} + \mathscr{L}_{Maxwell} + \mathscr{L}_{int} \\ &= \bar{\psi}(i\partial\!\!\!/ - m)\psi - \frac{1}{4}(F_{\mu\nu})^2 + Q\bar{\psi}\gamma^{\mu}\psi A_{\mu} \ ,\end{aligned}$$

[1] Do not worry if you are not familiar with this Lagrangian, for one can reformulate the whole theory using the gauge invariance as a fundamental principle. One just has to retrace the steps used for the case of non-abelian gauge theories, to the case of the gauge group $U(1)$.

where ψ is the Dirac field, A_μ is the electromagnetic vector potential, Q is the fermion charge, and $F_{\mu\nu}$ is the electromagnetic field tensor, which is given by $F_{\mu\nu} = \partial_\mu A_\nu - \partial_\nu A_\mu$, and $\not{\partial} = \gamma^\mu \partial_\mu$. One property of the QED Lagrangian is that it is invariant under the so-called gauge transformations

$$\psi(x) \to e^{i\alpha(x)}\psi(x), \quad A_\mu \to A_\mu + \frac{1}{Q}\partial_\mu \alpha(x) \,, \tag{2.1}$$

which corresponds to a local phase rotation on the Dirac field. In order to derive the Yang-Mills Lagrangian, one will generalize this invariance under local phase rotations to invariance under any continuous symmetry group[2].

Let us begin with any continuous group of transformations, depicted by a set of $n \times n$ unitary matrices V (one is interested in non-abelian theories corresponding to $SU(N)$, for Quantum Chromodynamics is defined on the gauge group $SU(3)$). Thus the fields $\psi(x)$ form an n-plet, transforming according to

$$\psi(x) \to V(x)\psi(x) \,, \tag{2.2}$$

noticing that the dependence of V on x makes the transformation local. In infinitesimal form, $V(x)$ may be expanded in terms of the generators of the symmetry group, which can be depicted as hermitian matrices t^a,

$$V(x) = 1 + i\alpha^a(x)t^a + \mathscr{O}(\alpha^2) \,. \tag{2.3}$$

In order to include terms that contains derivatives to the Lagrangian, a covariant derivative must be defined, since the fields that are subtracted on a usual derivative,

$$n^\mu \partial_\mu \psi = \lim_{\varepsilon \to 0} \frac{1}{\varepsilon}\left[\psi(x + \varepsilon n) - \psi(x)\right] \tag{2.4}$$

have completely different transformations under the symmetry (2.2). One ought to find a way to introduce a factor that compensates for the difference in gauge transformations of those two fields. One may define a quantity $U(y,x)$ (a comparator) that depends on the two points and transforms according to

$$U(y,x) \to V(y)U(y,x)V^\dagger(x) \,. \tag{2.5}$$

[2]Notice that the designation of non-abelian gauge theories comes from the fact that this generalization brings non-abelian objects, namely, a continuous symmetry group.

Of course, this scalar quantity must do nothing if the points are the same, so let us set $U(y,y) = 1$. Hence one can define a sensible derivative, designated as covariant derivative, as follows,

$$n^\mu D_\mu \psi = \lim_{\varepsilon \to 0} \frac{1}{\varepsilon} \left[\psi(x+\varepsilon n) - U(x+\varepsilon n, x)\psi(x) \right] . \tag{2.6}$$

At points in which $x \neq y$, $U(y,x)$ may be restricted to a unitary matrix. Thus any matrix near $U = \mathbf{1}$ may be expanded in terms of the Hermitian generators of $SU(N)$. One is interested in such a case, for one is dealing with a subtraction of fields with infinitesimal separation, and therefore, U may be written as (assuming that the comparator is a continuous function of x and y),

$$U(x+\varepsilon n, x) = 1 + \varepsilon n^\mu \partial_\mu^i U(x+\varepsilon n, x)\big|_{\varepsilon=0} t^i + \mathscr{O}(\varepsilon^2) . \tag{2.7}$$

Next, $\partial_\mu^i U(x+\varepsilon n, x)\big|_{\varepsilon=0} t^i$ is rewritten as $igA_\mu^i t^i$, where A_μ^i are gauge fields, one for each generator, and g is a constant (analogous to the electric charge for the case of QED). Inserting this expression into (2.6), the following expression for the covariant derivative is obtained,

$$D_\mu = \partial_\mu - igA_\mu^a t^a . \tag{2.8}$$

It can be shows that the transformation law for A_μ^a is [36],

$$A_\mu^a(x) t^a \to A_\mu^V(x) = V(x) \left(A_\mu^a(x) t^a + \frac{i}{g} \partial_\mu \right) V^\dagger(x) . \tag{2.9}$$

On the other hand, it can be shown as well that the infinitesimal transformation laws for ψ and A_μ^a are [36]

$$\begin{aligned} &\psi \to (1 + i\alpha^a t^a)\psi ; \\ &A_\mu^a \to A_\mu^a + \tfrac{1}{g}\partial_\mu \alpha^a + f^{abc} A_\mu^b \alpha^c , \end{aligned} \tag{2.10}$$

where f^{abc} is a set of numbers called structure constants and comes from $[t^a, t^b] = if^{abc}t^c$. Using these transformations laws, one may verify that the covariant derivative of ψ has the same transformation law of ψ itself.

To complete the construction of a Lagrangian which is locally invariant under any continuous symmetry group, one must find a kinetic energy term for the gauge fields A_μ, i.e., a term depending only on A_μ and its derivatives. As it has been discussed before, the covariant derivative has the same transformation law of that of the field itself. The same conclusion

holds for the second covariant derivative and, more generally, for the commutator of covariant derivatives,

$$[D_\mu, D_\nu]\psi(x) \to e^{i\alpha(x)}[D_\mu, D_\nu]\psi(x) \; .$$

However, notice that the commutator is not itself a derivative,

$$[D_\mu, D_\nu] = -igF^a_{\mu\nu}t^a \; , \tag{2.11}$$

with,

$$F^a_{\mu\nu} = \partial_\mu A^a_\nu - \partial_\nu A^a_\mu + g f^{abc} A^b_\mu A^c_\nu \; . \tag{2.12}$$

On the other hand, the field strength is not itself gauge-invariant. However, it may be turned into one, in the following way,

$$\mathscr{L} = -\frac{1}{2}\mathrm{tr}\left[(F^a_{\mu\nu}t^a)^2\right] = -\frac{1}{4}(F^a_{\mu\nu})^2 \; . \tag{2.13}$$

One has the essencial ingredients to construct the most general locally invariant Lagrangian for the fermion field ψ and the gauge field A_μ. This general Lagrangian ought to be a function of ψ and its covariant derivatives, include the kinetic energy term for the gauge fields A_μ, so one gets a generalization of the QED Lagrangian density function,

$$\mathscr{L}_{\mathrm{YM}} = \bar{\psi}(i\not{D} - m)\psi - \frac{1}{4}(F^a_{\mu\nu})^2 \; . \tag{2.14}$$

This is the Yang-Mills Lagrangian.

2.2 Quantization of Non-Abelian Gauge Theories

2.2.1 Faddeev-Popov Method

Let us consider the gauge fields A_μ, and their Lagrangian $\mathscr{L} = (-\frac{1}{4}F^a_{\mu\nu})^2$. Recall that in order to compute correlation functions (Cf. equation (1.24)), one has to perform on the denominator an integral of the form:

$$\int \mathscr{D}A \, e^{iS[A]} \; . \tag{2.15}$$

Given any gauge field A_μ, a gauge orbit may be defined as the set of all gauge fields related to the first by a gauge transformation (Cf. eq. (2.9)). Due to gauge-invariance, the functional integral is badly defined, for one is redundantly integrating over physically equivalent field

configurations – the integrand is constant on the gauge orbits and, therefore, the integral is proportional to the infinite volume of these gauge orbits. To fix this problem, one would like to isolate the part of the integral consisting of non-physically equivalent fields. To this end, the Faddeev-Popov Method may be used. In order to integrate over each orbit once, a hypersurfaces which intersects each orbit just once is defined. Let $G(A) = 0$ be the equation that defines such hypersurface. The condition $G(A) = 0$ is known as gauge condition and this procedure as gauge-fixing. This means that even if some gauge field A_μ does not intersect the hypersurface, there is one (unique[3]) gauge transformed field that does.

In order to consider only the gauge fields that satisfy the gauge condition one inserts a functional delta function[4] $\delta\left(G(A)\right)$. One is allowed to do so if 1 is inserted under the integral, using the following identity,

$$1 = \int \mathscr{D}\alpha(x)\delta\left(G(A^\alpha)\right)\det\left(\frac{\delta G(A^\alpha)}{\delta\alpha}\right), \tag{2.16}$$

where A^α is the gauge-transformed field, which may be written in the infinitesimal form as (Cf. (2.10)),

$$(A^\alpha)^a_\mu = A^a_\mu + \frac{1}{g}D_\mu\alpha^a\,. \tag{2.17}$$

Notice that (2.16) is the continuum generalization of the identity[5],

$$1 = \left(\prod_i \int da_i\right)\delta^{(n)}\left(\mathbf{g}(\mathbf{a})\right)\det\left(\frac{\partial g_i}{\partial a_j}\right) \tag{2.18}$$

for discrete n-dimensional vectors. One considers linear gauge-fixing functions $G(A)$, so that its functional derivative $\delta G(A^\alpha/\delta\alpha)$ is independent of α. Then A is replaced by $A' = A^\alpha$ in the exponential of (2.15) (Notice that by gauge invariance $S[A] = S[A^\alpha]$). Notice that this transformation is just a linear shift of the A^a_μ proceeded by a unitary rotation of the different components of $A^a_\mu(x)$ at each point x, which both preserves the measure

$$\mathscr{D}A = \prod_x \prod_{a,\mu} dA^a_\mu\ . \tag{2.19}$$

[3]This is true in perturbation theory. Notice that in the case of a non-perturbative approach, Gribov copies have to be considered. See section 3.4 for further informations on Gribov copies.

[4]One could see it as an infinite product of delta functions, one for each point x.

[5]Which is itself a generalization of $\int \delta(f(x))\left|\frac{df}{dx}\right|_{x_0} dx = 1$.

Therefore, $\mathscr{D}A = \mathscr{D}A'$. At the moment, renaming A' back to A and factoring out the integral over α into an overall normalization, one has

$$\int \mathscr{D}A e^{iS[A]} = \int (\mathscr{D}\alpha) \int \mathscr{D}A e^{iS[A]} \delta(G(A)) \det\left(\frac{\delta G(A^\alpha)}{\delta\alpha}\right) . \tag{2.20}$$

To go any further one must indicate a gauge-fixing function $G(A)$, which one chooses to be the general class of functions

$$G(A) = \partial^\mu A_\mu(x) - \imath(x) . \tag{2.21}$$

The equality (2.20) holds for any $\imath(x)$, so it must hold, most generally, if the right-hand side is replaced by a properly normalized linear combination using different functions $\imath(x)$. Thus one can integrate over all $\imath(x)$, with a Gaussian function centered on $\imath = 0$. Using the generalized Dirac delta $\delta(\partial^\mu A_\mu - \imath(x))$ this integral may be performed, leaving us with[6],

$$\int \mathscr{D}A e^{iS[A]} = N(\xi) \int \mathscr{D}\alpha \int \mathscr{D}A\, e^{iS[A]} \exp\left[-i\int d^4x \frac{1}{2\xi}(\partial^\mu A_\mu)^2\right] \det\left(\frac{\delta G(A^\alpha)}{\delta\alpha}\right) ,$$

where $N(\xi)$ is a normalization constant which is irrelevant. Notice that the same manipulations can be performed on the numerator of the correlation function formula (eq. 1.24), as long as the operator $\mathscr{O}(A)$ is gauge invariant[7].

The functional derivative $\delta G(A^\alpha)/\delta\alpha$ may be evaluated by means of (2.17),

$$\frac{\delta G(A^\alpha)}{\delta\alpha} = \frac{1}{g}\partial^\mu D_\mu . \tag{2.22}$$

This operator depends on A, therefore the functional determinant of the aforementioned expression will add some new terms to the Lagrangian. This determinant may be represented as a functional integral taken over a set of Grassmann fields [8] using the following identity,

$$\det\left(\frac{1}{g}\partial^\mu D_\mu\right) = \int \mathscr{D}c\mathscr{D}\bar{c} \exp\left[i\int d^4x \bar{c}(-\partial^\mu D_\mu)c\right] , \tag{2.23}$$

where the factor $1/g$ was absorbed into the normalization of the integral. Notice, however, that these fields do not represent any physical particles for they have the wrong relation between statistics and spin - they are merely a mathematical artifact. These ficticious particles

[6] One has inserted the gaussian weighting function $\int \mathscr{D}\imath \exp\left[-i\int d^4x \frac{\omega^2}{2\xi}\right]$.

[7] If this is not true, one may not change A to A^α.

[8] One introduces in Appendix C the Grassmann variables.

are known as the Faddeev-Popov ghosts. Thus, one finishes with

$$\langle\Omega|\,T\mathscr{O}(\phi)\,|\Omega\rangle = \lim_{T\to\infty(1-i\varepsilon)} \frac{\int \mathscr{D}c\mathscr{D}\bar{c}\int \mathscr{D}A\mathscr{O}(A)\exp\left[i\int_{-T}^{T}d^4x\left[\mathscr{L}-\frac{1}{2\xi}(\partial^\mu A_\mu)^2+\bar{c}(-\partial^\mu D_\mu)c\right]\right]}{\int \mathscr{D}c\mathscr{D}\bar{c}\int \mathscr{D}A\exp\left[i\int_{-T}^{T}d^4x\left[\mathscr{L}-\frac{1}{2\xi}(\partial^\mu A_\mu)^2+\bar{c}(-\partial^\mu D_\mu)c\right]\right]}\,.$$

From this, a new Lagrangian, which counts these new terms due to the quantization of non-abelian gauge theories, may be written, called the Faddeev-Popov Lagrangian,

$$\mathscr{L} = \bar{\psi}(i\not{D}-m)\psi - \frac{1}{4}(F^i_{\mu\nu})^2 - \frac{1}{2\xi}(\partial^\mu A^a_\mu)^2 + \bar{c}^a(-\partial^\mu D^{ac}_\mu)c^c\,. \tag{2.24}$$

2.3 Perturbation Theory

The exact computation of correlation functions is often not possible. However, if the coupling constant is sufficiently small, perturbation theory may be used. Let us consider the Lagrangian without fermions,

$$\mathscr{L} = -\frac{1}{4}(F^i_{\mu\nu})^2 - \frac{1}{2\xi}(\partial^\mu A^a_\mu)^2 + c^a(-\partial^\mu D^{ac}_\mu)c^c = \mathscr{L}_{gluon}+\mathscr{L}_{ghost}\,, \tag{2.25}$$

where $\mathscr{L}_{gluon} = -\frac{1}{4}(F^i_{\mu\nu})^2 - \frac{1}{2\xi}(\partial^\mu A^a_\mu)^2$ is the part of the Lagrangian which depends on the gauge field, and $\mathscr{L}_{ghost} = c^a(-\partial^\mu D^{ac}_\mu)c^c$ is the part of the Lagrangian which depends on the ghost fields. The gluon part of the Lagrangian may be rewritten more explicitly as

$$\begin{aligned}\mathscr{L}_{gluon} = {}& \frac{1}{2}A^a_\mu\left(\partial^2 g^{\mu\nu}-\left(1-\frac{1}{\xi}\right)\partial^\mu\partial^\nu\right)A^a_\nu - \frac{1}{2}\partial_\mu\left[A_{a\nu}\left(\partial^\mu A^{a\nu}-\partial^\nu A^{a\mu}\right)\right]\\ & -\frac{1}{2\xi}\partial^\mu(A^a_\mu\partial^\nu A^a_\nu) - gf^{abc}(\partial^\mu_x A^\nu_a)A_{b\mu}A_{c\nu} - \frac{1}{4}g^2 f^{eab}f^{ecd}A^a_\mu A^b_\nu A^{c\mu}A^{d\nu}\,.\end{aligned}$$

The terms $-\frac{1}{2}\partial_\mu\left[A_{a\nu}\left(\partial^\mu A^{a\nu}-\partial^\nu A^{a\mu}\right)\right]$ and $-\frac{1}{2\xi}\partial^\mu(A_\mu\partial^\nu A_\nu)$, may be turned into a surface term which one ignores (notice that the correlation function depends on the action, in which these mentioned terms may be ignored).

On the other hand, the ghost part may be rewritten as

$$\mathscr{L}_{\text{ghost}} = c^a(-\partial^2\delta^{ac} - g\partial^\mu f^{abc}A^b_\mu)c^c\,. \tag{2.26}$$

Then the lagrangian $\mathscr{L}$ is decomposed into two parts: one containing the quadractic terms on the fields, denoted by $\mathscr{L}_0$, and another containing the remaining ones, denoted by $\mathscr{L}_I$, i.e.,

$$\mathscr{L}_0 = \int d^4x A^a_\mu \left(\partial^2 g^{\mu\nu} - \left(1 - \frac{1}{\xi}\right)\partial^\mu\partial^\nu\right) A^a_\nu + \int d^4x c^a(-\partial^2\delta^{ac})c^c \tag{2.27}$$

and,

$$\begin{aligned}\mathscr{L}_1 = &\int d^4x(-gf^{abc}(\partial^\mu A^\nu_a)A_{b\mu}A_{c\nu} - \frac{1}{4}g^2 f^{eab}f^{ecd}A^a_\mu A^b_\nu A^{c\mu}A^{d\nu}) + \\ &\int d^4x(c^a(-g\partial^\mu f^{abc}A^b_\mu)c^c)\ .\end{aligned} \tag{2.28}$$

On the correlation function (see (1.20)) one has factors of the form

$$e^{i\int d^4x\mathscr{L}} = e^{i\int d^4x\mathscr{L}_0 + \int d^4x\mathscr{L}_I} = e^{i\int d^4x\mathscr{L}_I}e^{i\int d^4x\mathscr{L}_0} \tag{2.29}$$

and then assuming g is small the exponencial $e^{i\int d^4x\mathscr{L}_I}$ is expanded as

$$e^{i\int d^4x\mathscr{L}} = \left(1 + i\int d^4x\mathscr{L}_I + ...\right)e^{i\int d^4x\mathscr{L}_0}\ . \tag{2.30}$$

2.3.1 The Gluon and Ghost Propagators

In this thesis, one is interested on the gluon and ghost propagators. Only the derivation of the gluon propagator will be presented. The one for the ghost propagator follows from similar considerations. The gluon propagator is defined as the 2-correlation function of the gauge field,

$$D^{ab}_{\mu\nu}(x-y) = \langle A^a_\mu(x)A^b_\nu(y)\rangle = \lim_{T\to\infty(1-i\varepsilon)} \frac{\int \mathscr{D}A\, A^a_\mu(x)A^b_\nu(y)\exp\left[i\int_{-T}^{T} d^4x\mathscr{L}\right]}{\int \mathscr{D}A\exp\left[i\int_{-T}^{T} d^4x\mathscr{L}\right]}\ . \tag{2.31}$$

In the lowest order perturbation theory[9], one has

$$D^{ab}_{\mu\nu}(x-y) = \frac{\int \mathscr{D}A\, A^a_\mu(x)A^b_\nu(y)\exp\left[\frac{1}{2}i\int_{-T}^{T} d^4x A^c_\mu(x)\left(\partial^2 g^{\mu\nu} - \left(1-\frac{1}{\xi}\right)\partial^\mu\partial^\nu\right)A^c_\nu(x)\right]}{\int \mathscr{D}A\exp\left[\frac{1}{2}i\int_{-T}^{T} d^4x A^c_\mu(x)\left(\partial^2 g^{\mu\nu} - \left(1-\frac{1}{\xi}\right)\partial^\mu\partial^\nu\right)A^c_\nu(x)\right]}\ . \tag{2.32}$$

[9] In this case, the lowest order perturbation theory gives the first term of the expansion of the exponencial (2.30).

Before going any further, one may introduce the expression for the ratio between functional gaussian integrals for the same matrix B (which is deduced in the Appendix B)

$$\frac{(\prod_k \int d\xi_k) \exp\left[-\frac{1}{2}\sum_{ij}\xi_i B_{ij}\xi_j\right]\xi_m\xi_n}{(\prod_k \int d\xi_k) \exp\left[-\frac{1}{2}\sum_{ij}\xi_i B_{ij}\xi_j\right]} = (B)^{-1}_{mn} \,. \tag{2.33}$$

The 2-correlation function has precisely this form. From this, one may find the propagator solving the following equation,

$$\left(\partial^2 g_{\mu\nu} - \left(1-\frac{1}{\xi}\right)\partial_\mu\partial_\nu\right) D^{\nu\rho}_{ab}(x-y) = i\delta^\rho_\mu \delta^{ab}\delta^{(4)}(x-y) \,. \tag{2.34}$$

Then one performs a Fourier transform on the gluon propagator as

$$D^{ab}_{\mu\nu}(x,y) = \int \frac{d^4k}{(2\pi)^4} e^{-ik(x-y)} \tilde{D}^{ab}_{\mu\nu}(k) \,, \tag{2.35}$$

which results in

$$\left(-k^2 g_{\mu\nu} + \left(1-\frac{1}{\xi}\right)k_\mu k_\nu\right)\tilde{D}^{\nu\rho}_{ab}(k) = i\delta^\rho_\mu\delta^{ab} \,. \tag{2.36}$$

This has as its solution,

$$\tilde{D}^{\mu\nu}_{ab}(k) = \frac{-i}{k^2+i\varepsilon}\left(g^{\mu\nu} - (1-\xi)\frac{k^\mu k^\nu}{k^2}\right)\delta^{ab} \,. \tag{2.37}$$

The ghost propagator is defined as the 2-correlation function of the ghost fields. The same manipulations may be performed for its computation, which leads us to the following expression for the case of the lowest order perturbation theory,

$$\tilde{G}^{\mu\nu}_{ab}(k) = \frac{i}{k^2}\delta^{ab} \,. \tag{2.38}$$

2.3.2 Three-Gluon Vertex

In the previous subsection, the perturbative results for the gluon and ghost propagators were derived. One is also interested in the three-gluon vertex, which is described in the 3-correlation function of the gauge fields,

$$\langle A^a_\alpha(x_1)A^b_\beta(x_2)A^c_\gamma(x_3)\rangle = \frac{\int \mathscr{D}\mathscr{A}\, A^a_\alpha(x_1)A^b_\beta(x_2)A^c_\gamma(x_3)e^{i\int d^4x\mathscr{L}}}{\int \mathscr{D}\mathscr{A}\, e^{i\int d^4x\mathscr{L}}} \,. \tag{2.39}$$

Notice that the first term of the expansion (2.30) makes the numerator of (2.39) vanish, for it gets an odd integrand, therefore, for the numerator, $e^{i\int d^4x\mathscr{L}_I} \approx i\int d^4x\mathscr{L}_I$ is used. For the denominator, one may continue to use $e^{i\int d^4x\mathscr{L}_I} \approx 1$. Therefore, one has

$$\begin{aligned}&\langle A^a_\alpha(x_1)A^b_\beta(x_2)A^c_\gamma(x_3)\rangle = \\ &-igf^{lmn}\frac{\int \mathscr{D}\mathscr{A}\ \int d^4x(\partial^\mu A^{l\nu}(x))A^m_\mu(x)A^n_\nu(x)A^a_\alpha(x_1)A^b_\beta(x_2)A^c_\gamma(x_3)e^{i\int d^4x\mathscr{L}^{gl}_0}}{\int \mathscr{D}\mathscr{A}\ e^{i\int d^4x\mathscr{L}^{gl}_0}}\,,\end{aligned} \tag{2.40}$$

which may be rewritten as,

$$\begin{aligned}&\langle A^a_\alpha(x_1)A^b_\beta(x_2)A^c_\gamma(x_3)\rangle = \\ &-igf^{lmn}g^{\mu\sigma}g^{\nu\tau}\frac{\int \mathscr{D}\mathscr{A}\ \int d^4x(\partial_\sigma A^l_\tau(x))A^m_\mu(x)A^n_\nu(x)A^a_\alpha(x_1)A^b_\beta(x_2)A^c_\gamma(x_3)e^{i\int d^4x\mathscr{L}^{gl}_0}}{\int \mathscr{D}\mathscr{A}\ e^{i\int d^4x\mathscr{L}^{gl}_0}}\,.\end{aligned} \tag{2.41}$$

In order to solve this expression, the following generalization of [10] (2.33) may be used,

$$\frac{(\prod_k\int d\xi_k)\exp\left[-\frac{1}{2}\xi_iB_{ij}\xi_j\right]\,\xi_1\ldots\xi_N}{(\prod_k\int d\xi_k)\exp\left[-\frac{1}{2}\xi_iB_{ij}\xi_j\right]} = \sum_{\text{pairings}}\prod_{\text{pairs}}(B)^{-1}_{\text{index pair}} \tag{2.42}$$

if N is even. Otherwise, one has an odd integrand on the numerator, then the integral vanishes. Applying this formula, one sees that there are six non-vanishing terms, which correspond to the 3! ways of pairing the three fields due to interaction with the other three. However, notice that these terms differ from one another by interchanging

$$(l,\alpha,x_1)\quad(m,\beta,x_2)\quad(n,\gamma,x_3)\,. \tag{2.43}$$

Thus, one may compute only one of the terms and then use symmetry to retrieve the others. Let us consider the following pairing of terms,

$$\overbrace{A^m_\mu(x)A^a_\alpha(x_1)}\overbrace{A^n_\nu(x)A^b_\beta(x_2)}\partial_\sigma\overbrace{A^l_\tau(x)A^c_\gamma(x_3)}\,.$$

Then the formula (2.42) gives,

$$-igf^{abc}g^{\mu\sigma}g^{\nu\tau}\int d^4xD^{am}_{\mu\alpha}(x-x_1)D^{nb}_{\nu\beta}(x-x_2)\partial_\sigma D^{lc}_{\tau\gamma}(x-x_3)\,. \tag{2.44}$$

[10] The derivation of this expression is described in Appendix B.

Applying the Fourier transform, in order to have the aforementioned result in the momentum space[11],

$$-gf^{abc}g^{\nu\tau}\delta(k_1+k_2+k_3)(2\pi)^4 k_3^{\mu}\tilde{D}^{am}_{\mu\alpha}(k_1)\tilde{D}^{nb}_{\nu\beta}(k_2)\tilde{D}^{lc}_{\tau\gamma}(k_3)\ . \tag{2.45}$$

By interchanging indices and taking into account the antisymmetry of f^{abc}, the perturbative 3-point correlation function may be found,

$$\langle A^a_\alpha(k_1)A^b_\beta(k_2)A^c_\gamma(k_3)\rangle = (2\pi)^4\delta(k_1+k_2+k_3)\tilde{D}^{am}_{\mu\alpha}(k_1)\tilde{D}^{nb}_{\nu\beta}(k_2)\tilde{D}^{lc}_{\tau\gamma}(k_3)\Gamma^{abc}_{\nu\tau\sigma} \tag{2.46}$$

where,

$$\Gamma^{abc}_{\alpha\beta\gamma} = gf^{abc}\left[g^{\nu\mu}(k_3-k_2)^{\tau}+g^{\mu\tau}(k_2-k_1)^{\nu}+g^{\tau\nu}(k_1-k_3)^{\mu}\right]\ . \tag{2.47}$$

2.4 Full Propagators

In section 2.3.1 the Feynman rules for the gluon and ghost propagators were derived. However, one dealt only with tree-level processes, i.e., without loops. To correct these expressions, one has to consider loops. For the gluon propagator, this means considering the vacuum polarization (also known as gluon self-energy). It can be regarded as a modification to the gluon structure by considering virtual fermion-antifermion pairs. As one may see in [36], the n-correlation function is the sum of all connected diagrams with n external points. One defines the one-particle irreducible (1PI) diagram as any diagram that cannot be separated in two by removing a single line. Let us denote their sum by $\Pi^{ab}_{\mu\nu}$ (the gluon self-energy). Therefore the most general case is that of a sum of diagrams as depicted in Fig. 2.1. Thus, one may relate the tree-level gluon propagator to the full one using the following[12],

$$\begin{aligned}\tilde{D}^{ab}_{\mu\nu}(k) =& \tilde{D}^{ab}_{(\mathrm{tr})\mu\nu}(k)+\tilde{D}^{ac}_{(\mathrm{tr})\mu\lambda}(k)\Pi^{cd,\lambda\rho}(k)\tilde{D}^{db}_{(\mathrm{tr})\rho\nu}(k)+\\ &\tilde{D}^{ac}_{(\mathrm{tr})\mu\lambda}(k)\Pi^{cd,\lambda\rho}(k)\tilde{D}^{de}_{(\mathrm{tr})\rho\sigma}\Pi^{ef,\sigma\theta}(k)\tilde{D}^{fb}_{(\mathrm{tr})\theta\nu}(k)+\ldots\quad .\end{aligned} \tag{2.48}$$

The previous equation is equivalent to

$$\tilde{D}^{ab}_{\mu\nu}(k) = \tilde{D}^{ab}_{(\mathrm{tr})\mu\nu}(k)+\tilde{D}^{ac}_{(\mathrm{tr})\mu\lambda}(k)\Pi^{cd,\lambda\rho}(k)\tilde{D}^{db}_{\rho\nu}(k)\ . \tag{2.49}$$

One uses the generalization of the Ward identities of QED (which tells us that the photon self-energy is transverse, $k^{\mu}\Pi^{\mu\nu}=0$). This is generalized by the Slavnov-Taylor identities,

[11] On has chosen the convention of all momenta pointing inward.

[12] This is the Dyson equation for the self-energy.

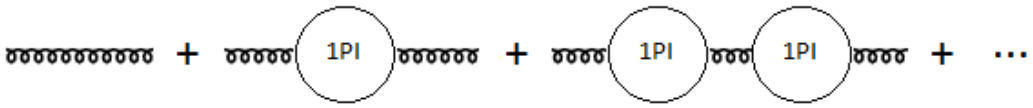

Fig. 2.1 The full gluon two-point correlation function written as a series of Feynamn diagrams. The curvy lines represent the tree-level gluon propagator, and the circle, in which "1PI" is written, represents the sum of all 1PI diagrams, i.e., the gluon self-energy.

which read for the gluon propagator, in momentum space,

$$\frac{1}{\xi}k^{\mu}k^{\nu}\tilde{D}^{ab}_{\mu\nu} = \delta_{ab}\,. \tag{2.50}$$

If one applies (2.50) in (2.49), one finds that

$$k^{\mu}k^{\nu}\Pi^{ab}_{\mu\nu}(k) = 0\,. \tag{2.51}$$

From this, one may isolate the tensorial structure of the gluon self-energy as

$$\Pi^{ab}_{\mu\nu} = \delta_{ab}(k_{\mu}k_{\nu} - k^2 g_{\mu\nu})\Pi^{(\mathrm{gl})}(k^2)\,. \tag{2.52}$$

Using (2.52) and (2.51) in (2.49), one finds that:

$$\tilde{D}^{\mu\nu}_{ab}(k) = \frac{-i}{k^2}\left(\frac{g^{\mu\nu} - k^{\mu}k^{\nu}/k^2}{1+\Pi^{gl}(k^2)} + \xi\frac{k^{\mu}k^{\nu}}{k^2}\right)\delta^{ab}\,. \tag{2.53}$$

From similar considerations, one may obtain the full ghost propagator, considering the inclusion of the ghost self-energy, i.e.,

$$\tilde{G}^{\mu\nu}_{ab}(k) = \frac{i}{k^2}\delta^{ab}\frac{1}{1+\Pi^{gh}(k^2)}\,, \tag{2.54}$$

where $\Pi^{gh}(k^2)$ is the ghost self-energy.

2.5 Regularization and Renormalization

In the previous section, one defined the full propagators using the self-energy. However, in general, loop contributions to the Green functions generate divergencies, which have to be taken care of. The first step to take care of loop divergencies is to regularize the theory, making the divergent integrals into finite ones by introducing a convergence procedure [44].

One of the most used regularizations in QCD is that of the discretization of space-time contemplated in Lattice QCD[13].

One must renormalize the theory, afterwards, i.e., rescale physical quantities. However, these rescaling is not unique and depends on what is called the renormalization scheme. For the purpose of this thesis one used the MOM scheme, consisting in defining the renormalization such that the Green functions corresponds to their tree level counterpart for a specific momentum μ [46].

2.6 General Form of the Three-gluon vertex

The general form of the three-gluon vertex was introduced in [35]. The goal is to define a general tensor structure which ought to be consistent with the generalized Ward identities and regularized (due to the inclusion of one loop divergencies). Let us assume that the color dependence of the vertex is, in analogy with its tree level form, due to the structure constant $f^{a_1a_2a_3}$ of $SU(3)$,

$$\Gamma^{a_1a_2a_3}_{\mu_1\mu_2\mu_3}(p_1,p_2,p_3) = f^{a_1a_2a_3}\Gamma_{\mu_1\mu_2\mu_3}(p_1,p_2,p_3)\ . \tag{2.55}$$

One requires $\Gamma_{\mu_1\mu_2\mu_3}(p_1,p_2,p_3)$ to satisfy Bose symmetry, i.e., symmetric under the interchange of any triplet (p_i,a_i,μ_i). Due to $f^{a_1a_2a_3}$ antisymmetry, Γ has to change sign under the switch of any two Lorentz indices and the respective momenta, in order to satisfy Bose symmetry. Thus one forms tensors which are odd under the interchanges of pairs (p_i,μ_i). Let us separate Γ into a transverse part (i.e., which is ortogonal to momenta) and a longitudinal part. The most general transverse tensor is then

$$\begin{aligned}\Gamma^{(t)}_{\mu_1\mu_2\mu_3} &= F(p_1^2,p_2^2;p_3^2)(g_{\mu_1\mu_2}p_1\cdot p_2 - p_{1\mu_2}p_{2\mu_1})B^3_{\mu_3}\\ &+H[-g_{\mu_1\mu_2}B^3_{\mu_3}+\frac{1}{3}(p_{1\mu_3}p_{2\mu_1}p_{3\mu_2}-p_{1\mu_2}p_{2\mu_3}p_{3\mu_1})]+\text{cyclic permutations}\ ,\end{aligned} \tag{2.56}$$

where

$$B^3_{\mu_3} = (p_{1\mu_3}p_2\cdot p_3 - p_{2\mu_3}p_1\cdot p_3)\ , \tag{2.57}$$

and $F(p_1^2,p_2^2;p_3^2)$ is a scalar function symmetric under the interchange of its first two arguments and $H(p_1^2,p_2^2;p_3^2)$ is totally symmetric in momenta. On the other hand, one has the

[13] Other methods of regularization may be seen in [44].

longitudinal part of Γ which accounts the remaining 10 terms,

$$\begin{aligned}\Gamma^{(l)}_{\mu_1\mu_2\mu_3} &= A(p_1^2,p_2^2;p_3^2)g_{\mu_1\mu_2}(p_1-p_2)_{\mu_3}+B(p_1^2,p_2^2;p_3^2)g_{\mu_1\mu_2}(p_1+p_2)_{\mu_3}\\ &+C(p_1^2,p_2^2;p_3^2)(p_{1\mu_2}p_{2\mu_1}-g_{\mu_1\mu_2}p_1\cdot p_2)(p_1-p_2)_{\mu_3}\\ &+\frac{1}{3}S(p_1^2,p_2^2;p_3^2)(p_{1\mu_3}p_{2\mu_1}p_{3\mu_2}+p_{1\mu_2}p_{2\mu_3}p_{3\mu_1})+\text{cyclic permutations}\,,\end{aligned} \tag{2.58}$$

where $A(p_1^2,p_2^2;p_3^2)$ and $C(p_1^2,p_2^2;p_3^2)$ are symmetric in their first arguments, $B(p_1^2,p_2^2;p_3^2)$ is antisymmetric and $S(p_1^2,p_2^2;p_3^2)$ under interchange of any pair of arguments.

Now, one may relate the three gluon vertex tensor to the three point complete Green's function in analogy with the perturbative approach,

$$\langle A^{a_1}_{\mu_1}(p_1)A^{a_2}_{\mu_2}(p_2)A^{a_3}_{\mu_3}(p_3)\rangle = V\delta(p_1+p_2+p_3)G^{a_1a_2a_3}_{\mu_1\mu_2\mu_3}\,, \tag{2.59}$$

in which,

$$G^{a_1a_2a_3}_{\mu_1\mu_2\mu_3} = D^{a_1b_1}_{\mu_1\nu_1}(p_1)D^{a_2b_2}_{\mu_1\nu_2}(p_2)D^{a_3b_3}_{\mu_3\nu_3}(p_3)\Gamma^{b_1b_2b_3}_{\nu_1\nu_2\nu_3}(p_1,p_2,p_3)\,, \tag{2.60}$$

where $D^{a_ib_i}_{\mu_i\nu_i}$ are the gluon propagators (see (2.53)). Taking the colour trace of the aforementioned expression one gets

$$\begin{aligned}G_{\mu_1\mu_2\mu_3}(p_1,p_2,p_3) =&\text{tr}\langle A_{\mu_1}(p_1)A_{\mu_2}(p_2)A_{\mu_3}(p_3)\rangle = V\delta(p_1+p_2+p_3)\frac{N_c(N_c^2-1)}{4}\\ &\times D(p_1^2)D(p_2^2)D(p_3^2)P_{\mu_1\nu_1}(p_1)P_{\mu_2\nu_2}(p_2)P_{\mu_3\nu_3}(p_3)\Gamma_{\nu_1\nu_2\nu_3}(p_1,p_2,p_3)\,,\end{aligned} \tag{2.61}$$

where $P_{\mu\nu}(p)=\delta_{\mu\nu}-\frac{p_\mu p_\nu}{p^2}$ is the transverse projector.

2.7 Summary

In short, one has written the expression of the Yang-Mills Lagrangian using as a starting point the gauge the invariance under any continuous symmetry group,

$$\mathscr{L}_{\text{YM}} = \bar{\psi}(i\not{D})\psi-\frac{1}{4}(F^a_{\mu\nu})^2-m\bar{\psi}\psi\,, \tag{2.62}$$

where $D_\mu=\partial_\mu-igA^a_\mu t^a$ is the covariant derivative, ψ is a spinor field, $F^a_{\mu\nu}=\partial_\mu A^a_\nu-\partial_\nu A^a_\mu+gf^{abc}A^b_\mu A^c_\nu$ and A_μ is the gauge field. After that, one quantized it using Faddeev-Popov method, to avoid the redundant integration over a continuous infinity of equivalent fields due

to gauge invariance. One ended up with the quantized lagrangian,

$$\mathscr{L} = \bar{\psi}(i\not{\partial} - m)\psi - \frac{1}{4}(F^i_{\mu\nu})^2 - \frac{1}{2\xi}(\partial^\mu A^a_\mu)^2 + c^a(-\partial^\mu D^{ac}_\mu)c^c \; . \tag{2.63}$$

Then one derived some Feynman rules, namely those of the gluon and ghost propagators and of the three gluon vertex, which was obtained using perturbation theory, i.e., assuming the coupling constant was small in order to expand $e^{i\int d^4x \mathscr{L}_I}$. To summarize, one derived, in momentum space,

Gluon Propagator

$$D^{(tr)\,\mu\nu}_{ab}(k) = \frac{-i}{k^2 + i\varepsilon}\left(g^{\mu\nu} - (1-\xi)\frac{k^\mu k^\nu}{k^2}\right)\delta^{ab} \; ; \tag{2.64}$$

Ghost Propagator

$$G^{(tr)\,\mu\nu}_{ab}(k) = \frac{i}{k^2}\delta^{ab} \; ; \tag{2.65}$$

Three Gluon Vertex

$$\Gamma^{(tr)\,abc}_{\alpha\beta\gamma} = g f^{abc}\left[g^{\nu\mu}(k_3 - k_2)^\tau + g^{\mu\tau}(k_2 - k_1)^\nu + g^{\tau\nu}(k_1 - k_3)^\mu\right] \; . \tag{2.66}$$

Finally, one presented the derivation of the full gluon and ghost propagator as well as the general form of the three-gluon vertex,

Full gluon propagator

$$\tilde{D}^{\mu\nu}_{ab}(k) = \frac{-i}{k^2}\left(\frac{g^{\mu\nu} - k^\mu k^\nu/k^2}{1 + \Pi^{gl}(k^2)} + \xi\frac{k^\mu k^\nu}{k^2}\right)\delta^{ab} \; ; \tag{2.67}$$

Full ghost propagator

$$\tilde{G}^{\mu\nu}_{ab}(k) = \frac{i}{k^2}\delta^{ab}\frac{1}{1 + \Pi^{gh}(k^2)} \; ; \tag{2.68}$$

General Form of the Three-gluon Vertex

$$\Gamma^{a_1a_2a_3}_{\mu_1\mu_2\mu_3}(p_1,p_2,p_3) = f^{a_1a_2a_3}\left\{\Gamma^{(t)}_{\mu_1\mu_2\mu_3}(p_1,p_2,p_3) + \Gamma^{(l)}_{\mu_1\mu_2\mu_3}(p_1,p_2,p_3)\right\} \; , \tag{2.69}$$

where the transverse part is given by

$$\begin{aligned}\Gamma^{(t)}_{\mu_1\mu_2\mu_3} &= F(p_1^2,p_2^2;p_3^2)(g_{\mu_1\mu_2}p_1\cdot p_2 - p_{1\mu_2}p_{2\mu_1})B^3_{\mu_3}\\ &+ H[-g_{\mu_1\mu_2}B^3_{\mu_3} + \frac{1}{3}(p_{1\mu_3}p_{2\mu_1}p_{3\mu_2} - p_{1\mu_2}p_{2\mu_3}p_{3\mu_1})] + \text{cyclic permutations}\,,\end{aligned} \tag{2.70}$$

in which

$$B^3_{\mu_3} = (p_{1\mu_3}p_2\cdot p_3 - p_{2\mu_3}p_1\cdot p_3)\,, \tag{2.71}$$

and $F(p_1^2,p_2^2;p_3^2)$ is a scalar function symmetric under the interchange of its first two arguments and $H(p_1^2,p_2^2;p_3^2)$ is totally symmetric in momenta; and the longitudinal part given by

$$\begin{aligned}\Gamma^{(l)}_{\mu_1\mu_2\mu_3} &= A(p_1^2,p_2^2;p_3^2)g_{\mu_1\mu_2}(p_1-p_2)_{\mu_3} + B(p_1^2,p_2^2;p_3^2)g_{\mu_1\mu_2}(p_1+p_2)_{\mu_3}\\ &+ C(p_1^2,p_2^2;p_3^2)(p_{1\mu_2}p_{2\mu_1} - g_{\mu_1\mu_2}p_1\cdot p_2)(p_1-p_2)_{\mu_3}\\ &+ \frac{1}{3}S(p_1^2,p_2^2;p_3^2)(p_{1\mu_3}p_{2\mu_1}p_{3\mu_2} + p_{1\mu_2}p_{2\mu_3}p_{3\mu_1}) + \text{cyclic permutations}\,,\end{aligned} \tag{2.72}$$

where $A(p_1^2,p_2^2;p_3^2)$ and $C(p_1^2,p_2^2;p_3^2)$ are symmetric in their first arguments, $B(p_1^2,p_2^2;p_3^2)$ is antisymmetric and $S(p_1^2,p_2^2;p_3^2)$ under interchange of any pair of arguments.

Chapter 3

Lattice QCD

In order to study the region of low momenta of QCD, one has to adopt a non-perturbative approach. This can be achieved by a well-established non-perturbative approach – Lattice QCD. In Lattice QCD, space-time is discretized so that it is defined in a four-dimensional finite lattice. This discretization provides a way of regularizing QCD [44]. On one hand, the functional integrals become finite-dimensional integrals, after this discretization. On the other hand, LQCD is formulated in the Euclidean space-time. These combined allow us to evaluate numerically the functional integrals using Monte Carlo simulations.

In this chapter one commences with a discussion on the Euclidean space-time formulation of the theory [36, 47]. Then, the gauge links, which will replace the gauge fields, are defined [47, 48]. From these, one constructs the Wilson action – a discretized form of the action $S = \frac{1}{4}\int d^4x (F^c_{\mu\nu})^2$ [47]. Afterwards, the gauge-fixing to minimal Landau gauge [49] and the gluon and ghost propagators on the lattice [45, 50, 51] are discussed. Finally, from these propagators one may define a running coupling, which is a renormalization group invariant [52].

3.1 Euclidean Space-Time

One of the starting points in order to treat the theory by means of numerical computations is to switch from Minkowski space-time to the Euclidean one. This is achieved by a Wick rotation, i.e., a rotation by $\pi/2$ in the complex plane of time. This corresponds to the substitution of the real time t by the imaginary time τ, using $t = -i\tau$. Notice that this rotation makes the generating functional of a quantum field theory formally identical to the partition function of statistical mechanics in four dimensions,

$$\int \mathscr{D}\phi e^{iS[\phi]} \to \int \mathscr{D}\phi e^{-S^E[\phi]}\,, \tag{3.1}$$

where S^E is the action written in the Euclidean space-time. The metric tensor for the Euclidean space is simply $\delta_{\mu\nu} = diag(1,1,1,1)$. Notice, however, that an analytic continuation on the complex plane may be invalid if one encounters a pole. In the case of a Euclidean correlation function which obeys a certain set of axioms, it is possible to perform this analytic continuation by means of the Osterwalder-Schrader reconstruction (see [53, 54] for further informations on this topic).

3.2 Discretization of Space-Time: Gauge Links

The usual and simplest lattice used in Lattice QCD is an hypercubic one, in which the lattice spacing a is the same for every direction of space-time.

$$x_\mu \to x(i,j,k,t) = (i\mathbf{e}_1 + j\mathbf{e}_2 + k\mathbf{e}_3 + t\mathbf{e}_4)a \ . \tag{3.2}$$

Recall that the covariant derivative was defined by means of the comparator, which in the infinitesimal form reads (Cf. eq. 2.7),

$$C(x+\varepsilon n, x) = 1 + ig\varepsilon n^\mu A^i_\mu t^i + \mathscr{O}(\varepsilon^2) \ . \tag{3.3}$$

This comparator was introduced to compensate the difference in gauge transformations of the fields in different points of space-time (Cf. section 2.1). Now, let us consider two points on the lattice, x and $x + a\hat{e}_\mu$. One may consider the comparator between these two points as an infinite product of comparators of infinitesimally closed points along the line between x and $x + a\hat{e}_\mu$. Doing so, one ends up with an exponential of a path-ordered line integral connecting the two space-times points, which one calls the *link variable*[1],

$$U_\mu(x) := P\exp\left(ig\int_x^{x+a\hat{e}_\mu} ds^\mu A_\mu\right) \ , \tag{3.4}$$

where $A_\mu = A^i_\mu t^i$, and P is the path-ordering operator, which is defined as the operator that orders the terms of the power-series expansion of the exponential in order of a parameter labeling the path. On the lattice, the gluon fields are replaced by these link variables. Notice that from its definition, it is straightforward that $U_\mu(x)$ transforms under a gauge transformation according to,

$$U_\mu(x) \to V(x)U_\mu(x)V^\dagger(x+a\hat{e}_\mu) \ . \tag{3.5}$$

[1] This is a Wilson line defined between the point x and $x + a\hat{e}_\mu$.

These variables are called link variables, for they are oriented and can be associated with the links of the lattice. For instance, $U_\mu(x)$ refers to the link connecting the sites x and $x+a\hat{e}_\mu$. Due to the fact that links variables are oriented, one may also define link variables pointing in negative μ direction. Let us define it as $U_{-\mu}(x+a\hat{e}_\mu) := U_\mu^\dagger(x)$.

3.3 The Wilson Action

In this section, the simplest discretized form of the gluon action will be derived. Recall that one derived the kinetic energy term for the gauge field A_μ^a (see eq. 2.13), using the commutator of covariant derivatives. However, one could derive the field strength by means of the comparator, linking together comparators around a small square in spacetime. That approach will be used this time. Thus let us start by considering a spacing a sufficiently small so that (3.4) may be approximated as $e^{iagA_\mu(x+a\hat{e}_\mu/2)}$, where one took the value of the gauge field in the middle of the line. Within this approximation, one can show that the product of the links around a small square yields,

$$U_\mu(x)U_\nu^\dagger(x)U_\mu^\dagger(x+\hat{e}_\nu)U_\nu(x+\hat{e}_\mu) \approx \exp\left(ia^2g\left[\partial_\mu A_\nu(x)-\partial_\nu A_\mu(x)\right]+a^2g\left[A_\mu(x),A_\nu(x)\right]\right) .$$

One calls this product *plaquette*, where $P_{\mu\nu}$ is used to denote it. It gives rise to the first nontrivial gauge-invariant term[2]. Comparing the exponent of the expression of the plaquette to the definition of the field strength (Cf. (2.12)), one may write, for small a,

$$P_{\mu\nu}(x) = \left[\exp\left(ia^2gF_{\mu\nu}\right)\right] . \tag{3.6}$$

From this, the lattice version of the continuum gluon action may be constructed,

$$S_W = \beta \sum_{x,\mu>\nu}\left(1-\frac{1}{N}\mathrm{Re}\left(\mathrm{tr}[P_{\mu\nu}]\right)\right) , \tag{3.7}$$

where $\beta = 2N/g^2$ for $SU(N)$. This is the *Wilson* action and reproduces the usual action when the limit $a \to 0$ is taken. In fact, for small a the exponencial in (3.6) may be expanded,

$$S_W = \beta \sum_{x,\mu>\nu}\left(1-\frac{1}{N}\mathrm{Re}\left(\mathrm{tr}\left[1+ia^2gF_{\mu\nu}-\frac{1}{2}a^4g^2F_{\mu\nu}^2+\mathscr{O}(a^6)\right]\right)\right) . \tag{3.8}$$

[2]Notice that the trivial term would be $\mathrm{tr}\left[U_\mu(x_i)U_{-\mu}(x_i+a\hat{e}_\mu)\right] = \mathrm{tr}\left[U_\mu(x_i)U_\mu(x_i)^\dagger\right] = \mathrm{tr}[1] = N$, which is just a constant.

Notice that $\mathrm{tr}(1) = N$ and that $F_{\mu\nu} = F^a_{\mu\nu} t^a$,

$$S_W = \beta \sum_{x,\mu>\nu} \left(-\frac{1}{N} \mathrm{Re} \left(\mathrm{tr} \left[i a^2 g F^a_{\mu\nu} t^a \right] - \mathrm{tr} \left[\frac{1}{2} a^4 g^2 F^c_{\mu\nu} t^c F^d_{\mu\nu} t^d \right] + \mathscr{O}(a^6) \right) \right) . \tag{3.9}$$

Notice that the first trace in the r.h.s. vanishes due to the fact that the generators are traceless, i.e, $\mathrm{tr}[t^a] = 0$. On the other hand[3] $\mathrm{tr}[t^a t^b] = \frac{1}{2}\delta^{ab}$,

$$S_W = \frac{1}{2N} \sum_x a^4 g^2 \beta \sum_{\mu>\nu} \frac{1}{2} \left(F^c_{\mu\nu} F^c_{\mu\nu} \right) + \mathscr{O}(a^6) , \tag{3.10}$$

which may be turned into an integral, in the continuum limit,

$$S_W = \frac{1}{4} \int d^4x \left(F^c_{\mu\nu} \right)^2 + \mathscr{O}(a^2) . \tag{3.11}$$

Therefore the Wilson action reproduces the continuum action plus vanishing terms of order $\mathscr{O}(a^2)$.

3.4 Gauge-Fixing: Minimal Landau Gauge

In order to investigate correlation functions, one has to specify a gauge. One chose the Landau gauge in this work. The Landau gauge on the continuum is, by definition,

$$\partial_\mu A_\mu = 0 . \tag{3.12}$$

This defines a hyperplane of transverse configurations

$$\Gamma := \{ A : \ \partial \cdot A = 0 \} . \tag{3.13}$$

This region comprises more that one configuration from each gauge orbit [55], known as Gribov copies, so Gribov suggested to use some additional conditions: the restriction of the physical configurational space to the following region

$$\Omega := \{ A : \ \partial \cdot A = 0, M[A] \geqslant 0 \} \subset \Gamma , \tag{3.14}$$

where $M[A] := -\partial^\mu D_\mu[A]$ is the Faddeev-Popov operator (see (2.23)). However, this region is not yet free of Gribov copies, so further restrictions are needed. To this end, one identifies

[3] These relations are summarized in Appendix A.

the physical configurational space with the *fundamental modular region* $\Lambda \subset \Omega$, which is defined as the set of absolute minima of the following functional

$$F_U[V] = \int d^4x \sum_\mu \mathrm{tr}\left[A^V_\mu(x) A^V_\mu(x)\right] \ , \tag{3.15}$$

where $A^V_\mu(x)$ is defined in (2.9). This region is a convex manifold [56]. Each gauge orbit intersects its interior only once [57, 58], which means that the absolute minima are non-degenerate. However, this is not the case for the boundary $\partial\Lambda$, in which there are degenerate absolute minima, i.e, distinct points in the boundary are Gribov copies of each other [58–60]. This choice of gauge is called minimal Landau gauge[4].

The case of the lattice is similar to that of the continuum theory [61–63], i.e., the interior of the fundamental modular region Λ is free of Gribov copies, however, they might occur at the boundary $\partial\Lambda$. Nevertheless, the boundary of a finite lattice, in which degenerate absolute minima might occur, has measure zero for the partition function and thus may be ignored [62].

Landau gauge-fixing is performed on the lattice by maximizing the functional:

$$F_U[V] = C_F \sum_{x,\mu} Re\{\mathrm{tr}[V(x) U_\mu(x) V^\dagger(x+\hat{e}_\mu)]\} \ , \tag{3.16}$$

where $C_F = (N_{dim} N_C V)^{-1}$ is the normalization constant in which N_{dim} is the number of dimensions of the space-time, N_C is the number of colours and V is the number of points on the lattice. To see that, let us consider U_μ as the maximizing configuration of $F_U[V]$ on some given orbit. Then, one considers a configuration near U_μ and performs the following expansion[5],

$$F_U[1+i\omega(x)] \approx F_U[1] + \frac{C_F}{2} \sum_{x,\mu} i\omega^a(x) \mathrm{tr}\Big[t^a\left(U_\mu(x) - U_\mu(x-\hat{e}_\mu)\right) - t^a\left(U^\dagger_\mu(x) - U^\dagger_\mu(x-\hat{e}_\mu)\right)\Big] \ ,$$

where t^a are the generators of $SU(N)$. Recall that one has defined U_μ as the maximizing configuration of $F_U[V]$, therefore, U_μ is a stationary point of F, that is,

$$\frac{\partial F}{\partial \omega^a(x)} = \frac{iC_F}{2} \sum_\mu \mathrm{tr}\left[t^a\left(U_\mu(x) - U_\mu(x-\hat{e}_\mu)\right) - t^a\left(U^\dagger_\mu(x) - U^\dagger_\mu(x-\hat{e}_\mu)\right)\right] = 0 \ . \tag{3.17}$$

[4]Notice that some authors refers to the Landau gauge defined in Ω as the minimal Landau gauge, where Ω is defined in eq. 3.14.

[5]Notice that $V(x)$ in the infinitesimal form is $V(x) = 1 + i\omega(x) + \mathcal{O}(\omega^2)$.

Writting the aforementioned in terms of the gluon fields, expanding $U_\mu(x) = e^{iagA_\mu(x+a\hat{e}_\mu)}$, one has

$$\sum_\mu \mathrm{tr}\left[t^a\left(A_\mu(x+a\hat{e}_\mu/2) - A_\mu(x-a\hat{e}_\mu/2)\right)\right] + \mathscr{O}(a^2) = 0\,, \tag{3.18}$$

which is equivalent to[6]

$$\sum_\mu \partial_\mu A^a_\mu + \mathscr{O}(a) = 0\,, \tag{3.19}$$

which allows us to conclude that (3.17) is the lattice equivalent of the continuum Landau gauge condition.

One may define, in analogy with the continuum theory, the region of stationary points of the functional (3.16),

$$\Gamma := \{U : \partial \cdot A(U) = 0\}\,, \tag{3.20}$$

and the region containing the maxima of the functional (3.16) – the Gribov region,

$$\Omega := \{U : \partial \cdot A(U) = 0 \text{ and } M(U) \geqslant 0\}\,, \tag{3.21}$$

where $M(U)$ is the lattice equivalent of the continuum Faddeev-Popov operator. Then one defines the fundamental modular region Λ as the set of absolute maxima of the functional (3.16). The interior of this region is free from Gribov copies as in the continuum theory [62].

The choice of different maxima of $F[U]$ may lead to small changes in the propagators in the infrared region. For more informations on this subject see [64–66]. In the work developed on this thesis, one did not consider the possible influence of the Gribov copies.

3.5 Propagators

3.5.1 Gluon propagator

The gluon propagator is defined as the 2-correlation function of gauge fields. To define it on the lattice, one would like to relate the gluon field to the link variable. Considering a sufficiently small lattice spacing a, (3.4) may be approximated as $e^{iagA_\mu(x+a\hat{e}_\mu/2)}$, like one did for the computation of the Wilson action. Expanding the exponencial to quadratic terms of the lattice spacing one finds that,

$$aA_\mu(x+a\hat{e}_\mu/2) = \frac{1}{2ig}\left\{U_\mu(x) - U^\dagger_\mu(x)\right\} - \frac{1}{6ig}\mathrm{tr}\left\{U_\mu(x) - U^\dagger_\mu(x)\right\} + \mathscr{O}(a^2)\,. \tag{3.22}$$

[6] Notice that $A_\mu(x+\delta x) \approx A_\mu(x) + \delta x \partial_\mu A_\mu(x)$ (where there is no sum over the index μ in the last term).

The second term on the r.h.s. is due to the fact that A_μ is a traceless matrix, so that, to preserve that tracelessness, one had to correct the expression by the factor $-\frac{1}{2Nig}\mathrm{tr}\left\{U_\mu(x)-U_\mu^\dagger(x)\right\}$. Next, one uses a Fourier transform on the gluon field, representing the discrete momenta by $\hat{q}$,

$$A_\mu(\hat{q}) = \sum_x e^{-i\hat{q}(x+a\hat{e}_\mu/2)} A_\mu(x+a\hat{e}_\mu/2)\ . \tag{3.23}$$

Notice that from periodic boundary conditions, $\hat{q}_\mu$ is

$$\hat{q}_\mu = \frac{2\pi n_\mu}{aL_\mu}, \quad n_\mu = 0,1,...,L_\mu/2\ . \tag{3.24}$$

In momentum space, the 2-point correlation function is given by

$$\langle A^a_\mu(\hat{q}) A^b_\nu(\hat{q}')\rangle = D^{ab}_{\mu\nu}(\hat{q}) V \delta(\hat{q}+\hat{q}')\ , \tag{3.25}$$

where V is the number of points in the lattice. One now specifies the gauge parameter ξ of (2.53) to 0 (which corresponds to the Landau gauge), and rewrites it as,

$$\tilde{D}^{ab}_{\mu\nu}(q) = \delta^{ab}\left(\delta_{\mu\nu} - \frac{q_\mu q_\nu}{q^2}\right) D(q^2)\ , \tag{3.26}$$

where $D(q^2) = \frac{1}{q^2(1+\Pi(q^2))}$ is the scalar part of $D^{ab}_{\mu\nu}(q)$. One would like to relate this scalar gluon propagator to the gluon fields[7]. Combining (3.26) with (3.25), noticing that one has the special case of $q \neq 0$, one gets

$$D(q^2) = \frac{2}{(N_c^2-1)(N_d-\alpha)V} \sum_\mu \langle \mathrm{tr}[A_\mu(\hat{q}) A_\mu(-\hat{q})]\rangle\ , \tag{3.27}$$

where $\alpha = 0$ if $q = 0$ and $\alpha = 1$ otherwise. Finally, let us mention that the tree level propagator of a massless scalar field does not correspond to its continuum counterpart, so that a redefinition of the momentum is to be made in order to reproduce it. This redefinition is

$$q_\mu = \frac{2}{a}\sin\left(\frac{\hat{q}_\mu a}{2}\right)\ . \tag{3.28}$$

It is usual to define what is called a *dressing function*, which is nothing but the quocient between the full propagator with its tree level form, i.e.,

$$d_{gl}(q^2) = q^2 D(q^2)\ , \tag{3.29}$$

[7]Notice that eq. 3.26 is valid for all momenta except for $q = 0$.

which provides a way of comparing the non-perturbative result to the perturbative one.

3.5.2 Ghost propagator

The ghost propagator is defined as the inverse of the Faddeev-Popov operator M^{ab},

$$G^{ab}(x-y) := \langle c^a(x)\bar{c}^b(y)\rangle = \langle (M^{-1})^{ab}_{xy}[U]\rangle \,, \tag{3.30}$$

where U represents a lattice configuration and c are ghost fields. This operator is given by the second variation of the functional (3.16) with respect to the parameters of the gauge transformation,

$$\frac{\partial^2 F_U[V]}{\partial\omega^a(x)\partial\omega^b(y)} = M^{ab}_{xy} \,. \tag{3.31}$$

It is a real symmetric matrix in the (minimal) Landau gauge [62]. Let us consider an arbitrary vector V^b and apply the matrix M^{ab} to it. One may find that [62],

$$\begin{aligned} M^{ab}_{xy}V^b_y = \sum_\mu \Big\{ & S^{ab}_\mu(x)[V^b_x - V^b_{x+\hat{\mu}}] - (x \leftrightarrow x-\hat{\mu}) \\ & -\tfrac{1}{2}f^{abc}[A^b_\mu(x)V^c_{x+\hat{\mu}}] - A^b_\mu(x-\hat{\mu})V^c_{x-\hat{\mu}}]\Big\} \,, \end{aligned} \tag{3.32}$$

where $S^{ab} = -\frac{1}{2}\mathrm{tr}(\{t^a,t^b\}(U_\mu(x)+U^\dagger_\mu(x)))$. Now one would like to invert the matrix M. However, due to its large size the inversion would be too computationally demanding. To solve this issue, the following linear system may be solved instead,

$$M^{ab}_{xy}V^b_y = I^a_x \,, \tag{3.33}$$

where $I^a_x = \delta^{aa_0}\delta_{xx_0}$. However, the constant vectors are zero modes of the Faddeev-Popov matrix (i.e. eigenvectors with vanishing eigenvalues) [51]. Fortunately, this matrix is positive-definite in the subspace orthogonal to constant vectors. Thus, one may use the conjugate-gradient method[8] [68] provided that one works on that orthogonal subspace. This is possible if the aforementioned equation is multiplied by M, for Mv belongs to the orthogonal space for a generic vector v. Therefore, one ends up with

$$MMV = MI \,, \tag{3.34}$$

[8]Notice that the method is applicable for positive-definite, symmetric and real matrices. For further informations on this method, see [67].

which may solved by solving separately the following equations

$$MA = MI; \quad MV = A \; . \tag{3.35}$$

Afterwards, one gets the ghost propagator on the momentum space from (3.30),

$$G^{ab}(k) = \left\langle \sum_x (M^{-1})^{ab}_{xx_o} e^{ik(x-x_0)} \right\rangle \; . \tag{3.36}$$

Assuming that the ghost propagator on the lattice has the same tensorial structure as its continuum counterpart, one may write,

$$G^{ab}(k) = \delta^{ab} G(k^2) \; . \tag{3.37}$$

And now, the scalar function may be obtained from (3.37),

$$G(k^2) = \frac{1}{N_c^2 - 1} \sum_a G^{aa}(k) \; . \tag{3.38}$$

From which one can define the ghost dressing function,

$$d_{\mathrm{gh}}(k^2) = k^2 G(k^2) \; . \tag{3.39}$$

One would like to note that (3.36) corresponds to a *point-to-all* propagator, as opposed to the *all-to-all* one,

$$G^{ab}(k) = \frac{1}{V} \left\langle \sum_{x,y} (M^{-1})^{ab}_{xy} e^{ik(x-y)} \right\rangle \; . \tag{3.40}$$

In order to estimate this *all-to-all* propagator, one may average over several values *point-to-all*. This is what we did in the work described in this dissertation[9].

3.5.3 Running Coupling

From the dressing functions for the gluon and ghost propagators one can form a renormalization group invariant (i.e. does not depend on the renormalization scheme one uses) which defines a running coupling [52],

$$\alpha_S(q^2) = \frac{g^2}{4\pi} d_{\mathrm{gl}}(q^2) d^2_{\mathrm{gh}}(q^2) \; . \tag{3.41}$$

[9] There is a method described in [69] which allows us to determine the *all-to-all* for a specific momentum, using a plane wave as a source.

Chapter 4

Computational Methods

In this chapter one discusses the computational methods used in order to perform lattice computations. One commences with a discussion on Monte Carlo methods used to compute the correlation functions. To this end, one introduces the Markov chains and discuss the convergence of strongly ergodic Markov chains [70, 71]. Then, one discuss a simple algorithm that provides a way to generate a Markov chain that satisfies detailed balance – the Metropolis algorithm. Subsequently, two other algorithms are discussed, which were the ones used in our simulations – the Overrelaxation and the Heat-Bath algorithms [48, 72]. There is also a discussion on the Fourier Accelerated Steepest Descent algorithm, used in order to perform a gauge-fixing to the Landau gauge [49]. Finally, the method used in the work described in this dissertation for computing statistical errors is introduced - the bootstrap method [45, 73–76].

4.1 Monte Carlo Methods: Heat-Bath and Overrelaxation

One of the most useful quantities one wishes to determine on the lattice is the expectation value of some operator $\mathscr{O}(U)$ which depends on some gauge configuration U, i.e,

$$\langle \mathscr{O} \rangle = \frac{1}{Z} \int \mathscr{D}U e^{-S(U)} \mathscr{O}(U) \,, \tag{4.1}$$

where, S corresponds to some action, the Wilson one in our case. Our goal is to compute this integral numerically. However, notice that there is one integration per degree of freedom so that usual deterministic methods aren't suited for such computations, for these become too expensive for integrals on higher dimensional spaces. This issue may be solved resorting to Monte Carlo methods. The main idea is to identify probabilities with integration measures. This is due to the fact that the *Boltzmann factor* e^{-S} gives different importance to different

gauge configurations. To this end, one generates an ensemble of gauge configurations $\{U_i\}_{i=1}^N$ which are drawn from the probability distribution

$$P(U_i)\mathscr{D}U = \frac{1}{Z}e^{-S(U_i)}\mathscr{D}U \ . \tag{4.2}$$

This is achieved by means of Markov chains, which will be described in section 4.1.1. Then, one computes the average of the values of the operator $\mathscr{O}$ on each configuration,

$$\bar{\mathscr{O}} := \frac{1}{N}\sum_{t=1}^{N}\mathscr{O}(U_i) \ . \tag{4.3}$$

Using the *law of large numbers*, one knows that as the number of field configurations sampled is increased, the value of the sample average becomes closer to that of the expectation value, i.e.,

$$\langle\mathscr{O}\rangle = \lim_{N\to\infty}\bar{\mathscr{O}} \ . \tag{4.4}$$

According to the central limit theorem, the sample average tends to a Gaussian distribution with the expectation value as its mean and a standard deviation proportional to $1/\sqrt{N}$.

4.1.1 Markov Chains and their convergence

Let us define a Markov chain as a sequence of random variables A_t drawn from a specified state space Ω (in our case, the space of all gauge configurations) indexed by a totally ordered discrete set T ("time") with the following property[1]:

$$Pr(A_{t+1}|A_1,...,A_t) = Pr(A_{t+1}|A_t) \ , \tag{4.5}$$

that is, the conditional probability of moving to the next state depends only on the current state and not on the preceding states.

A probability distribution is defined as a mapping $Q : \Omega \to \mathbb{R}$ which is positive, $Q(U) > 0 \forall x \in \Omega$ and normalized, $\sum_\Omega Q(U) = 1$. Let us call the space of such mappings by S_Ω. Let us write $P(i \to j)$, where $i, j \in \Omega$ as the probability of transition from the state i to j, i.e. $Pr(j|i)$. The operator $P : S_\Omega \to S_\Omega$, such that

$$(PQ)(U) = \sum_{U'\in\Omega} P(U' \to U)Q(U) \tag{4.6}$$

[1] one has chosen T as the set of natural numbers $\mathbb{N}$

defines a Markov process. By definition, a Markov process P is strongly ergodic if

$$P(U \to U') > 0 \ \forall_{U,U'} \ . \tag{4.7}$$

One would like to prove that a Markov chain with a strongly ergodic P converges to a stationary distribution.

Before that, let us introduce some basic concepts of Metric Spaces. They are needed for one is interested in a generalization of the concept of distance.

Def. Let M be a set. A metric d is a function $d : M \times M \to \mathbb{R}$ which satisfies the following conditions[2]:

$$\begin{aligned} &\bullet\ d(x,y) = 0 \text{ if and only if } x = y; \\ &\bullet\ \forall_{x,y\in M}\ d(x,y) = d(y,x); \\ &\bullet\ \forall_{x,y,z\in M}\ d(x,z) \leqslant d(x,z) + d(z,y). \end{aligned} \tag{4.8}$$

The pair (M,d) is called the metric space. The metric can be viewed as a generalization of the concept of distance. In our case, one will present a function which measures the "distance" between probability distributions.

Def. Let (M,d) be a metric space and (u_n) a sequence of elements of M. One may refer to (u_n) as a *Cauchy sequence.* if:

$$\forall_{\varepsilon>0}\, \exists_{n_0}\, \forall_{m,n} : m,n \geqslant n_0 \implies d(u_n,u_m) < \varepsilon \ . \tag{4.9}$$

Def. One says that a metric space (M,d) is *complete* if every Cauchy sequence of elements of M has its limit in[3] M.

Def. Let (M,d) and (M',d') be metric spaces. Let $f : M \to M'$ be a function. One says that f is a *Lipschitz function* if there is $K \in \mathbb{R}$(non-negative) such that:

$$\forall_{x,y\in M}\ d'(f(x),f(y)) \leqslant K\, d(x,y) \ , \tag{4.10}$$

where K is called the *Lipschitz constant*. If $K < 1$, one calls the function a *contraction*.

[2] It is easy to prove that from these conditions one gets $d \geqslant 0$.

[3] Let (M,d) be a metric space and (u_n) a sequence of elements of M and $c \in M$. One says that c is the limit of the sequence if $\forall_{\varepsilon>0}\exists_{n_0}\forall_n : n \geqslant n_0 \implies d(u_n,c) < \varepsilon$.

Def. Let (M,d) be a metric space and $f : M \to M$ a function. One says that x^* is a fixed point if:

$$f(x^*) = x^* \ . \tag{4.11}$$

Now that some basic concepts from metric spaces have been introduced, one may present the following theorem, which will enable us to prove the convergence of ergodic Markov chains,

Banach Fixed Point Theorem. Let (M,d) be a complete metric space and let $f : M \to M$ be a contraction with Lipschitz constant K. It follows that:

• f admits a unique fixed point x^* in M. Moreover, x^* may be found by starting with an arbitrary element $x_0 \in X$ and define the sequence of $x_n = f(x_{n-1})$. It follows that $x_n \to x^*$;

• $d(x_n, x^*) \leqslant \frac{K^n}{1-K} d(x_1, x_0) \forall_{n \in \mathbb{N}}$.

Next, let us define a metric on the space introduced, S_Ω, as follows,

$$d(Q_1, Q_2) := \sum_{U \in \Omega} |Q_1(U) - Q_2(U)| \ . \tag{4.12}$$

In order to prove the convergence of the (strongly) ergodic Markov chains, one has to prove that the function $P_M : S_\Omega \to S_\Omega$ is a contraction. This is done in [70]. On the other hand, the space of probability distributions S_Ω is complete [70], so one concludes that the (strongly) ergodic Markov chains converges to a unique distribution using Banach fixed point theorem.

4.1.2 Detailed Balance and the Metropolis Algorithm

Now, one wishes to construct a Markov chain with a precise fixed point, that is,

$$P^*(U) = \sum_{U' \in \Omega} P(U' \to U) P^*(U') \ \ \forall_{U \in \Omega} \ . \tag{4.13}$$

A sufficient condition [70] is to make the chain satisfy *detailed balance*,

$$P(U \to U') P^*(U) = P(U' \to U) P^*(U') \ . \tag{4.14}$$

To generate the elements of a Markov chain which satisfies detailed balance one may use the well-known Metropolis Algorithm. It is defined as follows,

Metropolis Algorithm

• Start with some arbritrary U;
• Choose a test U' from some *a priori selection probability* $P(U'|U)$;
• Accept the test U' with probability[4]

$$P_A(U \to U') = \min\left(1, \frac{P^*(U)}{P^*(U')}\right) \tag{4.15}$$

• Continue from second step; It is an easy exercise to see that this algorithm fullfils detailed balance condition. Notice that in our case of interest, $P^*(x)$ is defined in (4.2), so that one may write,

$$\frac{P^*(U)}{P^*(U')} = e^{-\delta S}\,, \tag{4.16}$$

where $\delta S = S(U') - S(U)$.

4.1.3 Metropolis Algorithm applied on the Lattice

In this section, the Metropolis Algorithm applied to the Wilson gauge action is discussed. To this end, let us start from a configuration U. In the simplest case, the test U' for the Metropolis algorithm update differs from the first by the value of just a single link variable $U_\mu(n)'$. Therefore, only six plaquettes are affected when one updates $U_\mu(n) \to U_\mu(n)'$ for the link is shared solely by those six plaquettes (of course, considering a four dimensional lattice). Then, it is easy to see that the change of action is (See (3.7)),

$$\delta S = S[U_\mu(x)']_{\rm loc} - S[U_\mu(x)]_{\rm loc} = -\frac{\beta}{N}\mathrm{Re\,tr}[U_\mu(x)' - U_\mu(x)]P_6\,, \tag{4.17}$$

[4]Other choices are possible.

where the subscript *loc* stands for *local* and means one is considering only the six plaquettes shared by the link, and where

$$P_6 = \sum_{i=1}^{6} P_i = \sum_{\nu\neq\mu} \left\{ U_\nu(x+\hat{e}_\mu) U_{-\mu}(x+\hat{e}_\mu+\hat{e}_\nu) U_{-\nu}(x+\hat{e}_\nu) \right. \\ \left. + U_{-\nu}(x+\hat{e}_\mu) U_{-\mu}(x+\hat{e}_\mu-\hat{e}_\nu) U_\nu(x-\hat{e}_\nu) \right\} .$$

These products are called *staples*.

4.1.4 Problems with Simple Metropolis Algorithm

In order to get high acceptance, one has to choose U' in the vicinity of U, as one may see from (4.17). Unfortunately, this implies too small steps in the Markov chain. However, if a candidate U' is chosen too far from the original U, one has low acceptance, which is not desirable as well. Therefore, one would like to somehow improve the algorithm in order to get larger step sizes. This can be achieved by the Overrelaxation algorithm, which is explained in the next subsection for $SU(2)$. However this algorithm is not ergodic, for the configurations it generates belong to a subspace of constant energy. In order to get ergodicity, one has to combine it, for instance, with the heat bath algorithm.

4.1.5 Overrelaxation Method in SU(2)

Notice that in the Metropolis algorithm the candidates are always accepted if the action is not changed. Therefore, if one chooses U' in such a manner that it has the same probability weight as U, it will be automatically accepted. The starting point is the following local probability distribution,

$$dP(U) = \exp\left(\frac{\beta}{N} \mathrm{Re\ tr}[U P_6]\right) dU \ , \tag{4.18}$$

where, again, P_6 is defined in (4.17). Let us define the change of U according to the following ansatz

$$U \to U' = V^\dagger U^\dagger V^\dagger \ , \tag{4.19}$$

with V being a gauge group element such that the action remains invariant. Let us consider the case of $SU(2)$, before considering the case of $SU(3)$. This group is special, for the sum of two $SU(2)$ is proportional to some other $SU(2)$ matrix. Therefore, one may write P_6 as

$$P_6 = \alpha V; \quad \alpha = \sqrt{\det[P_6]} \ . \tag{4.20}$$

It can be proved that $det[P_6] \geqslant 0$. From this one defines the matrix[5] $V = P_6/a$. Within this definition, one find that,

$$\mathrm{tr}[U'P_6] = \mathrm{tr}[V^\dagger U^\dagger V^\dagger P_6] = \alpha \mathrm{tr}[V^\dagger U^\dagger] = tr[UP_6] \; . \tag{4.21}$$

Notice that in the last step one considered the fact that SU(2) matrices have real trace. Thus, one proved that this choice of U' keeps the action the same.

4.1.6 Heatbath in SU(2)

This algorithm updates to the new value $U'_\mu(n)$ according to the same local probability distribution as the overrelaxation algorithm, defined in (4.18). It is possible to prove that dU (called Haar measure) is invariant under left and right multiplications with another element V of $SU(2)$, therefore, one may write $dU = d(UV)$. Let us define $X := UV$, one may write,

$$dP(X) = \exp\left[\frac{1}{2}\alpha\beta \mathrm{Re\ tr}[X]\right] dX \; . \tag{4.22}$$

Then, one may write $U_\mu(n)'$ in terms of the generated X, according to

$$U_\mu(n)' = U = XV^\dagger = XP_6^\dagger \frac{1}{\alpha} \; . \tag{4.23}$$

One transformed the problem of generating U to that of generating X, distributed according to the distribution (4.22). Let us consider a general $SU(2)$ matrix. One knows that it can be written as,

$$U = \begin{pmatrix} a & b \\ -b^* & a^* \end{pmatrix} \quad \text{with} \;\; |a|^2 + |b|^2 = 1 \; . \tag{4.24}$$

If one writes $a = x_0 + ix_3$ and $b = x_2 + ix_1$, this turns out to be equivalent to writting the four vector $(x_0, \mathbf{x})$ in the representation,[6]

$$U = x_0 \mathbb{I} + i\mathbf{x} \cdot \boldsymbol{\sigma} \; . \tag{4.25}$$

[5] Notice that in the particular case of $det[P_6] = 0$, one may choose a random $SU(2)$ matrix for U'.

[6] σ denotes the vector of Pauli matrices.

Notice that $\det[U] = |x|^2 = x_0^2 + |\mathbf{x}|^2 = 1$. In this representation, the Haar measure may be written as[7]

$$\begin{aligned} dX &= \frac{1}{\pi^2}\delta(x_0^2 + |\mathbf{x}|^2 - 1)d^4x \\ &= \frac{1}{\pi^2}\frac{1}{2\sqrt{1-x_0^2}}\left\{\delta\left(|\mathbf{x}| - \sqrt{1-x_0^2}\right) + \delta\left(|\mathbf{x}| + \sqrt{1-x_0^2}\right)\right\}d^4x\,. \end{aligned}$$

Now the hyper-volume element may be written as:

$$d^4x = d|\mathbf{x}||\mathbf{x}|^2 d\Omega dx_0\,, \tag{4.26}$$

where $d\Omega$ stands for the spherical angle due to $\mathbf{x}$. If one integrates over $|x|$, one sees that this is the same as to specify the value of $|x| = \sqrt{1-x^0}$. On the other hand, writting $d\Omega = d\cos\theta d\phi$[8] and noting that $\mathrm{tr}[X] = 2x_0$, one may write the distribution as,

$$P(X)dX = \frac{1}{2\pi^2}d\cos\theta\, d\phi\, dx_0\sqrt{1-x_0^2}e^{\alpha\beta x_0}\,. \tag{4.27}$$

Now one asks the question of how to generate randomly such values of x_0, $|x|$, $|cos\theta|$ and $|\phi|$. To generate x_0 according to the distribution $\sqrt{1-x_0^2}e^{\alpha\beta x_0}$ one would like to write the previous as a gaussian distribution. This can be achieved by performing the following change of variables,

$$x_0 = 1 - 2\xi^2\,. \tag{4.28}$$

This implies that

$$dx_0\sqrt{1-x_0^2}e^{\alpha\beta x_0} \propto d\xi\,\xi^2\sqrt{1-\xi^2}e^{-2\alpha\beta\xi^2} \text{ with } \xi \in [0,1]\,. \tag{4.29}$$

Next, one has to generate ξ with the density (called modified Gaussian distribution density),

$$p_1(\xi) = \xi^2 e^{-2\alpha\beta\xi^2}\,, \tag{4.30}$$

and accept it with probability

$$p_2(\xi) = \sqrt{1-\xi^2}\,. \tag{4.31}$$

Algorithms to compute random numbers with Gaussian distributions are well-known. After generating ξ, one recovers x_0 from $x_0 = 1 - 2\xi^2$.

[7] One used the property of Dirac-delta δ, that $\delta(g(x)) = \sum_i \frac{\delta(x-x_i)}{|g'(x_i)|}$, where x_i are the roots of g.

[8] One has $\cos\theta \in [-1,1]$ and $\phi \in [0,2\pi)$.

On the other hand, generating $|\mathbf{x}|$ is easy, for one just has to recall that $|\mathbf{x}| = \sqrt{1-x_0^2}$. The angular variables $\cos\theta$ and ϕ are generated from a uniform distribution. From all these, it is possible to reconstruct X. Now the heatbath algorithm is summarized,

Heatbath Algorithm

1. Determine P_6 and $\alpha = \sqrt{\det[P_6]}$, and then initialize $V = P_6/\alpha$;
2. Find X according to the aforemention distribution (4.22);
3. Set the new variable as $U = XV^\dagger$.

4.1.7 Generalization to SU(3)

Unfortunately, there is not a heatbath algorithm that directly makes $SU(3)$ link variables. In order to solve this, one may apply this algorithm for the $SU(2)$ subgroups of $SU(3)$. This method [72] consists in selecting a set $\mathscr{S}$ of k $SU(2)$ subgroups of $SU(3)$, such that there is no invariant subset of $SU(3)$ under left multiplication by $\mathscr{S}$, with the exception of the whole group. Then, one performs an update on a given link by multiplying it by k matrices belonging to each subgroup $(SU(2))_i$, $i = 1,...,k$, i.e., (see (4.23))

$$U = XV^\dagger, \text{ where } X = X_1X_2...X_k\ , \tag{4.32}$$

for $X_i \in SU(2)_i$, $i = 1,...,k$.

The same reasoning may be applied to the overrelaxation algorithm for the matrix V in (4.19).[9]

4.2 Gauge Fixing Algorithm

Fourier Accelerated Steepest Descent Method

In order to search for a maximum of the functional (3.16), one used the *Fourier Accelerated Steepest Descent* method, in the work described in this dissertation. Unfortunately, the naive steepest descent method, when applied to large lattices, encounters an issue of critical slowing down (i.e. the number of iterations necessary to converge to some fixed accuracy grows drastically with the volume). One may ameliorate this by performing a Fourier acceleration.

[9] Notice that there is also a method of overrelaxation for $SU(3)$ [77].

In this method, one chooses the matrices V, which appeared on (3.5), to be

$$V(x) = \exp\left[\hat{F}^{-1}\frac{\alpha}{2}\frac{p^2_{\max}a^2}{p^2a^2}\hat{F}\left(\Delta(x)\right)\right] , \tag{4.33}$$

where a is the lattice spacing, p^2 are the eigenvalues of $-\partial^2$, $\hat{F}$ represents the fast Fourier transform (FFT), α is a parameter which we have set to the recommended value of 0.08 [78] in the work presented in this dissertation, and where[10]

$$\Delta(x) = \sum_{\nu}\left[U_\nu(x - a\hat{e}_\nu) - U_\nu(x) - h.c. - trace\right] , \tag{4.34}$$

is the lattice version of the continuum Landau gauge condition $\partial_\mu A_\mu = 0$. In order to compute V it is sufficient to expand the exponential to first order in α. To keep it an element of $SU(3)$ one has to reunitarize it afterwards. The monitorization of the convergence of the gauge fixing process is done with

$$\theta = \frac{1}{VN_C}\sum_{x}\mathrm{tr}\left[\Delta(x)\Delta^\dagger(x)\right] , \tag{4.35}$$

which corresponds to the mean value of $(\partial_\mu A_\mu)^2$ performed over all lattice points per color degree of freedom. In our work, the algorithm stops when $\theta \leqslant 10^{-15}$. The algorithm is defined below:

Fourier Accelerated Steepest Descent Algorithm

1. determine $\Delta(x), F[U]$ and θ.
2. while $\theta > 10^{-15}$
3. loop for all elements of $\Delta(x)$
4. FFT forward
5. apply $p^2_{\max}/p^2$
6. FFT backward
7. normalize
8. end loop

[10] Notice that here h.c. means "hermitian conjugate" of the previous terms.

9. loop for all x
10. determine $V(x)$ and reunitarize
11. end loop
12. loop for all x
13. loop for all μ
14. $U_\mu(x) \to V(x)U_\mu(x)V^\dagger(x+\hat{e}_\mu)$
15. end internal loop
16. end external loop
17. Determine $\Delta(x), F[U]$ and θ
18. end while loop

4.3 Error Analysis: Bootstrap Method

In the work described in this dissertation, we used the bootstrap method in order to compute the statistical errors. The bootstrap method may be applied to cases in which no mathematical model is used for the probability distribution function (non-parametric). For instance, it is suited when one does not know the probability density function or when the estimation of standard errors require complicated formulas. One of the advantages of this method is its simplicity. It is explained briefly in what follows. For a complete description of this subject, one recomends [73–76].

Let us consider a given sample of n independent quantities which are identically distributed $X_1, X_2, ..., X_N$ and a real-valued estimator $\hat{\theta} = \hat{\theta}(X_1, ..., X_N)$. In the case one is interested in, the estimator is the mean value. One is interested in the standard deviation of the estimator. The idea is to replace the (possibly) unknown population distribution with the empirical distribution. The empirical distribution F_n is a probability distribution in which each sample value has the probability $1/n$ assigned to it. Then one performs independent samplings with replacement from the empirical distribution F_n: it consists in generating N_{boot} samples of N elements which were drawn from the empirical distribution, F_n (it doesn't matter if the elements are drawn more than once or never at all). For each bootstrap sample

one determines the average, which will be denoted by A_i^{boot}, where i denotes the bootstrap sample (which runs from 1 to N_{boot}). One computes the asymmetric errors from

$$\sigma_B^{up} = \langle A \rangle - a^* \ , \ \sigma_B^{down} = b^* - \langle B \rangle \ , \tag{4.36}$$

where a^* and b^* are such that

$$\frac{\#\{A \in A_i^{boot} | A_i^{boot} < a^*\}}{N_{boot}} = \frac{1-C}{2} \ , \ \frac{\#\{A \in A_i^{boot} | A_i^{boot} < b^*\}}{N_{boot}} = \frac{1+C}{2} \ , \tag{4.37}$$

where C is the confidence coefficient ($C \in [0,1]$) and $\#\{\bullet\}$ denotes the cardinality of the set. One set $C = 0.675$. In the work developed, one used for the statistical error the greater of both asymetric values σ_B^{up}, σ_B^{down}, i.e.,

$$\sigma_B = \max\{|\sigma_B^{up}|, |\sigma_B^{down}|\} \ . \tag{4.38}$$

Chapter 5

Results

This chapter is a result of the work developed throughout the year by the author of this dissertation in association with his supervisors and it is divided into three sections. In section 5.1, we describe the lattice setup.

In section 5.2, we studied the dependence on the lattice spacing and physical volume of the Landau gauge two-point correlation functions of the gluon and ghost fields for pure $SU(3)$ Yang-Mills theory in four dimensions using lattice simulations. We used several lattice volumes, from 64^4 to 128^4, and different lattice spacings. On the other hand, one may define, as already discussed in section 3.5.3 a renormalization group invariant from the gluon and ghost propagators, the running coupling constant. We also studied the dependence of this coupling running constant on the lattice spacing and physical volume.

In section 5.3, we studied the three gluon one particle irreducible function (defined in section 2.6) in Landau gauge for pure $SU(3)$ Yang-Mills theory in four dimensions as well. It is expected from DSE (Dyson-Schwinger Equations) that there is a change of sign of certain form factors associated with this function in the IR region [26, 27]. Therefore, we investigated this zero crossing demanded in order to define properly the set of Dyson-Schwinger equations for the gluon.

5.1 Lattice setup

In order to perform computational simulations of the pure gauge $SU(3)$ Yang-Mills theory we adopted the Wilson action (See (3.7)) at several values of β and physical volumes, which we report in Table 5.1, concerning section 5.2 and Table 5.6, concerning section 5.3. On the other hand, we converted into physical units using the string tension as measured in [79]. However, the lattice spacing for $\beta = 6.3$ was not measured in [79], thus, in that case, we used the procedure described in [80].

We generated the gauge configurations using a combined Monte Carlo sweep of seven overrelaxations with four heatbath updates (See sections 4.1.5, 4.1.6 and 4.1.7) using the Chroma library [81]. Each generated configuration $U_\mu(x)$ was gauge fixed to the Landau gauge as described in section 4.2, using a computer code based in the Chroma and PFFT libraries [82]. As mentioned before in section 4.2, the algorithm was stopped for values of $\theta \leqslant 10^{-15}$.

On the other hand, we performed the cylindrical and conic cuts [83] for momenta above 1 GeV in order to reduce lattice artefacts. For momenta below 1 GeV we simply included all lattice data points. To define the cylindrical cut, one starts by choosing momenta that lies within a cylinder directed along $(x,y,z,t) = (1,1,1,1)$, which is a diagonal of the lattice. The distance between a momentum vector $\hat{q}$ and the diagonal is denoted by δq and is given by,

$$\delta q = |\hat{q}| \sin(\theta_q) \, , \tag{5.1}$$

where θ_q is given by

$$\theta_q = \arccos \frac{\hat{q} \cdot \hat{n}}{|\hat{q}|} \, , \tag{5.2}$$

and $\hat{n} = \frac{1}{2}(1,1,1,1)$ is the unit vector along the diagonal. On the computations performed, we chose momenta which satifies $\delta q < 1$. On the other hand, we imposed further restrictions on the angle, namely, $\theta_q < 20^\circ$ – conic cut.

It is also important to notice that we performed an averaging over all permutations of the components of $n_\mu = (n_x, n_y, n_z, n_t)$ (see (3.24)) when we computed the quantities of interest (the propagators and the 1PI function). This is done in order to minimize the possible break of rotational invariance on the lattice.

5.2 Gluon and Ghost Propagators and the Strong Coupling: Finite Lattice Spacing and Volume Effects

In order to compare the data of different simulations, one has to choose a renormalization scheme. The renormalization of the propagators was performed in the MOM scheme, with the following definition of renormalized propagators (see section 2.5 for further informations),

$$D(q^2)\big|_{q^2=\mu^2} = Z_A D_{lat}(\mu^2) = \frac{1}{\mu^2} \, ;$$
$$G(q^2)\big|_{q^2=\mu^2} = Z_\eta G_{lat}(\mu^2) = \frac{1}{\mu^2} \, ,$$

β	a(fm)	1/a(GeV)	L	La(fm)	# Conf	Sources
5.7	0.1838(11)	1.0734(63)	44	8.087	100	3
6.0	0.1016(25)	1.943(47)	64	6.502	100	2
			80	8.128	70	2
			128	13.005	35	1
6.3	0.0627(24)	3.149(46)	128	8.026	54	3

Table 5.1 Lattice setup. The last column refers so the number of point sources, per configurations, used to invert the Faddeev-Popov matrix, necessary to compute the ghost propagator.

where D_{lat} and G_{lat} indicates the bare lattice propagators. In the work described in this dissertation, we used $\mu = 4\,\text{GeV}$. In order to obtain the renormalization constants we fit the bare lattice propagators to the functional form

$$D(q^2) = z\frac{q^2+m_1^2}{q^4+m_2^2q^2+m_3^4} \tag{5.3}$$

for the gluon propagator (where we fit the data in the range of momentum $q \in [0,6]\,GeV$), and

$$G(q^2) = z\frac{\left[\log\frac{q^2}{\Lambda^2}\right]^{\gamma_{\text{gh}}}}{q^2} \tag{5.4}$$

for the ghost propagator (where one fit the data in the range of momentum $q \in [2,6]\,GeV$). The parameters obtained from the fit of the bare propagator data set to these funtional forms are presented in Table 5.2 (*gluon*) and Table 5.3 (*ghost*). The renormalization constants are presented in Table 5.4. Notice that the fittings of the functional forms (5.3) and (5.4) were performed in *Gnuplot*, from which one retrieved the fitting parameters as well as their associated errors. On the other hand, the errors of the value of the bare lattice propagators at $\mu = 4\,GeV$, extracted from the fit, and of the renormalization constants were determined using the Gaussian error propagation formula[1].

5.2.1 Gluon Propagator

The data concerning the renormalized gluon propagator may be seen in Fig.5.1 and Fig. 5.2. In order to see the effects of volume and lattice spacing, we performed two different plots. In the first plot (Fig. 5.1) we chose data with approximately the same volume ($V \sim (8fm)^4$)

[1] Let f be a function of uncorrelated variables $x_1,...,x_N$. Then, the standard error of f can be approximated by $\delta f(x_1,...,x_N) = \sqrt{\left(\frac{\partial f}{\partial x_1}\delta x_1\right)^2 + ... + \left(\frac{\partial f}{\partial x_N}\delta x_N\right)^2}$.

β	L	z	m_1	m_2	m_3	$\chi/d.o.f.$
5.7	44	1.470(8)	1.991(22)	0.747(13)	-0.7725(27)	2.528
6.0	64	4.931 (18)	2.054(18)	0.779(12)	-0.7625(23)	1.213
	80	4.904 (18)	2.054(18)	0.774(11)	-0.7617(21)	1.373
	128	4.907(18)	2.056(14)	0.772(8)	-0.7637(15)	1.264
6.3	128	13.166(54)	2.091(19)	0.799(12)	-0.7801(24)	1.141

Table 5.2 Parameters from the fit in the range $q \in [0,6]\,GeV$ of the bare gluon propagator data set using the functional form (5.3).

β	L	z	Λ	γ_{gh}	$\chi/d.o.f.$
5.7	44	2.00(14)	0.71(14)	-0.264(35)	0.101
6.0	64	9.27 (72)	0.28(5)	-0.395(29)	0.043
	80	8.56 (7)	0.33(7)	-0.367(29)	0.192
	128	5.36 (5)	1.40(5)	-0.151(5)	0.147
6.3	128	16.4(10)	0.77(17)	-0.206(29)	0.248

Table 5.3 Parameters from the fit in the range $q \in [2,6]\,GeV$ of the bare ghost propagator data set using the functional form (5.4), except for the lattices corresponding to $\beta = 6.0$, $L = 80$ and $L = 128$, in which the range was $q \in [2,8]\,GeV$.

β	L	$D(\mu = 4)\,(GeV)$	Z_A	$G(\mu = 4)\,(GeV)$	Z_η
5.7	44	0.1106(5)	0.5650(25)	0.090(8)	0.693(61)
6.0	64	0.3747(11)	0.1668(5)	0.299(29)	0.209(20)
	80	0.3730 (11)	0.1676(5)	0.298(17)	0.210(12)
	128	0.3736(11)	0.1674(5)	0.299(3)	0.209(2)
6.3	128	1.0062(34)	0.0621(2)	0.800(61)	0.078(6)

Table 5.4 Values of the bare lattice propagators at $\mu = 4\,GeV$ and renormalization constants.

and compared its values for different lattice spacings $(a \sim 0.18fm; 0.10fm; 0.06fm)$. On the other hand, in the second plot (Fig. 5.2), we chose data with the same lattice spacing $(a \sim 0.10fm)$ and different volumes $\left(V \sim (6.5fm)^4; (8.1fm)^4; (13.0fm)^4\right)$.

From Fig. 5.1 (constant physical volume), one may see a dependence on the lattice spacing, although it may seem rather non trivial (look, for instance, at the propagator for momenta below 0.5 GeV - there is no direct correspondence between it and the lattice spacing). On the other hand, one may see that the largest lattice spacing underestimates the lattice data in the IR region.

From Fig. 5.2 (constant lattice spacing), one may see that there is substancially no physical volume dependence, at least, for the volumes considered here in this work (above $(6.5\,fm)^4$ and below $(13\,fm)^4$).

These results obtained here about the relative importance of the effects due to the use of a finite lattice spacing and finite volume are in accordance with those of [10].

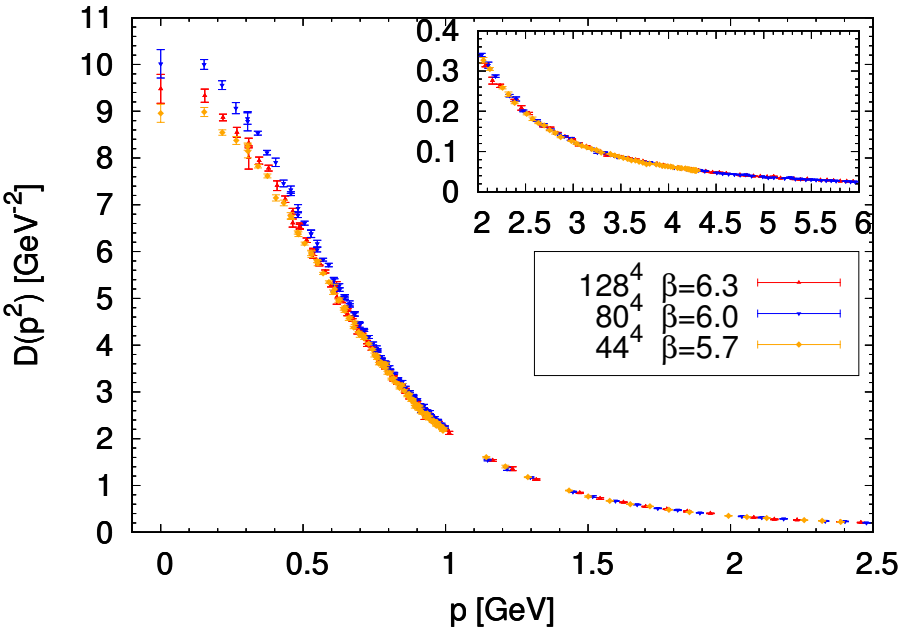

Fig. 5.1 Gluon propagator renormalized at $\mu = 4\,GeV$ for the same physical volume of $(8fm)^4$ and different lattice spacings.

5.2.2 Ghost Dressing Function

The analysis of the ghost two point correlation function was performed using its dressing function (see 3.39). Once again one has two plots, one (Fig. 5.3) for essentially the same

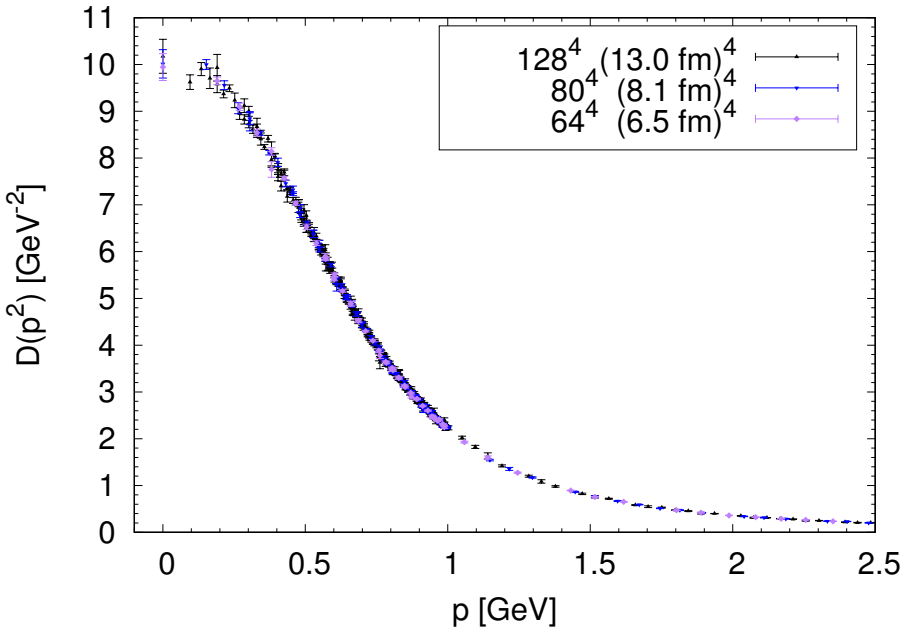

Fig. 5.2 Gluon propagator renormalized at $\mu = 4\,GeV$ for the same lattice spacing ($a = 0.1016(25)$fm) and different volumes.

volume of $V \sim (8fm)^4$ and different lattice spacings, as for the gluon propagator; and another (Fig. 5.4) for the same lattice spacing of $a \sim 0.10fm$ and different volumes.

From Fig. 5.3 (constant physical volume), one may see that a smaller lattice spacing seems to suppress the ghost propagator on the infrared region. On another note, the lattice with larger spacing ($\beta = 5.7$) differs from the others up to 2 GeV in the sense that its data is above the ones from other simulations, so one may say that it provides an upper bound to the continuum correlation function. Notice that this is opposed to the case of the gluon propagator in which the lattice with $\beta = 5.7$ provided a lower bound to the corresponding continuum correlation function. Note that the results corresponding to the two lattices with smaller spacing are compatible within one standard deviation as from momenta above ~ 1 GeV. However, for two standard deviations all dressing functions are compatible for almost the entire range of momenta.

From Fig. 5.4, one may conclude essentially the same as for the gluon propagator. There is no evident dependence on the physical volume. In fact, within one standard deviation the simulations are compatible for the full range of momenta. On a different note, the data corresponding to the largest physical volume seems not as smooth as the others. However, this may be due to its larger errors which is possibly caused by the limited statistical ensemble considered for this largest volume.

For completeness, we also report the dressing functions for all simulations in Fig. 5.5. They seem to be compatible within two standard deviations, except for the lattice corresponding to $\beta = 5.7$.

We would also like to mention the fact that the functional form depicted in (5.4), which concerns the perturbative one-loop result at high momenta, allows us to reproduce the lattice data over a vast range of momenta. In fact, if Λ is taken as a fitting parameter, the functional form may fit the lattice data that runs from approximately $1 GeV$ up to the largest momenta one had available. On the other hand, if one sets $\Lambda \sim \Lambda_{\mathrm{QCD}} \sim 200 MeV$, the functional form fits the lattice data from momenta about $\sim 2 GeV$ up to the largest momenta one simulated. This may be seen as an indication of a behaviour of the ghost propagator which is essencially described by its pertubative form for momenta as small as $\sim 1 GeV$. The plots and respective fittings are presented in Appendix D.

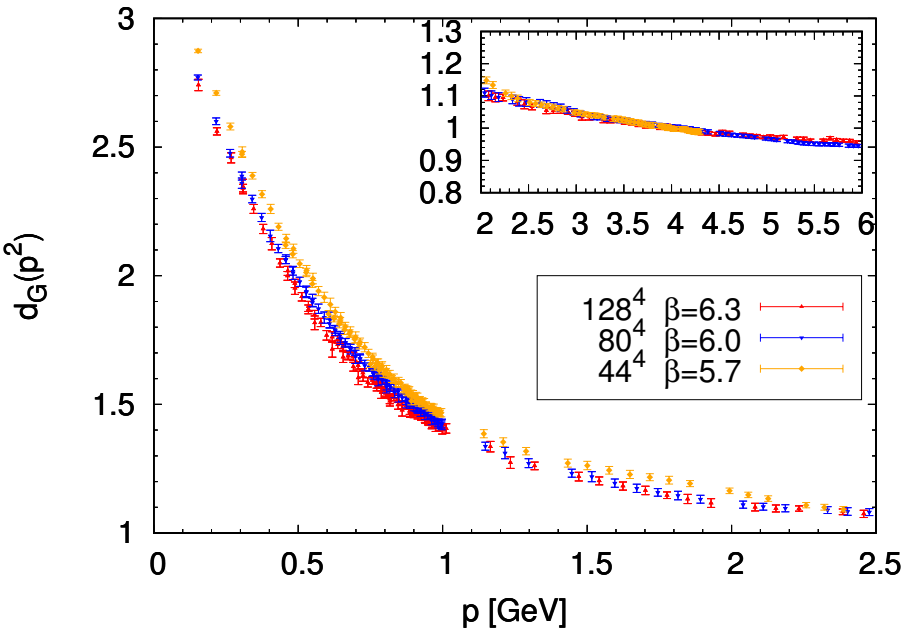

Fig. 5.3 Ghost dressing function renormalized at $\mu = 4 GeV$ for the same physical volume of $(8 fm)^4$ and different lattice spacings.

5.2.3 Running Coupling

Finally, we studied the dependence on the lattice spacing and volume of the running coupling, defined in section 3.5.3. As done in previous cases, one has two graphs with the same characteristics (Fig. 5.6 and Fig. 5.7). Notice that the axis of p^2 is in logarithmic scale.

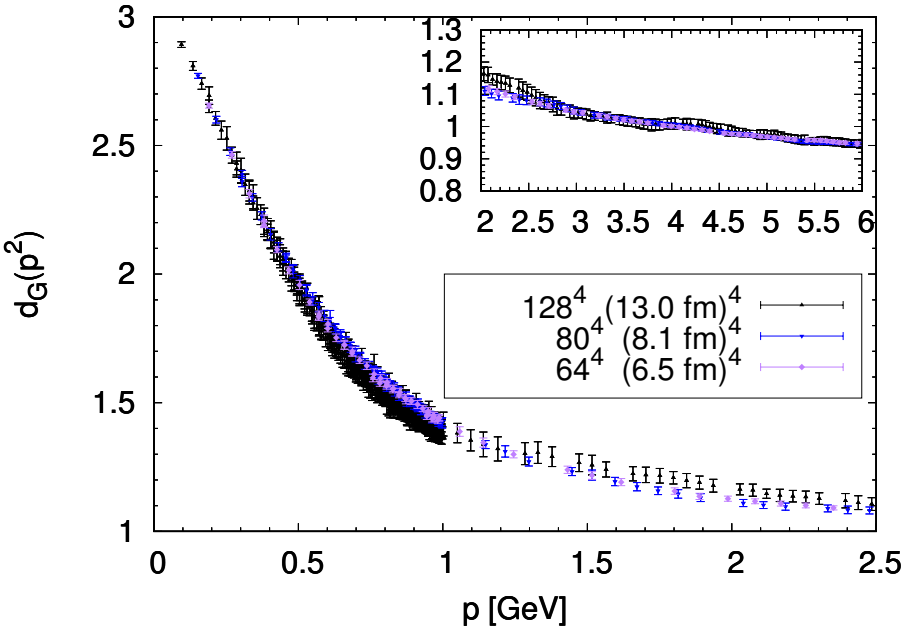

Fig. 5.4 Ghost dressing function renormalized at $\mu = 4\,GeV$ for for the same lattice spacing ($a = 0.1016(25)$fm) and different volumes.

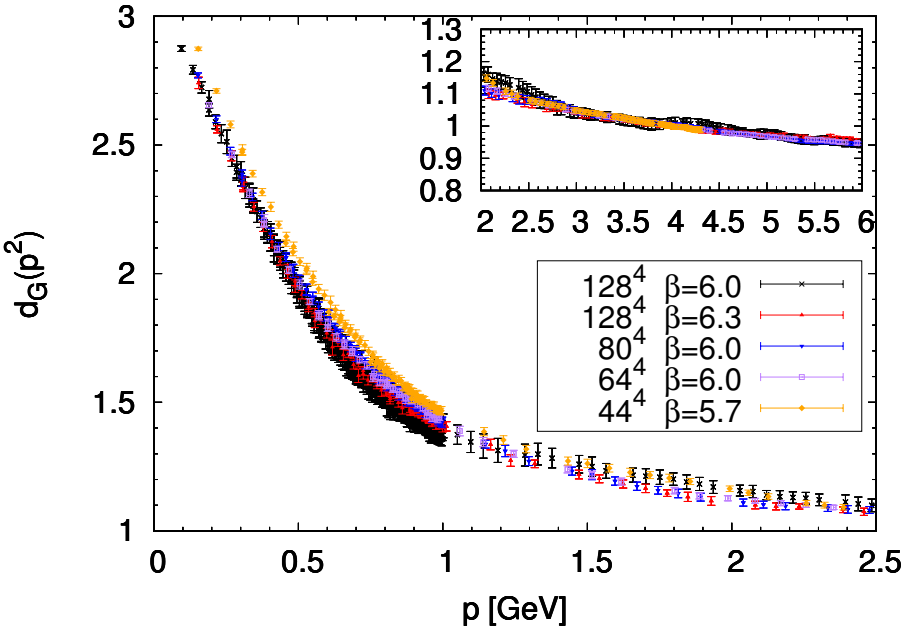

Fig. 5.5 Ghost dressing function renormalized at $\mu = 4\,GeV$ for the simulations reported in Table 5.1.

From Fig. 5.6, one may see that the running coupling is slightly suppressed for smaller lattice spacings in a range of momenta essentially below 1 GeV.

From Fig. 5.7, one concludes the same as for the gluon propagator and the ghost dressing function: no noticeable dependence on the physical volume.

We also studied the dependence on the lattice spacing and physical volume of the position of the maximum of $\alpha_S(p^2)$. There seems to be no significant variation on the position of the maximum. The maximum occurs approximately at $p^2 \sim 250\,\mathrm{MeV}^2$. Nevertheless, its own value seems to be supressed for smaller lattice spacings (i.e. when one gets closer to the continuum limit). In fact, the value of the maximum of the running coupling for $\beta = 6.3$ seems to be about 15% smaller in comparison to the values of the other simulations.

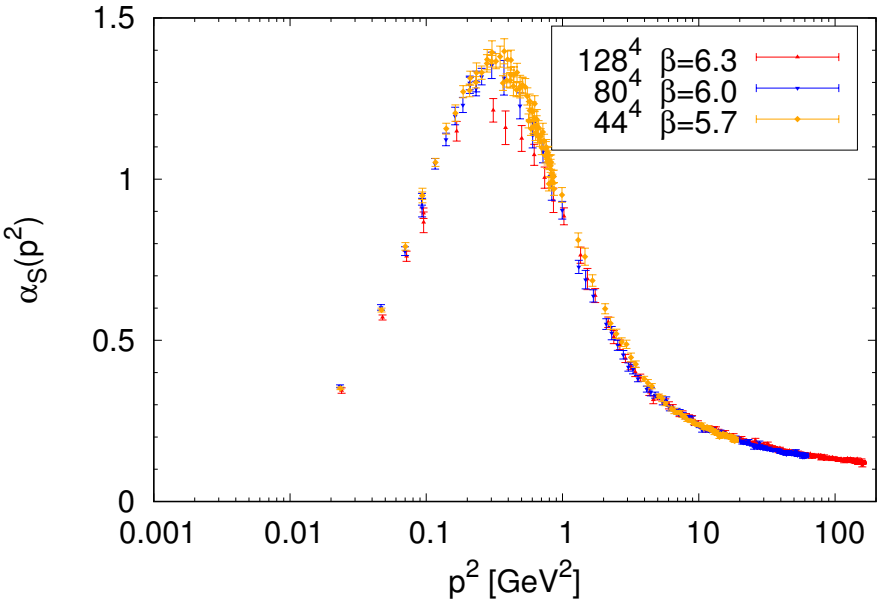

Fig. 5.6 Running coupling for the same physical volume of $(8\,fm)^4$ and different lattice spacings.

5.2.4 Comparison with previous works

In this section, we compare our lattice results with those of [3], which were performed using the largest physical volumes for an $SU(3)$ simulation to date. Before we proceeds with the comparison of the results we obtained with those of the Berlin-Moscow-Adelaide group, it is important to mention that we had to rescale the propagators, due to the use of different definitions of the lattice spacing (which affects the conversion into physical units); we used a different algorithm to compute the maxima of the functional $F[U]$ defined in eq. 3.16, which,

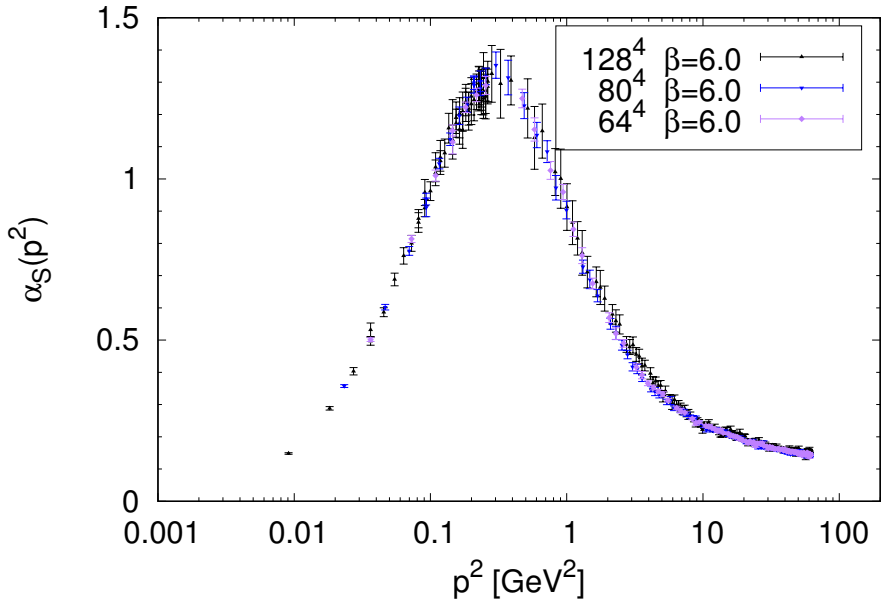

Fig. 5.7 Running coupling for the same lattice spacing of $(a = 0.1016(25)\text{fm})$ and different volumes.

as already discussed (see section 3.4), may cause differences on the values of propagators in the infrared region.

The lattice setup of Berlin-Moscow-Adelaide simulations may be seen in Table 5.5. The values presented are already those resulting of the previously mentioned rescaling.

Gluon Propagator

In order to compare our results with those of Berlin-Moscow-Adelaide, we used the lattice with $\beta = 5.7$ so we could have a plot with the same β value. This plot is presented in

β	a(fm)	1/a(GeV)	L	La(fm)	#Conf Gluon	Ghost
5.7	0.1838(11)	1.0734(63)	64	11.763	14	14
			72	13.234	20	—
			80	14.704	25	11
			88	16.174	68	—
			96	17.645	67	—

Table 5.5 Lattice setup considered by the Berlin-Moscow-Adelaide group [3]. Notice that the values presented in this table are those already rescaled.

Fig. 5.8. In this case, there is a more noticeable dependence on the volume, where one may see a decrease of the propagator in the infrared region when moving through volumes from $(8.1\,fm)^4$ to $(17.6\,fm)^4$. This dependence becomes more distinct for momenta below $\sim 0.4\,GeV$.

We also presents in Fig. 5.9 a plot of all our data sets considering, in addition, the lattice data with the largest volume of the Berlin-Moscow-Adelaide group (the lattice data with $\beta = 5.7$). One may see that all data appears to define a unique curve when looking at momenta above $\sim 0.7\,GeV$. In contrast, when looking at smaller momenta, one may see that data from the two lattices with $\beta = 5.7$ (i.e., with the largest lattice spacing) are always below the remaining ones. In order to obtain the infinite volume limit, we compares the values obtained with the smallest β values and, from that, estimate a value of $\sim 8/9$ as the factor one may multiply by when dealing with propagator with higher values of β (in the infrared region).

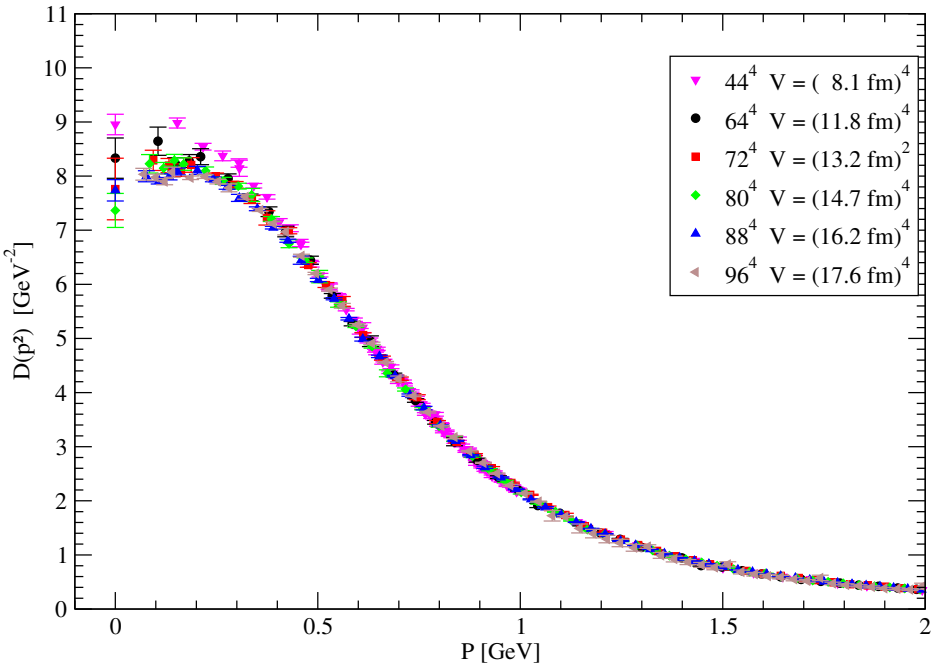

Fig. 5.8 Renormalized gluon propagator for the Berlin-Moscow-Adelaide lattice data. The plot also includes the results of our simulation with the same β value ($\beta = 5.7$). This figure was taken from our article [1].

Ghost Propagator

Unfortunately, in the case of the ghost propagator, it is not possible to rescale the Berlin-Moscow-Adelaide data to compare with our own, for their ghost data goes up to momenta

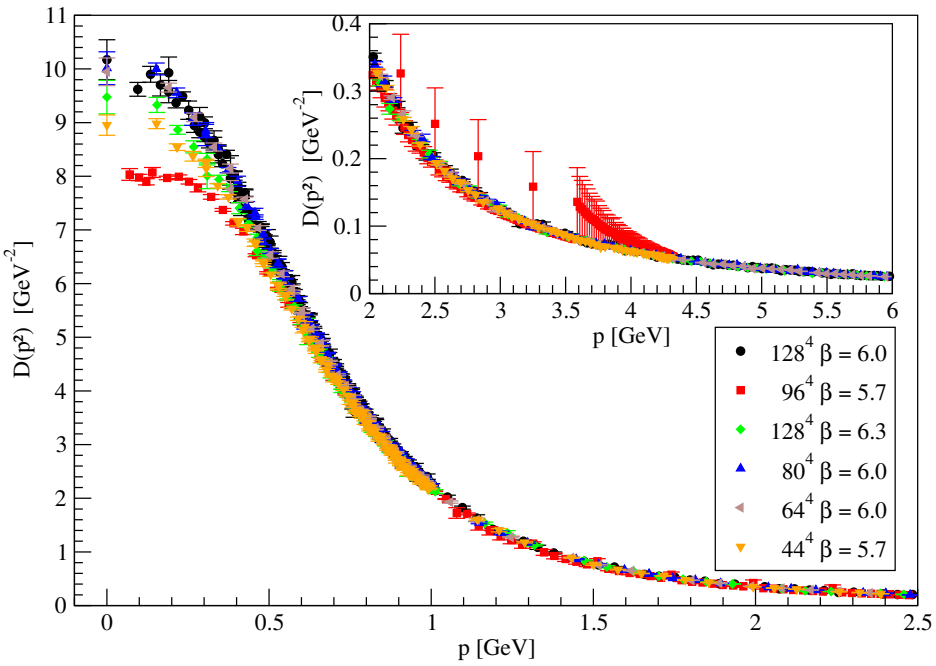

Fig. 5.9 Renormalized gluon propagator for all our data and the data corresponding largest volume of the Berlin-Moscow-Adelaide group. This figure was taken from our article [1].

$\sim 3\,GeV$ for $\beta = 5.7$, 64^4 or $\sim 1.5\,GeV$ for $\beta = 5.7$, 80^4, which is not sufficient due to the fact that we are considering as the renormalization scale $\mu = 4\,GeV$.

Therefore, we used our data for the bare ghost dressing function and rescale it to reproduce their 64^4 value at the highest accessible momentum. These are presented in Fig. 5.10. For higher momenta (above $\sim 0.7\,GeV$), the results seems to define a unique curve.

On the other hand, for smaller momenta, it seems that the increase of the physical volume of the lattice decreases the ghost dressing function. Notice that this volume dependence was not observed in our simulations.

Running Coupling

We gather our results with those obtained by the Berlin-Moscow-Adelaide group for the running coupling in Fig. 5.11. One may see the difference between our results and those obtained by Berlin-Moscow-Adelaide for momenta below $p \sim 1\,GeV$, in which the estimations of the running coupling are smaller than ours. Moreover, there is some noticeable dependence on the lattice volume in the low momenta region if one compares the different lattices with $\beta = 5.7$. For momenta above $p \sim 1\,GeV$ the results from the various lattices become compatible.

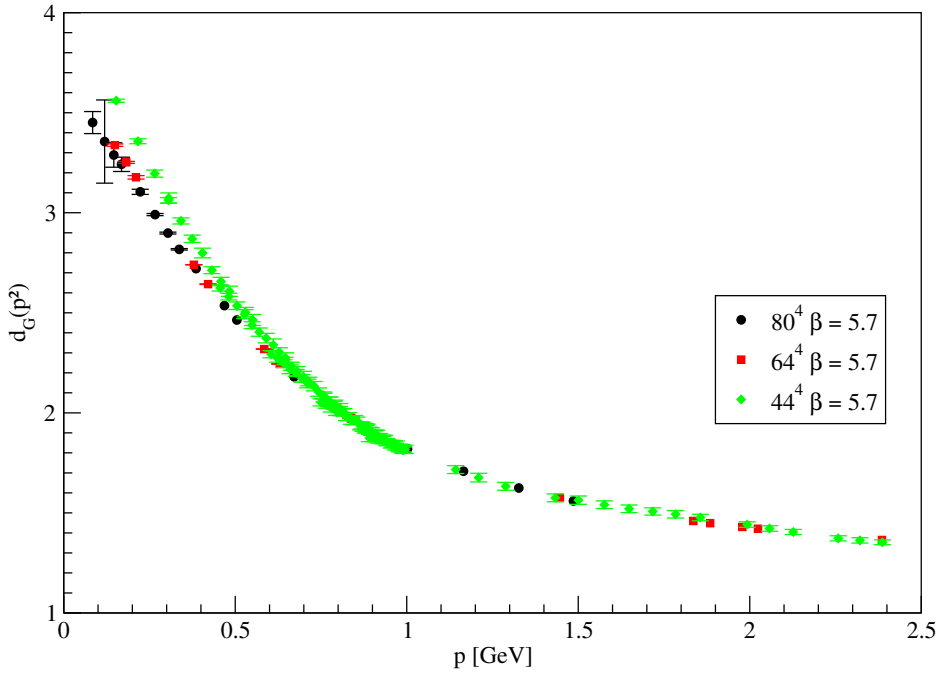

Fig. 5.10 Bare ghost dressing function corresponding to $\beta = 5.7$ simulations. Our lattice was rescaled in order to reproduce the 64^4 Berlin-Moscow-Adelaide numbers at its largest momentum. This figure was taken from our article [1].

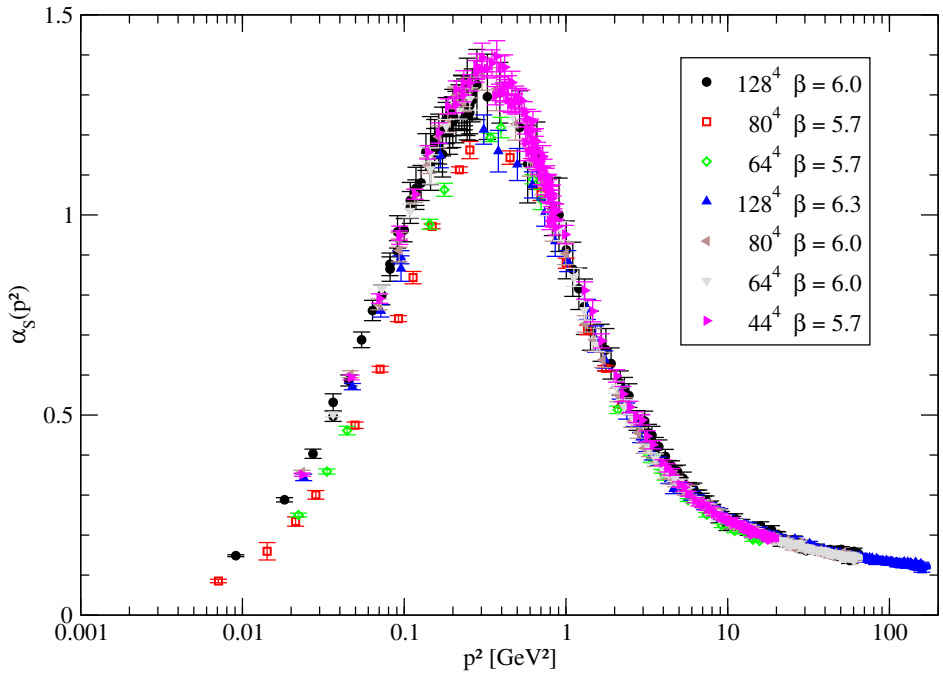

Fig. 5.11 Comparison of the results for the strong coupling computed from the simulations reported in Tab. 5.1 and Tab 5.5. This figure was taken from our article [1].

5.3 The Three Gluon Vertex

In order to study the three gluon vertex, we focused on the three point Green's function $G^{(3)}{}^{a_1a_2a_3}_{\mu_1\mu_2\mu_3}(p_1,p_2,p_3)$ and its corresponding 1PI (one particle irreducible) function, $\Gamma^{(3)}{}^{a_1a_2a_3}_{\mu_1\mu_2\mu_3}(p_1,p_2,p_3)$ (see section 2.6 for more informations). If one is considering a pure Yang-Mills theory, in order to make the gluon Dyson-Schwinger equations finite, it is expected that some form factors related to the three-gluon 1PI change their sign for momentum in the infrared region (and, consequently become zero at a certain point), on the condition that the ghost propagator is essentially described by its tree level form and that the four-gluon vertex is subleading in the IR (see [26, 27]).

We would like to note that in previous works regarding the three gluon 1PI some authors considered a different function (see [28, 29, 25] for more informations).

5.3.1 Results and discussion

In order to study the three gluon vertex, we performed a simulation on a 64^4 and a 80^4 lattices, both for $\beta = 6.0$ (thus, one has a lattice spacing of $a = 0.1016\,fm$). The details of the lattice setup is presented in Table 5.6.

β	a(fm)	1/a(GeV)	L	La(fm)	p_{min}(MeV)	#Conf
6.0	0.1016(25)	1.943(47)	64	6.502	191	2000
			80	8.128	153	279

Table 5.6 Lattice setup used to study the three-gluon vertex.

Gluon propagator and dressing function

The bare gluon propagator and dressing function (in Landau gauge) as a function of momenta are reported in Fig. 5.12 and Fig. 5.13. Once again, one performed the conic cuts for momenta above $1\,GeV$, and included all data below this limit. As one may see, there are no noticeable finite lattice spacing and volume effects. In fact, if one plots $D(p^2)$, distinguishing the different types of momenta, i.e., $(n_x\,0\,0\,0)$, $(n_x\,n_y\,0\,0)$ and $(n_x\,n_y\,n_z\,0)$ from each other, the bare lattice data suggestes a unique curve – see Fig. 5.14.

Three-gluon vertex

In order to study the three point correlation function one considered the case of one vanishing momentum, i.e. $p_2 = 0$. The first lattice study of the three gluon vertex was performed within

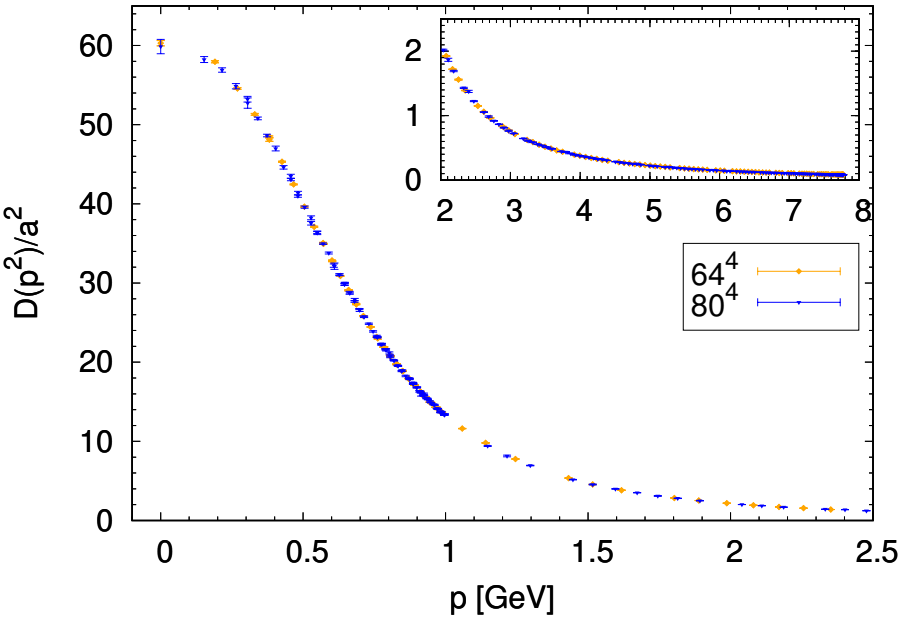

Fig. 5.12 Bare gluon propagator in Landau gauge.

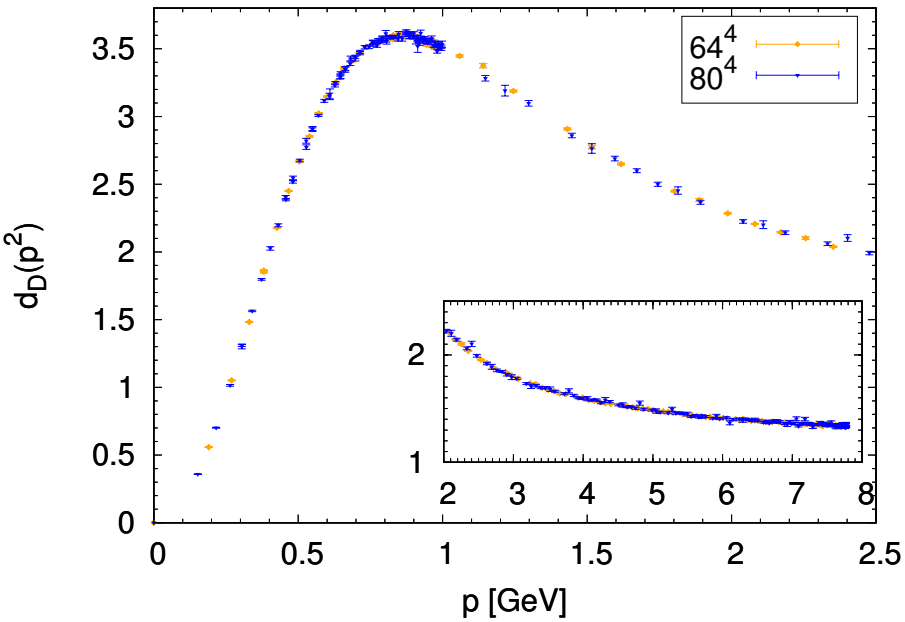

Fig. 5.13 Dressing function $d(p^2) = p^2 D(p^2)$ in Landau gauge.

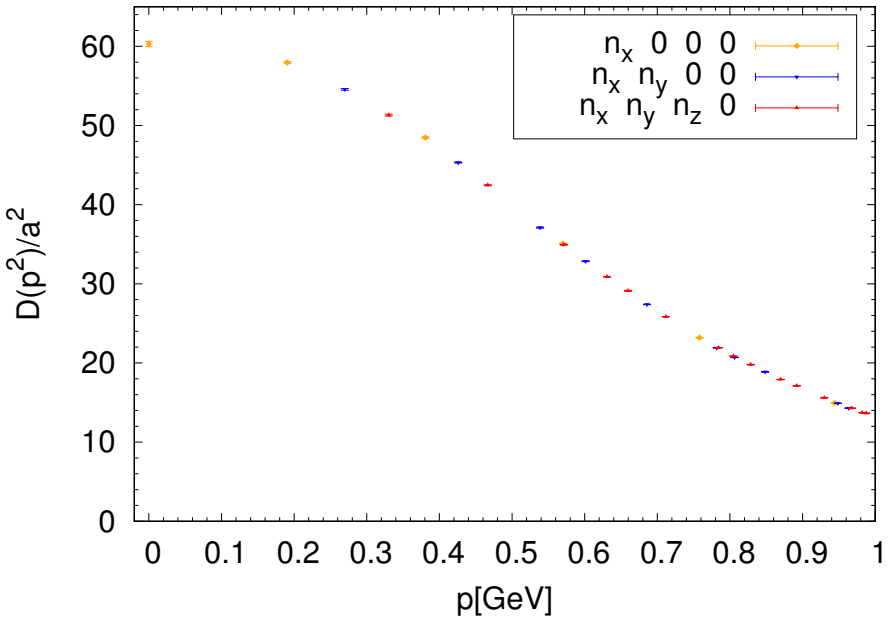

Fig. 5.14 Bare gluon propagator in the Infrared for different types of momenta, performed in the 64^4 lattice, in Landau gauge.

this specific kinematical configuration, where it was used to determine the strong coupling constant [18]. The continuum complete three point Green's function (see section 2.6) in this case depends solely one the knowledge of the following two longitudinal form factors[2],

$$\Gamma(p^2) = 2\left[A(p^2,p^2;0) + p^2 C(p^2,p^2;0)\right] , \tag{5.5}$$

and, therefore, one may write eq. 2.61 as

$$G_{\mu_1\mu_2\mu_3}(p,0,-p) = V\frac{N_c(N_c^2-1)}{4}\left[D(p^2)\right]^2 D(0)\frac{\Gamma(p^2)}{3}p_{\mu_2}P_{\mu_1\mu_3}(p) . \tag{5.6}$$

In order to determine the form factor $\Gamma(p^2)$, one considered the contraction of the indexes as follows,

$$G_{\mu\alpha\mu}(p,0,-p)p_\alpha = V\frac{N_c(N_c^2-1)}{4}\left[D(p^2)\right]^2 D(0)\Gamma(p^2)p^2 , \tag{5.7}$$

where one uses the momentum definition reported in eq. 3.28.

The authors [28, 29] considered in $SU(2)$, instead of $\Gamma(p^2)$, the following function, which results from the contraction of the complete correlation function with the lattice tree level

[2]Notice that one has an overall minus sign when compared with the results reported in (2.58) due to Wick's rotation to Euclidean space.

tensor structure of the three gluon vertex $\Gamma^{(tr)}$ (defined in (2.66)), as follows,

$$R(p^2) = \frac{\Gamma^{(tr)}{}^{a_1a_2a_3}_{\mu_1\mu_2\mu_3}(p,0,-p)G^{a_1a_2a_3}_{\mu_1\mu_2\mu_3}(p,0,-p)}{\Gamma^{(tr)}{}^{a_1a_2a_3}_{\mu_1\mu_2\mu_3}(p,0,-p)D^{a_1b_1}_{\mu_1\nu_1}D^{a_2b_2}_{\mu_2\nu_2}D^{a_3b_3}_{\mu_3\nu_3}\Gamma^{(tr)}{}^{b_1b_2b_3}_{\nu_1\nu_2\nu_3}(p,0,-p)} \,. \tag{5.8}$$

Assuming the continuum expression for the different quantities, and assuming the same decomposition of the 1PI three gluon vertex, one may show that $R(p^2) = \Gamma(p^2)/2$.

In order to compute the form factor $\Gamma(p^2)$, one has to compute the ratio

$$\Gamma(p^2) = \frac{G_{\mu\alpha\mu}(p,0,-p)p_\alpha}{V\frac{N_c(N_c^2-1)}{4}\left[D(p^2)\right]^2 D(0)\,p^2} \,. \tag{5.9}$$

Unfortunately, the computation of this ratio leads to large statistical fluctuations which inhibits us from a good estimation of $\Gamma(p^2)$ at high momenta. As a matter of fact, if one assumes a gaussian error propagation for estimating the statistical error on $\Gamma(p^2)$, denoted by $\delta\Gamma(p^2)$, it follows that[3]

$$\delta\Gamma(p^2) = \frac{1}{\left[D(p^2)\right]^2 p^2}\sqrt{\left[\frac{\delta G_{\mu\alpha\mu}p_\alpha}{D(0)}\right]^2 + \left[2\delta D(p^2)\frac{G_{\mu\alpha\mu}p_\alpha}{D(p^2)D(0)}\right]^2 + \left[\delta D(0)\frac{G_{\mu\alpha\mu}p_\alpha}{\left[D(0)\right]^2}\right]^2} \,, \tag{5.10}$$

and, therefore, for large momenta[4], $\delta\Gamma(p^2) \sim p^2$. One could argue that a very large number of configurations would do the trick for it would lead us to smaller statistical errors for the gluon propagator, however, the statistical errors arising from the three point correlation function dominate and thus $\delta\Gamma(p^2) \sim p^2$. Consequently, in order to solve this issue, for large momentum one may consider instead of $\Gamma(p^2)$ the quantity $\left[D(p^2)\right]^2 D(0)\Gamma(p^2)$. This limitation to the computation of the 1PI of the three gluon in the lattice is a common feature of 1PI functions with larger number of external legs. This pose a problem only for the UV region, for in IR $D(p^2)$ is approximately constant and thus the statistical error may be ameliorated by using larger ensembles of configurations.

Finite size effects on $\Gamma(p^2)$

We would like to study finite size effects that may eventually occur on the computation of $\Gamma(p^2)$ on the lattice. To this end, we plotted $\Gamma(p^2)p^2$ as a function of the momenta in Fig. 5.15 (for the 64^4 data set) and Fig. 5.16 (for the 80^4 data set), for different types of momenta.

[3] Notice that the factor $V\frac{N_c(N_c^2-1)}{4}$ has been omitted.

[4] Recall that for large momenta one has $D(p^2) \sim 1/p^2$.

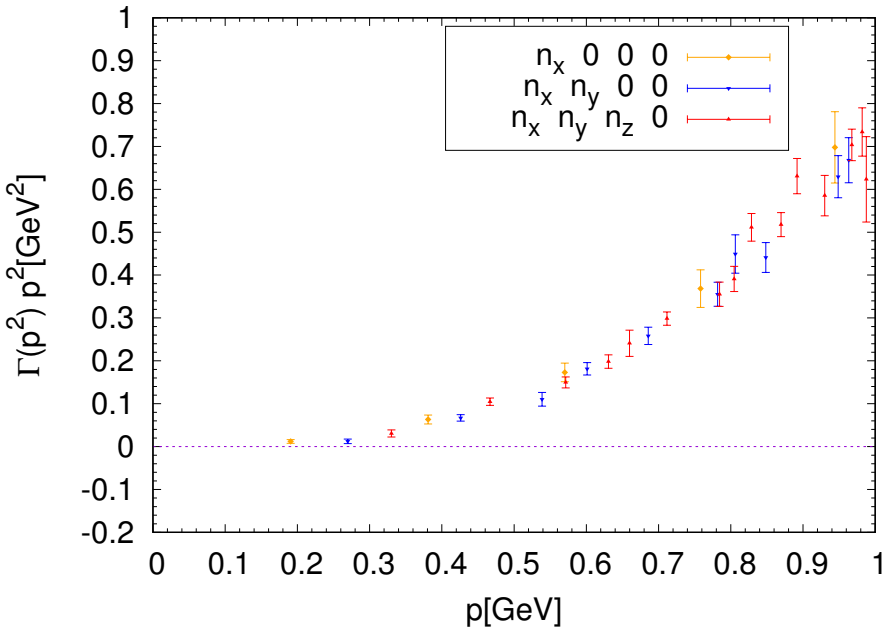

Fig. 5.15 Infrared $\Gamma(p^2)p^2$ computed using the 64^4 data sets for different types of momenta.

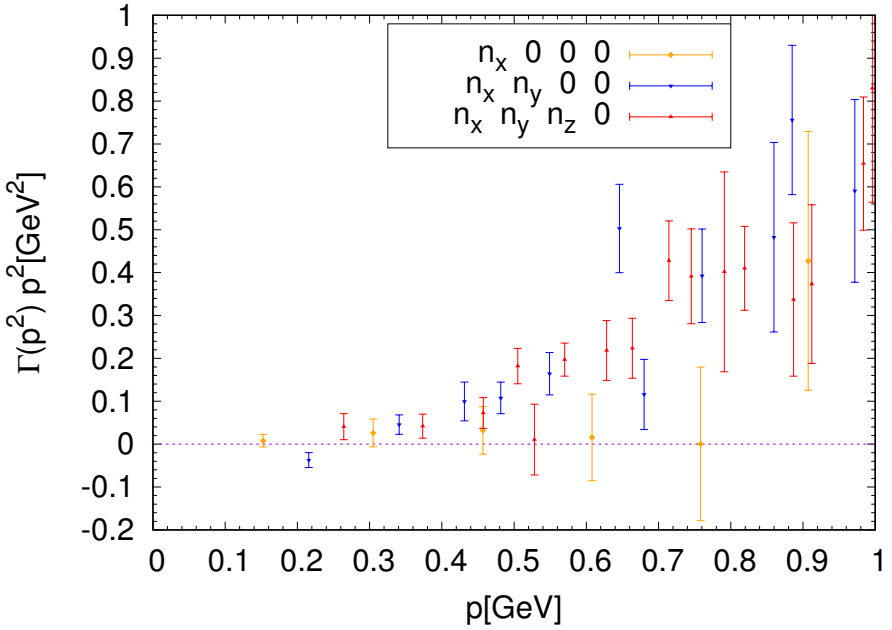

Fig. 5.16 Infrared $\Gamma(p^2)p^2$ computed using the 80^4 data sets for different types of momenta.

In the 64^4 data set one may observe that the $\Gamma(p^2)p^2$ data for momenta of the type $(n\,0\,0\,0)$ is above the data for other types of momenta for the smallest momenta. This may be viewed as an indication of rotational symmetry breaking effects.

Unfortunately, in the 80^4 data set, there is no conclusive observation one may derive due to the fact that the statistical errors are too large and, therefore, becomes compatible with a constant value. Thus, one cannot conclude much about finite size effects in that case.

On both lattices, apart from the momenta of type $(n\,0\,0\,0)$, the results coming from the different type of momenta seems to be essentially the same.

Notice that the difference between the statistial errors corresponding to the two different lattices is due to the difference in the number of configurations available in each ensemble. Moreover, from now on one will ignore the results coming from momenta of type $(n\,0\,0\,0)$, because of the expected larger finite size effect for momenta of this type.

Low momenta region

In order to study $\Gamma(p^2)$ in the low momenta region, one plotted it as a function of momenta in Fig. 5.17 for momenta below $2\,GeV$. One excluded the data corresponding to higher momenta in this analysis, due to their associated large statistical errors, which was already discussed. As one may see, the statistical errors associated with the 80^4 lattice are larger, as expected, and both data sets are substantially compatible within one standard deviation.

On the other hand, for momenta $p = 216MeV$ (of the 80^4 data set) the value of the form factor $\Gamma(p^2)$ becomes negative, $\Gamma(p^2) = -0.80(37)$, being compatible with zero only within 2.2 standard deviations. The closest momenta for the lattices 64^4 and 80^4 gives $\Gamma(p = 270MeV) = 0.171(73)$ and $\Gamma(p = 264MeV) = 0.58(43)$, respectively, which allows us to expect the zero crossing for momenta below $\sim 250MeV$. This is in concordance with the lattice simulation for $SU(3)$ which is described in [25], and the simulations performed in $SU(2)$ described in [28, 29].

However, no zero crossing is observed for the 64^4 data set, which may be due to the fact that no data was in the region of interest. For completeness, we present in Fig. 5.18 the data from the simulation performed on the 64^4 lattice for an extended momentum range.

UV region

As mentioned before, in order to study the three gluon vertex in the UV, one may consider

$$\Gamma_{UV}(p^2) = \left[D(p^2)\right]^2 D(0)\Gamma(p^2)p^2\,. \tag{5.11}$$

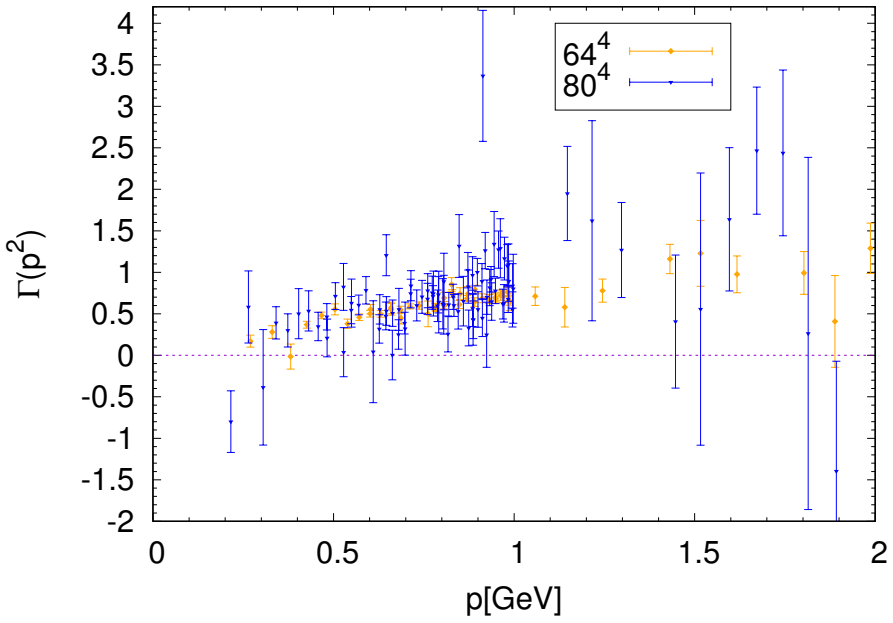

Fig. 5.17 Low momenta $\Gamma(p^2)$ from the 64^4 and 80^4 simulations.

We would like to compare the results obtained from the lattice with the expected from perturbation theory. At high momentum, the one-loop renormalization group improved result reads for the gluon

$$D(p^2) = \frac{Z}{p^2}\left[\ln\frac{p^2}{\mu^2}\right]^{-\gamma}, \tag{5.12}$$

where μ is a renormalization scale, Z is a constant and $\gamma = 13/22$ is the gluon anomalous dimension; and for $\Gamma(p^2)$,

$$\Gamma(p^2) = Z'\left[\ln\frac{p^2}{\mu^2}\right]^{\gamma_{3g}}, \tag{5.13}$$

where Z' is a constant and γ_{3g} is the anomalous dimension which is $\gamma_{3g} = 17/44$. Using the aforementioned results for $\Gamma_{UV}(p^2)$ it follows straighforwardly that for high momentum one has

$$\Gamma_{UV}(p^2) = \frac{Z''}{p^2}\left[\ln\frac{p^2}{\mu^2}\right]^{\gamma'}, \tag{5.14}$$

where Z'' is a constant and $\gamma' = \gamma_{3g} - 2\gamma = -35/44$.

Thus, in order to compare our results with the prediction of the renormalisation group improved perturbation theory and also of the tree level estimation of $\Gamma_{UV} = Z/p^2$, we present these in Fig. 5.19. Notice that we set the normalization constants to reproduce the lattice

result one obtained for momenta $p \sim 5\,GeV$ and used the value $\mu = 0.22\,GeV$ in order to generate the renormalization group improved result.

From the plot one may see that the data follows the prediction of perturbation theory for p above $\sim 2.5\,GeV$. This may be seen as a corroboration of the perturbative approach to QCD in the region of high momenta.

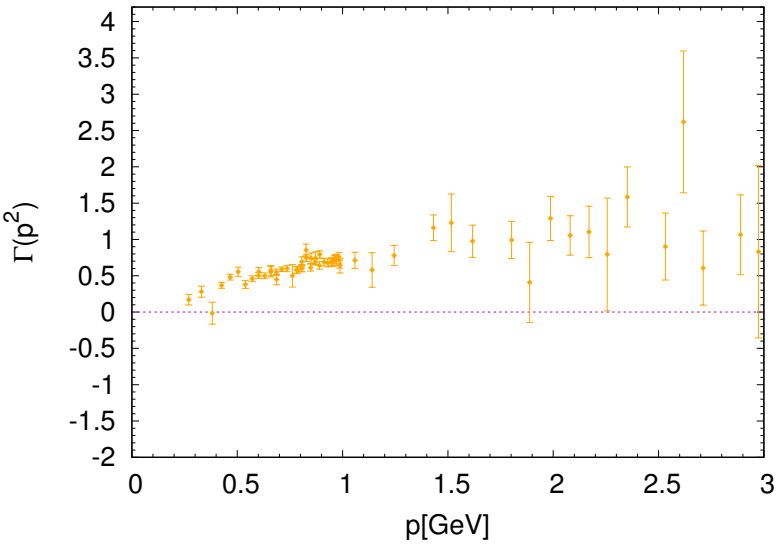

Fig. 5.18 $\Gamma(p^2)$ from the 64^4 simulation.

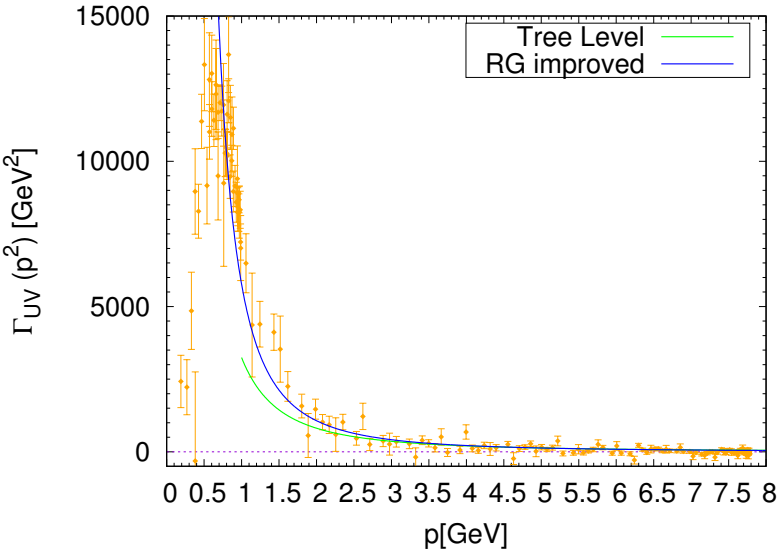

Fig. 5.19 $\Gamma_{UV}(p^2)$ from the 64^4 simulations. The curves represent predictions from perturbation theory. "RG imporved" stands for the one-loop renormalization group improved result.

Conclusion

In this work, we used lattice QCD techniques to study two and three-point correlation functions in Landau gauge.

In the first part of the work developed for this dissertation, we studied the dependence of the gluon propagator, ghost propagator and the running coupling on the lattice spacing and on the physical volume in a pure $SU(3)$ Yang-Mills theory in the Landau gauge. To this end, we ignored the contribution due to the presence of Gribov copies, which may be important when computing the propagators (and possibly the running coupling) [64–66, 84]. However, we ignored it, for the computational time required to analyse the effects of Gribov copies is extensive for the large lattices used, so that we cannot discern its contribution in the results we obtained.

The study of the gluon propagator reports essentially the behaviour observed in [10]. The data used shows no noticeable dependence on the physical volume, at least for the volumes we used which were above $(6.5\,fm)^4$, and for the range of momenta which were available. However, we could discern a non-trivial dependence on the lattice spacing in the infrared region and we observed that the lattice with the largest lattice spacing underestimates the value of the propagator.

In what concerns the ghost propagator, we may say that its data showed no evident dependence on the lattice volume, as well. However, we may see that the ghost propagator is supressed when the lattice spacing decreases, as opposed to what happened to the gluon propagator. On the other hand, the ghost propagator seems to be described by its perturbative expression (5.4) for momenta as small as ~ 1 GeV.

The results we obtained for the running coupling show no noticeable dependence on the lattice spacing and the physical volume for the position of its maximum. However, despite being seemingly independent of both variables, the value itself of the running coupling seems to be supressed as one gets closer to the continuum limit.

We may estimate how much the propagators are altered by changing the lattice spacing from Fig. 5.1 and Fig. 5.3: a change of $\sim 10\%$ from the decrease of the lattice spacing from $0.18\,fm$ to $0.06\,fm$ for the gluon propagator for zero momentum; a change of 7% for

the ghost propagator at the lower momenta accessible in the simulations we perfomed. In what concerns the running coupling, the value of the maximum of the running coupling for $\beta = 6.3$ seems to be about 15% smaller in comparison to the values of the other simulations.

Finally, we compared the results we obtained with those of the Berlin-Moscow-Adelaide group, which used the largest physical volume to date to simulate pure Yang-Mills theory in $SU(3)$ [3]. We obtained different results from theirs at low momenta. However, the qualitative behaviour of the quantities considered are similar. We can see that both results for the gluon and ghost propagators shows no depencence (or, at most, mild) on the physical volume. The differences between the values may be explained by the usage of distinct algorithms to perform gauge-fixing, which is related to the Gribov noise. If we compare directly the results we obtained with those of the Berlin-Moscow-Adelaide group, for $\beta \sim 5.7$, we may see that, at low momenta, the gluon propagator in the infinite volume limit should be supressed; the ghost propagator in the infinite volume limit should be enhanced.

In what concerns the study of the three gluon vertex, we used two different lattices, one with volume $(6.5\,fm)^4$ and the other with $(8.2\,fm)^4$. However, both had the same lattice spacing ($a = 0.102\,fm$), so that the study of possible effects arising from the use of a finite lattice spacing was infeasible. On the other hand, the study of the gluon propagators in these lattices (with a larger number of configurations than the ones used in the first part of the work – see Table 5.1 and Table 5.6) show no noticeable finite physical effects, and both results become compatible within one standard deviation. This is in good agreement with the previous results obtained.

We computed the three gluon one particle irreducible function and the results showed that it depended on the type of momenta considered in the infrared region. This was justified by rotational symmetry breaking effects. Notice that we had an overestimation of the 1PI function for the data related to momenta of the type $(n\,0\,0\,0)$ when compared to the other types, in the infrared region.

On the other hand, we observed a negative 1PI function for the 80^4 lattice and estimated the zero crossing at $p \sim 250\,MeV$. As mentioned before, there has been some studies that reported this change of sign, namely: lattice simulations of the pure Yang-Mills theory in four dimension for $SU(3)$ gauge group in [25]; lattice simulations of the pure Yang-Mills theory in three dimensions for $SU(2)$ gauge group in [28, 29]. These all seems to agree on the momentum scale for the zero crossing. These change of sign, again, is expected in order to get a properly defined Dyson-Schwinger equation for the gluon propagator [26, 27].

Finally, we studied the lattice data in the high momentum region in order to see its compatibility with the prediction of the renormalization group improved perturbation theory.

The data seems to corroborate the perturbative approach to quantum chromodynamics in the UV region.

Recall that we argued that the evaluation of the one particle irreducible function leads to a limitation of its calculation in the UV region. In fact, we discussed that within this region, the one particle irreducible function is associated with large statistical errors which could not be ameliorated with a larger set of configurations. To solve this issue, one may consider, for higher momenta, combinations of the 1PI function and correlation functions associated with a smaller number of external legs. This combination may still provide useful information about the behaviour of the 1PI in the UV region. In fact, the data is well-described by the predictions of perturbation theory for momenta starting essentially at $2.5\,GeV$, which may be seen as a corroboration of the perturbative approach to QCD in the region of high momenta.

As an extension of the work discussed in this dissertation, one could seek a way of improving the large statistical errors associated with the one particle irreducible function in the UV region, which, as discussed, goes beyond an increase on the number of configurations used (see [85]). One could also compute the three-gluon vertex for other kinemetical configurations. It would also be interesting to use some improved action instead of the Wilson one and study the differences. Another evident further work would be to study the four-vertex gluon.

References

[1] A. G. Duarte, O. Oliveira, and P. J. Silva, "Lattice gluon and ghost propagators, and the strong coupling in pure su(3) yang-mills theory: Finite lattice spacing and volume effects," *Phys. Rev. D 94, 014502 (2016)* , arXiv:1605.00594v1.

[2] A. G. Duarte, O. Oliveira, and P. J. Silva, "Further evidence for zero crossing on the three gluon vertex," arXiv:1607.03831v1.

[3] I. Bogolubsky, E.-M. Ilgenfritz, M. Müller-Preussker, and A. Sternbeck, "Lattice gluodynamics computation of Landau-gauge Green's functions in the deep infrared," *Phys.Lett.B676:69-73* (2009) , arXiv:0901.0736v3.

[4] A. Cucchieri and T. Mendes, "What's up with IR gluon and ghost propagators in Landau gauge? A puzzling answer from huge lattices," *PoS LAT2007:297* (2007) , arXiv:0710.0412 [hep-th].

[5] A. Cucchieri, T. Mendes, O. Oliveira, and P. Silva, "Just how different are SU(2) and SU(3) Landau-gauge propagators in the IR regime?," *Phys. Rev.D76:114507* (2007) , arXiv:0705.3367v2.

[6] D. Dudal, O. Oliveira, and N. Vandersickel, "Indirect lattice evidence for the Refined Gribov-Zwanziger formalism and the gluon condensate $\langle A^2 \rangle$ in the Landau gauge," *Phys. Rev.D81:074505* (2010) , arXiv:1002.2374v2.

[7] E.-M. Ilgenfritz, C. Menz, M. Müller-Preussker, A. Schiller, and A. Sternbeck, "SU(3) Landau gauge gluon and ghost propagators using the logarithmic lattice gluon field definition," *Phys. Rev.D83:054506* (2011) , arXiv:1010.5120v2.

[8] O. Oliveira and P. Bicudo *J. Phys. G38, 045003* (2011) .

[9] A. Cucchieri, D. Dudal, T. Mendes, and N. Vandersickel, "Modeling the Gluon Propagator in Landau Gauge: Lattice Estimates of Pole Masses and Dimension-Two Condensates," *Phys. Rev D.85, 094513* (2011) , arXiv:1111.2327.

[10] O. Oliveira and P. J. Silva, "The lattice Landau gauge gluon propagator: lattice spacing and volume dependence," *Phys. Rev D.86, 114513* (2012) , arXiv:1207.3029.

[11] A. Sternbeck and M. Müller-Preussker *Phys. Lett. B726, 396* (2013) .

[12] A. Sternbeck, E.-M. Ilgenfritz, and M. Mueller-Preussker, "Spectral properties of the Landau gauge Faddeev-Popov operator in lattice gluodynamics," *Phys. Rev. D73, 014502* (2006) , hep-lat/0510109.

[13] O. Oliveira and P. J. Silva, "Exploring the infrared gluon and ghost propagators using large asymmetric lattices ," *Braz.J.Phys.37:201-207* (2007) , hep-lat/0609036.

[14] T. M. Attilio Cucchieri, "Constraints on the IR behavior of the ghost propagator in Yang-Mills theories ," *Phys. Rev.D78, 094503* (2008) , arXiv:0804.2371.

[15] A. Cucchieri and T. Mendes *Phys. Rev D.88, 114501 (2013)* , arXiv:1308.1283.

[16] A. Cucchieri, D. Dudal, T. Mendes, and N. Vandersickel, "Modeling the Landau-Gauge Ghost Propagator in 2, 3 and 4 Space-Time Dimensions ," *Phys. Rev. D 93, 094513 (2016)* , arXiv:1602.01646.

[17] C. Parrinello *Phys. Rev D.50, R4247* (1994) .

[18] B. Allés, D. S. Henty, H. Panagopoulos, C. Parrinello, C. Pittori, and D. G. Richards *Nucl. Phys. B502, 325* (1997) .

[19] P. Boucaud, A. L. Yaouanc, J. Leroy, J. Micheli, O. Pène, and J. Rodríguez-Quintero *Phys. Lett. B493, 315* (2000) .

[20] F. de Soto and J. Rodríguez-Quintero *Phys. Rev. D64, 114003* (2001) .

[21] R. Alkofer, C. S. Fischer, and F. J. Llanes-Estrada, "Dynamically induced scalar quark confinement," *Mod.Phys.Lett. A23:1105-1113* (2008) , hep-ph/0607293.

[22] C. Kellermann and C. Fischer *Phys. Rev. D78, 025015* (2008) .

[23] J. m. Cornwall, "The QCD running charge and its RGI three-gluon vertex parent in the Pinch Technique," hep-ph/1211.2019.

[24] P. Boucaud, M. Brinet, F. D. Soto, V. Morenas, O. Pène, K. Petrov, and J. Rodríguez-Quintero *JHEP 1404, 086* (2014) .

[25] A. Athenodorou, D. Binosi, P. Boucaud, F. D. Soto, J. Papavassiliou, J. Rodriguez-Quintero, and S. Zafeiropoulos, "On the zero crossing of the three-gluon vertex," *Phys. Lett. B 761, 444-449 (2016)* .

[26] D. Binosi, D. Ibañez, and J. Papavassiliou *Phys. Rev. D87, 125026* (2013) .

[27] A. Aguilar, D. Binosi, D. Ibañez, and J. Papavassiliou *Phys. Rev. D89, 085008* (2014) .

[28] A. Cucchieri, A. Maas, and T. Mendes *Phys. Rev. D74, 0145003* (2006) .

[29] A. Cucchieri, A. Maas, and T. Mendes *Phys. Rev. D77, 094510* (2008) .

[30] A. Blum, M. Q. Huber, M. Mitter, and L. von Smekal *Phys. Rev. D89, 061703(R)* (2014) .

[31] G. Eichmann, R. Williams, R. Alkofer, and M. Vujinovic *Phys. Rev. D89, 105014* (2014) .

[32] D. R. Campagnari and H. Reinhardt *Phys. Rev. D82, 105021* (2010) .

[33] M. Peláez, M. Tissier, and N. Wschebor *Phys. Rev. D88, 125003* (2013) .

[34] R. Williams, C. S. Fischer, and W. Heupel *Phys. Rev. D93, 034026 (2016)* .

[35] J. Ball and T.-W. Chiu *Phys. Rev. D22, 2550 (1980)* .

[36] M. E. Peskin and D. V. Schroeder, *An Introduction to Quantum Field Theory*. Addison-Wesley, 1996.

[37] A. Das, *A path integral approach (2nd ed.)*. World Scientific, 2006.

[38] R. P. S. Mahler, *Statistical Multisource - Multitarget Information Fusion*. Artech House, 2007.

[39] S. Coleman and D. J. Gross. *Phys. Rev. Lett. 31 (1973) 851. (Sec. 1.1)* .

[40] L. Faddeev and V. Popov *Phys. Lett. B 25, 29 (1967)* .

[41] F. Mandl and G. Shaw, *Quantum Field Theory (2nd edition)*. Wiley, 2010.

[42] V. Kaplunovsky, "Functional quantization.". http://bolvan.ph.utexas.edu/~vadim/Classes/2017s/fq.pdf.

[43] P. Pascual, *QCD: Renormalization for the Practitioner*. Springer-Verlag Berlin Heidelberg New York Tokyo, 1984.

[44] T. Muta, *Foundations of Quantum Chromodynamics: An Introduction to Perturbative Methods in Gauge Theories*. World Scientific, 1987.

[45] P. de Jesus Henriques da Silva, *"Cópias de Gribov, Propagadores de Gluões e de Campos Fantasma, Sinais de Confinamento e Algoritmos para a Escolha da Gauge em Cromodinâmica Quântica sem Campos Fermiónicos na Rede"*. PhD thesis, Universidade de Coimbra, Department of Physics, 2007.

[46] W. Celmaster and R. J. Gonsalves *Phys. Rev. D20, 1420 (1979); Phys. Rev. Lett. 42, 1435 (1980)* .

[47] W. Greiner, S. Schramm, and E. Stein, *Quantum Chromodynamics (2nd edition)*. Springer.

[48] C. Gattringer and C. Lang, *Quantum Chromodynamics on the Lattice: An Introductory Presentation*. Springer.

[49] O. Oliveira and P. J. Silva, "A global optimization method for landau gauge fixing in lattice qcd," *Comput. Phys. Commun. 158 (2004) 73-88* , `arXiv:hep-ph/0309184v3`.

[50] J. E. Mandula *Phys. Rep. 315 (1999) 273* , `arXiv:hep-lat/9907020`.

[51] H. Suman and K. Schilling *Phys. Lett. B373* (1996) , `arXiv:hep-lat/9512003`.

[52] J. Bloch, "Multiplicative renormalizability and quark propagator," *Phys. Rev. D66 034032* (2002) , `arXiv:hep-ph/0202073v2`.

[53] J. Glimm and A. Jaffe, *Quantum Physics. A Functional Integral Point of View (2nd edition)*. (Springer, New York 1987) 21.

[54] K. Osterwalder and E. Seiler *Ann. Phys. 110, 440 (1978) 21* .

[55] V. Gribov *Nucl. Phys, B139 1*. (1978) .

[56] Semyonov-Tian-Shansky and Franke *Proc. Seminars of the Leningrad Math. Inst. (Plenum, New York, 1986) [English translation]* .

[57] G. Dell'Antonio and D. Zwanziger *Comm. Math. Phys. 138 (1991) 291.* .

[58] P. van Baal *Nucl. Phys. B369 (1992) 259* .

[59] P. van Baal *Nucl. Phys. B417 (1994) 215* .

[60] P. van Baal `hep-th/9511119`.

[61] D. Zwanziger *Nucl. Phys. B378 (1992) 525* .

[62] D. Zwanziger *Nucl. Phys. B412 (1994) 657* .

[63] A. Cucchieri *Nucl. Phys. B521 (1998) 365* , `hep-lat/9711024`.

[64] P. J. Silva and O. Oliveira *Nucl. Phys. B690, 177 (2004)* .

[65] P. J. Silva and O. Oliveira *PoS LAT2007 (2007) 333* .

[66] A. Sternbeck and M. Müller-Preussker *Phys. Lett. B726, 396-403 (2013)* .

[67] R. Barrett *et al.*, *Templates for the Solution of Linear Systems: Building Blocks for Iterative Methods*. (SIAM, Philadelphia 1994).

[68] J. Nocedal and S. J. Wright, *Numerical Optimization*. Springer.

[69] A. Cucchieri *Nucl. Phys. B508 (1997) 353* , `hep-lat/9705005`.

[70] A. Kennedy, J. Kuti, S. Meyer, and B. J. Pendleton, "Program for efficient monte carlo computations of quenched $su(3)$ lattice gauge theory using the quasi-heatbath method on a cdc cyber 205 computer," *J. Comp. Phys 64 133-160* (1986) .

[71] A. D. Kennedy, "Algorithms for dynamical fermions," `arXiv:hep-lat/0607038v2`.

[72] N. Cabibbo and E. Marinari, "A new method for updating su(n) matrices in computer simulations of gauge theories," *Phys. Lett. B 119, 387 (1982) 88* .

[73] B. Efron, *The Jackknife, the Bootstrap and Other Resampling Plans*. Department ot Statistics - Stanford University.

[74] B. Efron and R. Tibshirani, *An Introduction to the bootstrap*. Chapman & Hall.

[75] A. C. Davison and D. V. Hinkley, *Bootstrap Methods and their Applications*. Cambridge University Press.

[76] M. R. Chernick, *Bootstrap Methods: A Guide for Practitioners and Researchers (2nd Edition)*. Wiley.

[77] R. Petronzio and E. Vicari *Phys. Lett. B 248, 159 (1990) 89* .

[78] C. Davies, G. Batrouni, G. Katza, A. S. Kronfeld, G. Lepage, and et al., "Fourier acceleration in lattice gauge theories. i. landau gauge fixing," *Phys. Rev. D37 (1988) 1581.* .

[79] G. S. Bali and K. Schilling *Phys. Rev. D47, 661 (1993)* .

[80] P. J. Silva, O. Oliveira, P. Bicudo, and N. Cardoso *Phys. Rev. D89, 074503 (2014)* , arXiv:1310.5629.

[81] R. G. Edwards and B. Joó *(SciDAC Collaboration, LHPC Collaboration, UKQCD Collaboration) Nucl. Phys. Proc. Suppl. 140, 832 (2005)* , arXiv: hep-lat/0409003.

[82] M. Pippig *SIAM J. Sci. Comput. 35, C213 (2013)* .

[83] D. B. Leinweber, J. I. Skullerud, A. G. Williams, and C. Parrinello *Phys. Rev. D58, 031501 (1998)* .

[84] A. Sternbeck, E. M. Ilgenfritz, M. Müller-Preussker, and A. Schiller *Phys. Rev. D72, 014507 (2005)* , arXiv: hep-lat/0506007.

[85] A. Sternbeck, "Triple-gluon and quark-gluon vertex from lattice qcd in landau gauge - lattice 2016, southampton (uk).". https://conference.ippp.dur.ac.uk/event/470/session/17/contribution/286/material/slides/0.pdf.

[86] J. R. Magnus and H. Neudecker, *Matrix Differential Calculus with Applications in Statistics and Econometrics*. Wiley.

Appendix A

The Group SU(N)

The group $SU(N)$ stands for the group of $N \times N$ unitary matrices with determinant $det = 1$ in which the group operation is the matrix multiplication. Every matrix U of the group may be represented with the help of the generators t^a, $a = 1..., N^2 - 1$,

$$U(\alpha) = \exp(i\alpha^a t^a) \,, \tag{A.1}$$

where α are group parameters. Within this representation (A.1), the generators must be hermitian for the matrix is unitary. On the other had, the fact that $\det(U) = 1$ implies that the generators t^a must be traceless. The generators obey the following algebra

$$[t^a, t^b] = if^{abc}t^c \,, \tag{A.2}$$

and have the following normalization

$$\mathrm{tr}[t^a t^b] = \frac{1}{2}\delta^{ab} \,. \tag{A.3}$$

Notice that f^{abc} are the structure constant of the group (antisymmetric). One may write the completeness relation as well[1]

$$t^a_{ij} t^a_{kl} = \frac{1}{2}\delta_{il}\delta_{jk} - \frac{1}{2N}\delta_{ij}\delta_{kl} \,. \tag{A.4}$$

On the other hand, one may define the anticommutator as

$$\left\{t^a, t^b\right\} = \frac{1}{N}\delta^{ab} + d^{abc}t^c \,. \tag{A.5}$$

[1] Notice one uses upper indices to indicate the generator and lower indices to indicate the element of the matrix.

From the aforementioned relations one may derive the following identities

$$t^a_{ij}t^a_{jk} = \frac{N^2-1}{2N}\delta_{ik}\,; \tag{A.6}$$

$$\mathrm{tr}[t^a t^a] = \frac{N^2-1}{2}\,; \tag{A.7}$$

$$f^{acd}f^{bcd} = N\delta^{ab}\,; \tag{A.8}$$

$$f^{abc}f^{abc} = N(N^2-1)\,. \tag{A.9}$$

For $SU(3)$, the fundamental representation may be written as the following standard basis

$$t^1 = \frac{1}{2}\begin{pmatrix} 0 & 1 & 0 \\ 1 & 0 & 0 \\ 0 & 0 & 0 \end{pmatrix} \; t^2 = \frac{1}{2}\begin{pmatrix} 0 & -i & 0 \\ i & 0 & 0 \\ 0 & 0 & 0 \end{pmatrix} \; t^3 = \frac{1}{2}\begin{pmatrix} 1 & 0 & 0 \\ 0 & -1 & 0 \\ 0 & 0 & 0 \end{pmatrix}$$

$$t^4 = \frac{1}{2}\begin{pmatrix} 0 & 0 & 1 \\ 0 & 0 & 0 \\ 1 & 0 & 0 \end{pmatrix} \; t^5 = \frac{1}{2}\begin{pmatrix} 0 & 0 & -i \\ 0 & 0 & 0 \\ i & 0 & 0 \end{pmatrix}$$

$$t^6 = \frac{1}{2}\begin{pmatrix} 0 & 0 & 0 \\ 0 & 0 & 1 \\ 0 & 1 & 0 \end{pmatrix} \; t^7 = \frac{1}{2}\begin{pmatrix} 0 & 0 & 0 \\ 0 & 0 & -i \\ 0 & i & 0 \end{pmatrix} \; t^8 = \frac{1}{2\sqrt{3}}\begin{pmatrix} 1 & 0 & 0 \\ 0 & 1 & 0 \\ 0 & 0 & -2 \end{pmatrix}$$

And the antisymmetric structure constants are given by:

$$\begin{aligned} &f^{123} = 1; \\ &f^{147} = f^{165} = f^{246} = f^{257} = f^{345} = f^{376} = \frac{1}{2}; \\ &f^{458} = f^{678} = \frac{\sqrt{3}}{2}\,. \end{aligned}$$

and the remaining are zero unless related by antisymmetric permutation of indices. The symmetric structure constants are given by:

$$
\begin{aligned}
&d^{118} = d^{228} = d^{388} = -d^{888} = \frac{1}{\sqrt{3}};\\
&d^{448} = d^{558} = d^{668} = d^{778} = -\frac{1}{2\sqrt{3}};\\
&d^{146} = d^{157} = -d^{247} = d^{256} = d^{344} = d^{355} = -d^{366} = -d^{377} = \frac{1}{2}\,.
\end{aligned}
$$

and are zero otherwise.

Appendix B

Some proofs and calculations

This appendix includes some proofs and calculations one did not present in the theoretical chapters.

B.1 Weyl Ordering

A Hamiltonian is said to be Weyl ordered (which one represents by $H(p,q)_{\mathscr{W}}$) if it contains all possible combinations of the products of coordinates and momenta (divided by the number of such possibilities). One wants to prove that (see 1.2)

$$\langle q|\, H(p,q)_{\mathscr{W}}\, |q'\rangle = \int \frac{dp}{2\pi} e^{ip(q-q')} H\left(p, \frac{q+q'}{2}\right) . \tag{B.1}$$

Notice that one may relate Weyl-ordering with the binomial formula for non-commutative p and q

$$(\alpha q+\beta p)^N = \sum_{i+j=N} \frac{N!}{i!\,j!} \alpha^i \beta^j (x^i p^j)_{\mathscr{W}} . \tag{B.2}$$

Thus it is sufficient to prove

$$\langle q|\, (\alpha q+\beta p)^N\, |q'\rangle = \int \frac{dp}{2\pi} e^{ip(q-q')} \left(\beta p + \alpha \frac{q+q'}{2}\right)^N . \tag{B.3}$$

This is achieved by induction. Let us consider the case of $N = 1$. One has, using a set of momentum eigenstates,

$$\begin{aligned}\langle q|\left(\alpha q+\beta p\right)|q'\rangle &= \int \frac{dp}{2\pi}\frac{1}{2}\left(\langle q|p\rangle\langle p|\alpha q+\beta p|q'\rangle+\langle q|\alpha q+\beta|p\rangle\langle p|q'\rangle\right)\\ &= \int \frac{dp}{2\pi}\langle q|p\rangle\langle p|q'\rangle\frac{1}{2}\left\{(\alpha q'+\beta p)+(\alpha q+\beta p)\right\}\\ &= \int \frac{dp}{2\pi}e^{ip(q'-q)}\left(\alpha\frac{q+q'}{2}+\beta p\right).\end{aligned}$$

One used $e^{ipq}=\langle p|q\rangle$ to obtain the last line.

Now, let us assume that the formula is valid for N. Let us show that this implies the validity for $N+1$:

$$\begin{aligned}\langle q|\left(\alpha q+\beta p\right)^{N+1}|q'\rangle &= \int \frac{dp}{2\pi}e^{ip(q-q')}\left(\beta p+\alpha\frac{q+q'}{2}\right)^{N}\\ &= (\alpha q-i\beta\partial_q)\int \frac{dp}{2\pi}e^{ip(q-q')}\left(\beta p+\alpha\frac{q+q'}{2}\right)^{N}\\ &= \int \frac{dp}{2\pi}e^{ip(q-q')}\left(\beta p+\alpha\frac{q+q'}{2}-i\beta\partial_q+\alpha\frac{q-q'}{2}\right)\times\\ &\left(\beta p+\alpha\frac{q+q'}{2}\right)^{N}\\ &= \int \frac{dp}{2\pi}e^{ip(q-q')}\left(\beta p+\alpha\frac{q+q'}{2}\right)^{N+1}+\\ &\int \frac{dp}{2\pi}e^{ip(q-q')}\left(-i\beta\partial_q+\alpha\frac{q-q'}{2}\right)\left(\beta p+\alpha\frac{q+q'}{2}\right)^{N}.\end{aligned}$$

Finally, if one performs an integration by parts on the second integral of the last line, one may write

$$\begin{aligned}\int \frac{dp}{2\pi}e^{ip(q-q')}\left(\beta p+\alpha\frac{q+q'}{2}\right)^{N+1}+\int \frac{dp}{2\pi}e^{ip(q-q')}\left(-i\beta\partial_q-\frac{\alpha}{2}\partial_p\right)\left(\beta p+\alpha\frac{q+q'}{2}\right)^{N}\\ = \int \frac{dp}{2\pi}e^{ip(q-q')}\left(\beta p+\alpha\frac{q+q'}{2}\right)^{N+1}\ \blacksquare\end{aligned}$$

B.2 Generalization of Gaussian integrals

In this section, one would like to prove the following

$$\frac{\int d^N\xi\, exp\left(-\frac{1}{2}\xi_i B_{ij}\xi_j\right)\xi_m\xi_n}{\int d^N\xi\, exp\left(-\frac{1}{2}B_{ij}\xi_i\xi_j\right)} = (B^{-1})_{mn}\,, \tag{B.4}$$

where B is a symmetric positive-definite matrix. In order to avoid some confusions in some of the following reasonings, one writes explicitly the summations for repeated indices. One starts by noticing that one may write

$$\int d^N\xi\, exp\left(-\frac{1}{2}\sum_{ij}\xi_i B_{ij}\xi_j\right)\xi_m\xi_n = -2\frac{\partial}{\partial B_{mn}}\int d^N\xi\, exp\left(-\frac{1}{2}\xi_i B_{ij}\xi_j\right). \tag{B.5}$$

Therefore, one may write (B.4) as

$$\frac{\int d^N\xi\, exp\left(-\frac{1}{2}\sum_{ij}\xi_i B_{ij}\xi_j\right)\xi_m\xi_n}{\int d^N\xi\, exp\left(-\sum_{ij}\frac{1}{2}\xi_i B_{ij}\xi_j\right)} = -2\frac{\partial}{\partial B_{mn}}\ln\left[\int d^N\xi\, exp\left(-\frac{1}{2}\sum_{ij}\xi_i B_{ij}\xi_j\right)\right]. \tag{B.6}$$

Now, one wants to evaluate the following integral,

$$\int d^N\xi\, exp\left(-\frac{1}{2}\sum_{ij}\xi_i B_{ij}\xi_j\right). \tag{B.7}$$

From the fact that B is symmetric, one may diagonalize it,

$$\sum_{ij}\xi_i B_{ij}\xi_j = \sum_k \theta_k C_k \theta_k\,, \tag{B.8}$$

where θ_k are independent linear combinations of ξ_k. Therefore, due to this linearity in the transformation of variables, the jacobian associated with it is constant. Let's call it J. Thus

one may write

$$\begin{aligned}\int d^N\xi exp\left(-\frac{1}{2}\sum_{ij}\xi_i B_{ij}\xi_j\right) &= J\int d^N\theta e^{-\frac{1}{2}\sum_k C_k\theta_k^2}\\ &= J\prod_k^N\int d\theta_k e^{-\frac{1}{2}C_k\theta_k^2}\\ &= J\prod_k\sqrt{\frac{2\pi}{C_k}}\\ &= J\frac{(2\pi)^{N/2}}{\sqrt{\det C}}\,.\end{aligned}$$

One solved the last integral via the usual Gaussian integral and wrote $\prod_k B_k = \det B$ for the matrix B is diagonal. Now, one recovers the matrix B from

$$C = \left(\frac{\partial\xi}{\partial\theta}\right)^T B\left(\frac{\partial\xi}{\partial\theta}\right)\,. \tag{B.9}$$

Thus, one gets for the determinant

$$\det C = J^2\,\det B\,. \tag{B.10}$$

Finally, this means that

$$\int d^N\xi exp\left(-\frac{1}{2}\sum_{ij}\xi_i B_{ij}\xi_j\right) = \frac{(2\pi)^{N/2}}{\sqrt{\det B}}\,. \tag{B.11}$$

Returning to B.6, one may write

$$\frac{\int d^N\xi exp\left(-\frac{1}{2}\sum_{ij}\xi_i B_{ij}\xi_j\right)\xi_m\xi_n}{\int d^N\xi exp\left(-\sum_{ij}\frac{1}{2}\xi_i B_{ij}\xi_j\right)} = -2\frac{\partial}{\partial B_{mn}}\ln\frac{(2\pi)^{N/2}}{\sqrt{\det B}}\,. \tag{B.12}$$

Notice that

$$-2\frac{\partial}{\partial B_{mn}}\ln\frac{(2\pi)^{N/2}}{\sqrt{\det B}} = (\det(B))^{-1}\frac{\partial\det B}{\partial B_{mn}}\,. \tag{B.13}$$

It is possible to prove that [86]

$$\frac{\partial\det(B)}{\partial B_{mn}} = det(B)\left(\left(B^T\right)^{-1}\right)_{mn}\,. \tag{B.14}$$

Recall that the matrix B is symmetric, i.e., $B = B^T$. Therefore,

$$\frac{\partial \det(B)}{\partial B_{mn}} = \text{adj}(B^T)_{mn} = \text{adj}(B)_{mn} = \det(B)(B^{-1})_{mn} \,. \tag{B.15}$$

Thus, using the aforementioned in B.13, one gets

$$\frac{\int d^N\xi \, exp\left(-\frac{1}{2}\sum_{ij}\xi_i B_{ij}\xi_j\right)\xi_m\xi_n}{\int d^N\xi \, exp\left(-\sum_{ij}\frac{1}{2}\xi_i B_{ij}\xi_j\right)} = (B^{-1})_{mn} \blacksquare \tag{B.16}$$

The case of Grassman variables follows closely the aforementioned. It may be seen in [36, 37]. The general case

$$\frac{\left(\prod_k \int d\xi_k\right)\exp\left[-\xi_i B_{ij}\xi_j\right]\xi_1 \ldots \xi_N}{\left(\prod_k \int d\xi_k\right)\exp\left[-\xi_i B_{ij}\xi_j\right]} = \sum_{\text{pairings}}\prod_{\text{pairs}}(B)^{-1}_{\text{index pair}} \tag{B.17}$$

is just a generalization of the aforementioned. One just as to consider an expression similar to that of B.6, where, instead of one derivative, one has to perform a derivative for each pairing and consider each possible pairing, i.e., one substitutes

$$\begin{aligned}\frac{\int d^N\xi \, exp\left(-\frac{1}{2}\sum_{ij}\xi_i B_{ij}\xi_j\right)\xi_{a_1}\xi_{a_2}\ldots\xi_{a_N}}{\int d^N\xi \, exp\left(-\sum_{ij}\frac{1}{2}\xi_i B_{ij}\xi_j\right)} = &-2^{\#\{pairs\}}\sum_{pairings}\prod_{pairs}\frac{\partial}{\partial B_{index\,pair}} \\ &\times \ln\left[\int d^N\xi \, exp\left(-\frac{1}{2}\sum_{ij}\xi_i B_{ij}\xi_j\right)\right] \,.\end{aligned}$$

The rest of the proof is completely analogous.

Appendix C

Grassman variables

One introduces the Grassman variables in this appendix. These are used in order to quantize spinor fields by representing these fields by Grassman variables, for instance. On the other hand, one used Grassman variables to define the ghost fields (see 2.23). The basic property of the Grassman variables is that they anticommute with each other, i.e., let ξ and ϕ be two Grassman variables. One has

$$\xi\phi = -\phi\xi \ . \tag{C.1}$$

This implies that Grassman variables are nilpotent, i.e,

$$\xi^2 = 0 \ . \tag{C.2}$$

This has the straightforward consequence that a Taylor expansion of a function $f(\xi)$ of Grassman variables is simply given by

$$f(\xi) = a + b\xi \ . \tag{C.3}$$

One would like to define the derivative and integration of such variables. For starters, let us notice that the fact that Grassman variables are anticommuting implies that one has to define this operations carefully, in order to decide in which variable it operates first. For instance, let us define the derivative of Grassman variables as

$$\frac{\partial}{\partial\xi_a}\xi_b\xi_c = \left(\frac{\partial\xi_b}{\partial\xi_a}\right)\xi_c - \xi_b\left(\frac{\partial\xi_c}{\partial\xi_a}\right) = \delta_{ab}\xi_c - \delta_{ac}\xi_b \ . \tag{C.4}$$

Notice that like the Grassman variables, the derivative of Grassman variables anticommute, i.e.,

$$\frac{\partial}{\partial\xi_a}\frac{\partial}{\partial\xi_b} = -\frac{\partial}{\partial\xi_b}\frac{\partial}{\partial\xi_a} \ . \tag{C.5}$$

In particular, one has

$$\left(\frac{\partial}{\partial \xi_a}\right)^2 = 0 \,. \tag{C.6}$$

Now one turns to integration. Let us consider a function $f(\xi)$ which one wants to integrate. From its Taylor expansion one knows that

$$\int d\xi \, f(\xi) = \int d\xi (a + b\xi) \,. \tag{C.7}$$

One defines the integrals in order to satisfy the following relations:

$$ID = 0$$
$$DI = 0$$

where D stands for the differantiation operator and I the integration operator. These mean that the integral of a total derivative vanishes if the surface terms are ignored; the differentiation of an integral (which is independent of the variable) must be 0. Therefore, one may identify the integration with the differentiation due to the later being nilpotent, i.e,

$$\int d\xi f(\xi) = \frac{\partial f(\xi)}{\partial \xi} \,. \tag{C.8}$$

From this one obtains the following integrals

$$\int d\xi = 0$$
$$\int d\xi \, \xi = 1 \,.$$

One uses the convention that

$$\int d\phi \int d\xi \, \xi \, \phi = +1 \,. \tag{C.9}$$

From these, one may prove that

$$\left(\prod_i \int d\xi_i^* d\xi_i\right) e^{\xi_i^* B_{ij} \xi_j} = \det B \,, \tag{C.10}$$

and

$$\left(\prod_i \int d\xi_i^* d\xi_i\right) \xi_k \xi_l^* e^{\xi_i^* B_{ij} \xi_j} = \det B (B^{-1})_{kl} \,, \tag{C.11}$$

for a hermitian matrix B. Notice that one defines a complex Grassman variable just as for normal variables (with a real and imaginary part). Notice that the ratio of gaussian integrals determined in the previous appendix for normal variables gives the same result as the one for Grassman variables. See [36] and/or [37] for further informations.

Appendix D

Results: More Figures

In this appendix, one presents some extra figures and tables of the results we obtained.

D.1 Ghost Propagator and the Perturbative One-loop expression

In this section, we present the fits of the lattice data concerning the bare lattice ghost propagator to the functional form depicted in (5.4). We divide this section into two, in subsection D.1.1 we take all parameters of (5.4) as fitting parameters, as well as Λ; in subsection D.1.2, all parameters of the functional form are taken as fitting parameters, except for Λ, which we set $\Lambda \sim \Lambda_{QCD} \sim 200 MeV$. The discussion is presented in section 5.2.2.

D.1.1 Case in which Λ is taken as a fitting parameter

β	L	z	Λ	γ_{gh}	$\chi/d.o.f.$
5.7	44	2.20 (6)	0.59(4)	-0.315(15)	0.284
6.0	64	6.84 (4)	0.61(1)	-0.270(3)	0.062
	80	7.44 (14)	0.49(2)	-0.312(7)	0.213
	128	6.88 (13)	0.63(3)	-0.272(8)	0.297
6.3	128	18.08(31)	0.60(3)	-0.259(8)	0.499

Table D.1 Parameters from the fit of the bare ghost propagator data set using the functional form (5.4).

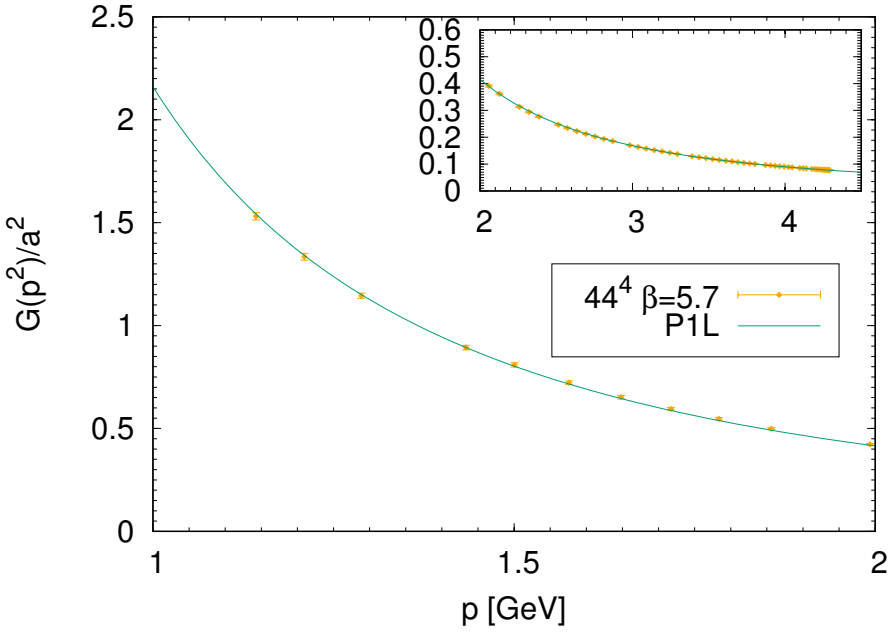

Fig. D.1 Bare Ghost Propagator and functional form (5.4) for the lattice with $\beta = 5.7$ and $L = 44$, in which Λ is a fitting parameter.

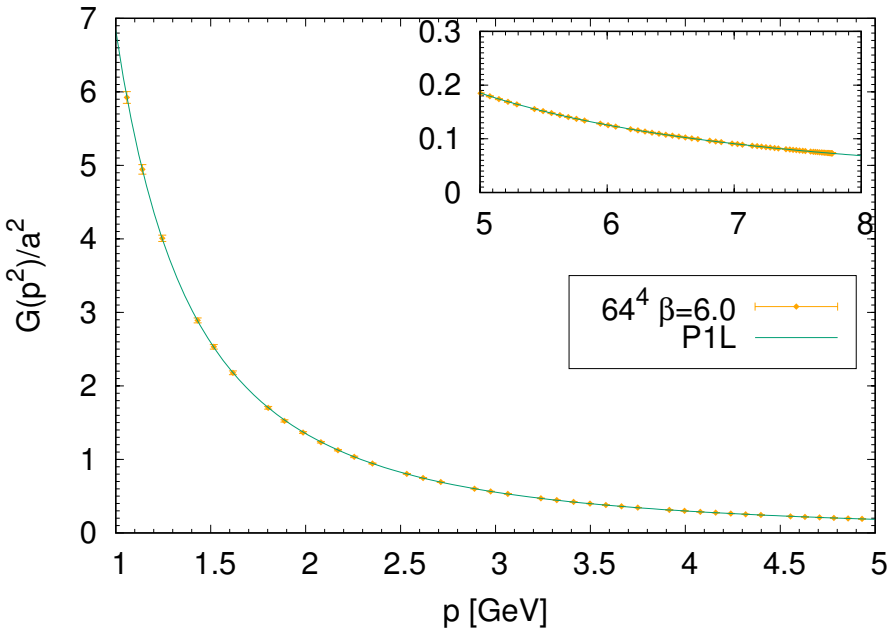

Fig. D.2 Bare Ghost Propagator and functional form (5.4) for the lattice with $\beta = 6.0$ and $L = 64$, in which Λ is a fitting parameter.

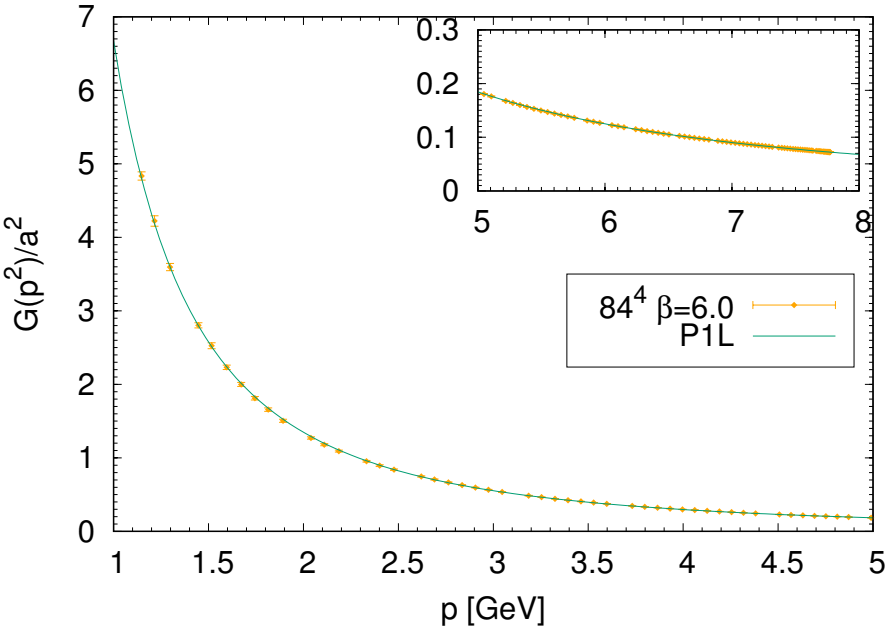

Fig. D.3 Bare Ghost Propagator and functional form (5.4) for the lattice with $\beta = 6.0$ and $L = 80$, in which Λ is a fitting parameter.

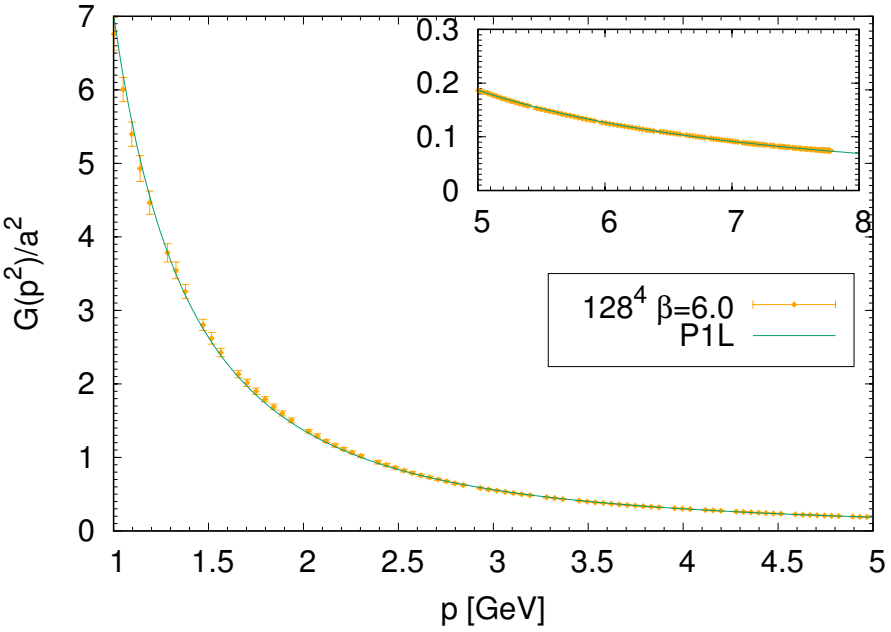

Fig. D.4 Bare Ghost Propagator and functional form (5.4) for the lattice with $\beta = 6.0$ and $L = 128$, in which Λ is a fitting parameter.

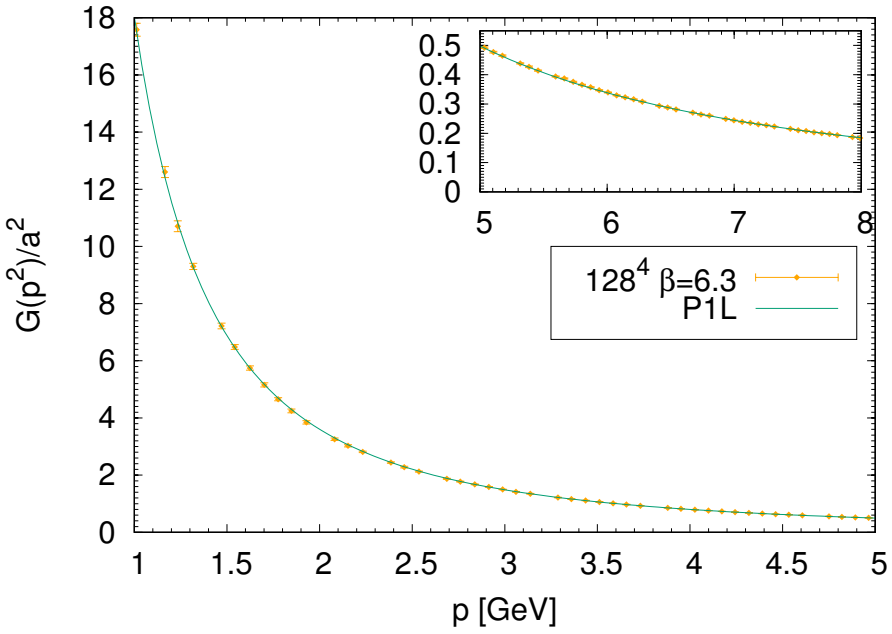

Fig. D.5 Bare Ghost Propagator and functional form (5.4) for the lattice with $\beta = 6.3$ and $L = 128$, in which Λ is a fitting parameter.

D.1.2 Case in which $\Lambda \sim \Lambda_{QCD} \sim 200MeV$

β	L	z	γ_{gh}	$\chi/d.o.f.$
5.7	44	3.97 (5)	-0.566(7)	0.677
6.0	64	10.69 (8)	-0.447(4)	0.827
	80	10.79 (7)	-0.456(3)	0.428
	128	11.11 (12)	-0.463(5)	0.520
6.3	128	27.81(30)	-0.430(5)	1.206

Table D.2 Parameters from the fit of the bare ghost propagator data set using the functional form (5.4) for $\Lambda \sim \Lambda_{QCD} \sim 200\,MeV$.

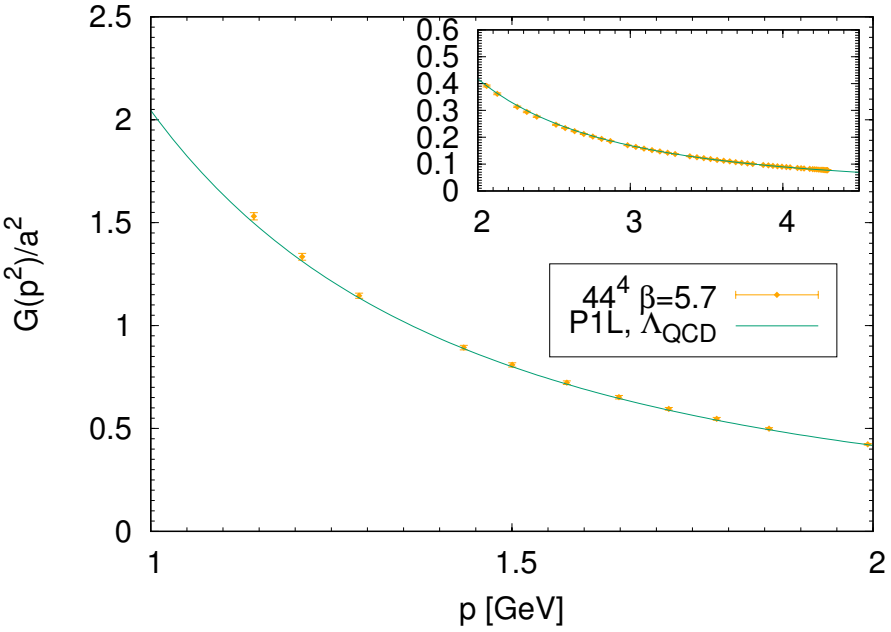

Fig. D.6 Bare ghost Propagator and functional form (5.4) for the lattice with $\beta = 5.7$ and $L = 44$, in which Λ is $\sim \Lambda_{QCD} \sim 200 MeV$.

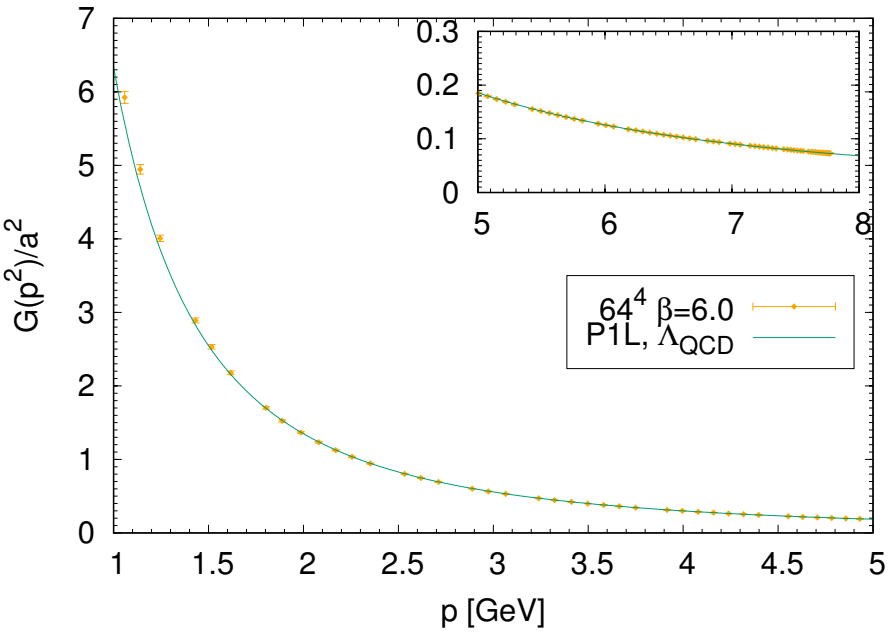

Fig. D.7 Bare ghost Propagator and functional form (5.4) for the lattice with $\beta = 6.0$ and $L = 64$, in which Λ is $\sim \Lambda_{QCD} \sim 200 MeV$.

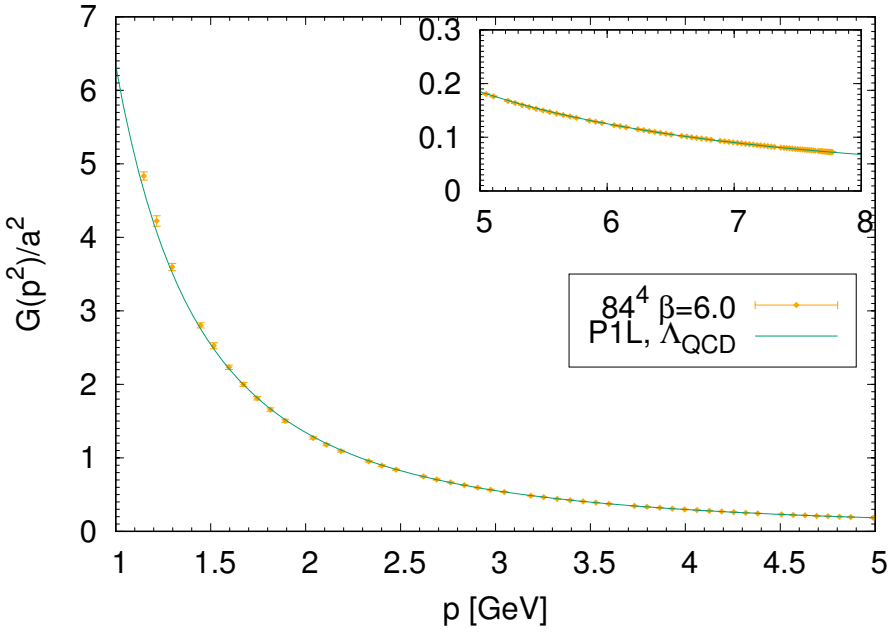

Fig. D.8 Bare ghost Propagator and functional form (5.4) for the lattice with $\beta = 6.0$ and $L = 80$, in which Λ is $\sim \Lambda_{QCD} \sim 200\,MeV$.

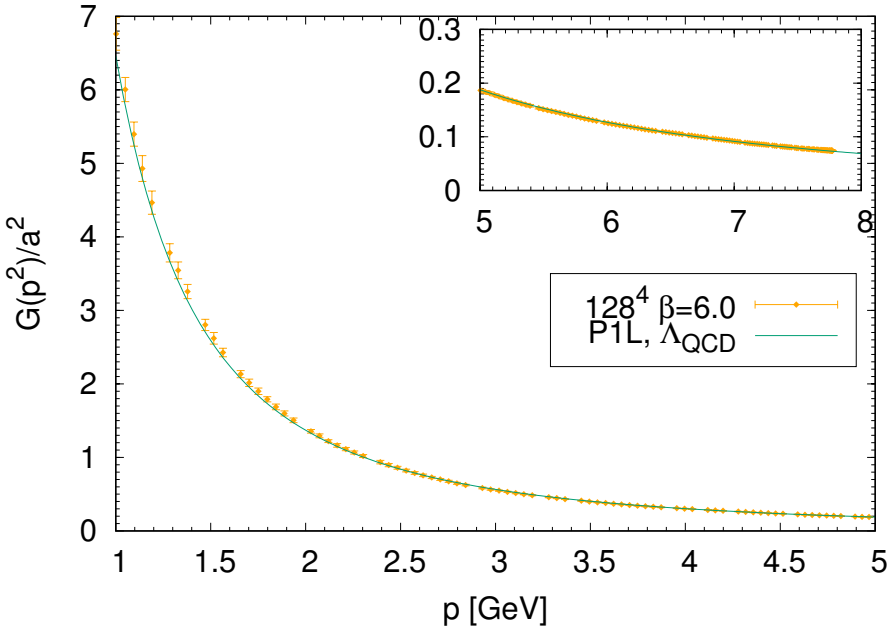

Fig. D.9 Bare ghost Propagator and functional form (5.4) for the lattice with $\beta = 6.0$ and $L = 128$, in which Λ is $\sim \Lambda_{QCD} \sim 200\,MeV$.

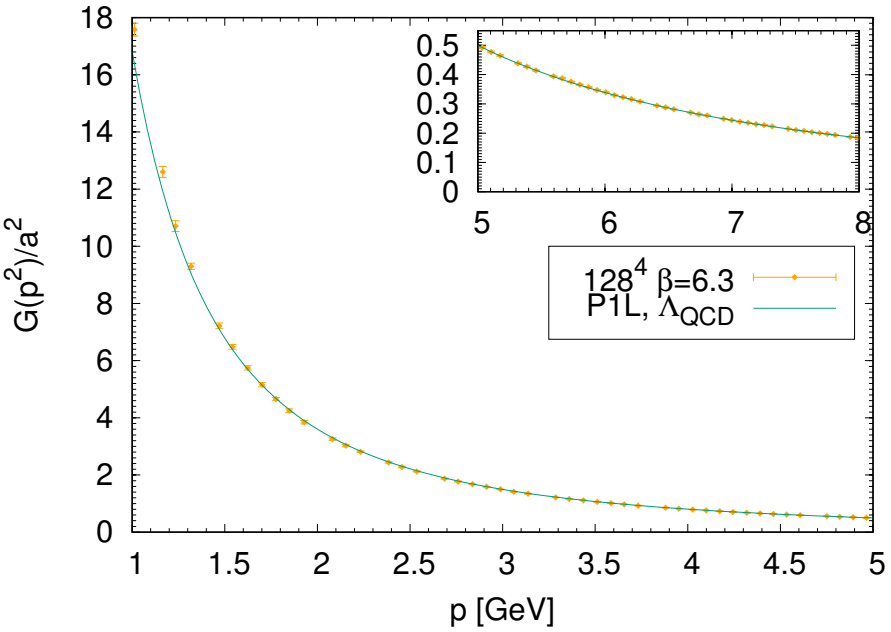

Fig. D.10 Bare ghost Propagator and functional form (5.4) for the lattice with $\beta = 6.3$ and $L = 128$, in which Λ is $\sim \Lambda_{QCD} \sim 200 MeV$.